INFORMATION TO USERS

This was produced from a copy of a document sent to us for microfilming. While the most advanced technological means to photograph and reproduce this document have been used, the quality is heavily dependent upon the quality of the material submitted.

The following explanation of techniques is provided to help you understand markings or notations which may appear on this reproduction.

1. The sign or "target" for pages apparently lacking from the document photographed is "Missing Page(s)". If it was possible to obtain the missing page(s) or section, they are spliced into the film along with adjacent pages. This may have necessitated cutting through an image and duplicating adjacent pages to assure you of complete continuity.

2. When an image on the film is obliterated with a round black mark it is an indication that the film inspector noticed either blurred copy because of movement during exposure, or duplicate copy. Unless we meant to delete copyrighted materials that should not have been filmed, you will find a good image of the page in the adjacent frame. If copyrighted materials were deleted you will find a target note listing the pages in the adjacent frame.

3. When a map, drawing or chart, etc., is part of the material being photographed the photographer has followed a definite method in "sectioning" the material. It is customary to begin filming at the upper left hand corner of a large sheet and to continue from left to right in equal sections with small overlaps. If necessary, sectioning is continued again—beginning below the first row and continuing on until complete.

4. For any illustrations that cannot be reproduced satisfactorily by xerography, photographic prints can be purchased at additional cost and tipped into your xerographic copy. Requests can be made to our Dissertations Customer Services Department.

5. Some pages in any document may have indistinct print. In all cases we have filmed the best available copy.

University
Microfilms
International

300 N. ZEEB RD., ANN ARBOR, MI 48106

Downloaded from SHAREOK. Persistent Handle URL: https://hdl.handle.net/11244/4972

8215906

Gibson, Thomas Loewen

A STUDY OF THE POLARIZATION INTERACTION WITH APPLICATION TO LOW-ENERGY ELECTRON-HYDROGEN COLLISIONS

The University of Oklahoma PH.D. 1982

University
Microfilms
International 300 N. Zeeb Road, Ann Arbor, MI 48106

THE UNIVERSITY OF OKLAHOMA
GRADUATE COLLEGE

A STUDY OF THE POLARIZATION INTERACTION WITH APPLICATION TO LOW-ENERGY ELECTRON-H_2 COLLISIONS

A DISSERTATION
SUBMITTED TO THE GRADUATE FACULTY
in partial fulfillment of the requirements for the
degree of
DOCTOR OF PHILOSOPHY

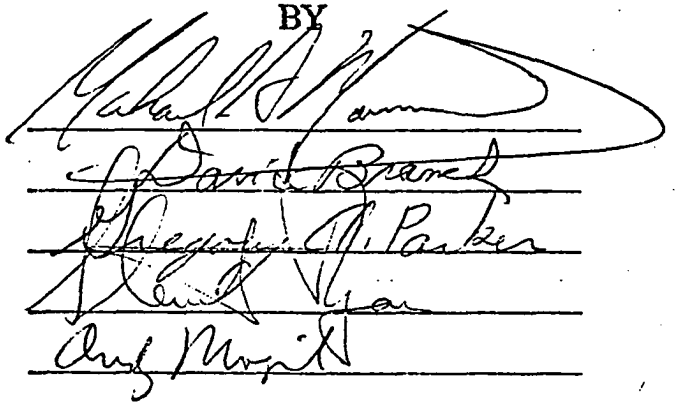
By
THOMAS LOEWEN GIBSON
1982

A STUDY OF THE POLARIZATION INTERACTION WITH APPLICATION TO LOW-ENERGY ELECTRON-H_2 COLLISIONS

A DISSERTATION

APPROVED FOR THE DEPARTMENT OF PHYSICS AND ASTRONOMY

BY



ACKNOWLEDGEMENTS

As with most endeavors of this kind, many people helped, encouraged, and provided support without which this work would have been made considerably more tedious. I wish to express my gratitude to Dr. Michael Morrison for pointing out the importance of this problem and for his patience and unflagging enthusiasm during this research. Much additional work on the scattering codes used to produce the results in Chapter IV was performed by Dr. Andrew Feldt who also provided the analytic fit of our BTAD potential. I would like to thank Drs. P. J. Hay and B. I. Schneider for their helpful suggestions during the early phases of this work and Drs. N. F. Lane, R. J. W. Henry and L. A. Collins for useful discussions regarding this research. I would like to acknowledge my office mates, especially Rick Weitzel, Bruce Hudson and Will Burgett, who provided moral support during the preparation of this dissertation. I would like to thank Jaquine Littell for the superb typescript she produced, and I am grateful to the Department of Physics and Astronomy for providing financial support during the last five years.

I want to express very special thanks to my wife Peggy for her patience and support during the years of graduate school.

ABSTRACT

The need for an understanding of the polarization interaction is discussed, and a procedure for calculating the electron-H_2 polarization potential based on a molecular structure code formulation of the problem is developed. In our treatment, nonadiabatic effects are approximated by a cutoff procedure which involves the numerical computation of certain integrals. Polarization potentials in which various multipole contributions were retained are presented. Scattering results in which the polarization interaction is represented by our calculated potentials are found to be in excellent agreement with a variety of recent experimental measurements. The possibility of extending this *ab initio* treatment of the polarization potential to include other electron-molecule systems is discussed.

TABLE OF CONTENTS

Page

Acknowledgements iii

List of Tables vii

List of Figures viii

Chapter

I. INTRODUCTION 1

II. A BRIEF INTRODUCTION TO THE POLARIZATION POTENTIAL IN ELECTRON-ATOM AND ELECTRON-MOLECULE COLLISIONS 8

2.1 Introduction 8

2.2 The Effects of Closed Channels: Electron-H Scattering, an Example 9

2.3 The Asymptotic Polarization Potential via Time Independent Perturbation Theory 11

2.4 The Importance of Being Nonadiabatic 14

2.5 The Polarization Potential for Electron-Molecule Collisions . . 19

Page

III. A PARAMETER-FREE NONADIABATIC POLARIZATION POTENTIAL FOR ELECTRON-H_2 SCATTERING 22

3.1 Introduction 22

3.2 On the Use of Structure Codes to Calculate the Adiabatic Polarization Potential 23

3.3 The Inclusion of Nonadiabatic Effects 28

3.4 Numerical Procedures 38

3.5 Calculation of the Polarization Potential 42

IV. ELECTRON-H_2 SCATTERING RESULTS 71

V. CONCLUSIONS 87

References 90

Appendix I. Comparison of Model Exchange Potentials for Low-Energy e-H_2 Collisions with and without Polarization Effects 95

Appendix II. Expansion of Gaussian Primitives 96

LIST OF TABLES

Page

1. Values of the corrected hydrogen atom dipole polarizability . . . 17
2. Definitions of the terms appearing in Gaussian primitives . . . 31
3. Relationships between the types of basis functions used and the spherical harmonics 32
4. Convergence characteristics of $E_0^P(\vec{C},R)$ 41
5. Exponents and contraction coefficients for the [6S3P/4S3P] basis set 43
6. Calculated values of $\alpha_{\|}$ and $\alpha_{\perp}$ for various values of C and R . 45
7. Integrated cross sections for the $j = 0$ to $j' = 2$ transition . . . 76

LIST OF FIGURES

Page

1. Coordinates used for the electron-H_2 system 51
2. The BTAD, BTADP23, AD, and BTA polarization potentials for $\theta = 0$ 52
3. The BTAD, BTADP23, AD, and BTA polarization potentials for $\theta = 90$ 53
4. A comparison of the BTAD, BTADP2, and BTADP23 polarization potentials for $\theta = 0$ 54
5. A comparison of the BTAD, BTADP2, and BTADP23 polarization potentials for $\theta = 90$ 55
6. A comparison of $v_0^{pol}(r)$ and $v_2^{pol}(r)$ for the BTAD and BTADP23 potentials 56
7. The BTAD, AD, and SNPD potentials for $\theta = 0$ 57
8. The BTAD, AD, and SNPD potentials for $\theta = 90$ 58
9. A comparison of $v_0^{pol}(r)$ for the BTAD and SNPD potentials . . . 59
10. A comparison of $v_2^{pol}(r)$ for the BTAD and SNPD potentials . . 60
11. The R-dependence of $v_0^{pol}(r)$ for the BTAD potential. 61
12. The R-dependence of $v_2^{pol}(r)$ for the BTAD potential. 62

Page

13. The AD and ADPOS polarization potentials for $\theta = 0$. 63
14. The AD and ADPOS polarization potentials for $\theta = 90$ 64
15. A comparison of $v_0^{pol}(r)$ for the AD and ADPOS potentials . . . 65
16. A comparison of $v_2^{pol}(r)$ for the AD and ADPOS potentials. . . 66
17. The $L = 0$ expansion coefficients for the AD, ADPOS and NEUTRAL molecular orbitals 67
18. The $L = 1$ expansion coefficients for the AD, ADPOS and NEUTRAL molecular orbitals 68
19. The $L = 2$ expansion coefficients for the AD, ADPOS and NEUTRAL molecular orbitals 69
20. A comparison of $v_0^{pol}(r)$ and $v_2^{pol}(r)$ for the BTAD potential and the ANALYTIC FIT 70
21. Total, integrated BFSMEP(BTAD), BFSMEP(BTADP2), and BFSMEP(BTADP23) cross sections 77
22. Total, integrated cross sections for very low-energy collisions. . 78
23. A comparison of various experimental and theoretical cross sections 79
24. A comparison of total integrated LFSMEP(BTAD) and BFESEP(BTAD) cross sections with measured values 80
25. Integrated rotational-excitation cross sections for the $j = 0$ to $j' = 2$ transition 81
26. Integrated rotational-excitation cross sections for the $j = 1$ to $j' = 3$ transition 82

Page

27. A comparison of BFESEP(OPT) and BFESEP(BTAD) eigenphase sums for the Σ_g symmetry 83
28. A comparison of BFESEP(OPT) and BFESEP(BTAD) cross sections for the Σ_g symmetry 84
29. A comparison of BFESEP(OPT) and BFESEP(BTAD) eigenphase sums for the Σ_u symmetry 85
30. A comparison of BFESEP(OPT) and BFESEP(BTAD) cross sections for the Σ_u symmetry 86

CHAPTER I
INTRODUCTION

The study of the quantum realm has led to the development of a very powerful branch of science known as collision physics. Here, where quantum phenomena can be observed only indirectly, measurements are usually performed by scattering a beam of projectiles off a target, and from an analysis of the scattering data, deducing something about the structure of the target and the nature of the interactions involved. Scattering theory is the theoretical tool used to analyze the experimental results.

Scattering theory can also be used to *predict* collision results, thereby testing our knowledge of the physics involved and providing theoretical guidance where the experimental results are uncertain or non-existent. This interplay between theory and experiment is especially prominent in the field of low-energy electron-molecule scattering and has proved quite beneficial to both.

We will use scattering theory to investigate the physics of the polarization potential for the electron-H_2 system. A comparison of our results with various experimental measurements and other theoretical treatments will be made. But first, we would like to sketch the development of the scattering equations in a body-fixed reference frame. Here we choose

the origin of coordinates at the molecular center-of-mass and pick the $\hat{z}$-direction to lie along the internuclear axis. We make the Born-Oppenheimer approximation[1] for the molecular wavefunctions, and in addition, we make the fixed-nuclei approximation[2] by freezing the position of the nuclei for the duration of the collision. (A very complete development of the theory of low-energy electron-molecule collisions can be found in reference 3.)

A theoretical formulation of the low-energy electron-molecule scattering problem usually begins with the non-relativistic time-independent Schrödinger equation

$$\hat{\mathcal{H}}\,\Psi_E = E\,\Psi_E \tag{1.1}$$

where E is the total energy of the system and the system Hamiltonian $\hat{\mathcal{H}}$ is given as

$$\hat{\mathcal{H}} = \hat{\mathcal{H}}_0 - \frac{1}{2}\nabla_r^2 + V_{e-m}. \tag{1.2}$$

Here, $\hat{\mathcal{H}}_0$ is the target Hamiltonian, while the second and third terms in Eq. (1.2) are the kinetic energy of the projectile and the electron-molecule interaction potential energy, respectively. Unless otherwise stated, atomic units* are used throughout. For the electron-H_2 system, V_{e-m} is written as

$$V_{e-m} = -\frac{1}{|\vec{r}-\vec{R}_a|} - \frac{1}{|\vec{r}-\vec{R}_b|} + \frac{1}{|\vec{r}-\vec{r}_1|} + \frac{1}{|\vec{r}-\vec{r}_2|} \tag{1.3}$$

which is just the sum of the Coulomb interactions between the scattering

---

*In atomic units $\hbar = m_e = a_0 = 1$. The unit of energy is $\hbar^2/(m_e a_0^2) = 1E_h = 2\,\mathrm{Ry} = 27.212$ eV. The unit of distance is the first Bohr radius $(a_0) = 1\,\mathrm{Bohr} = 0.52918 \times 10^{-10}\mathrm{m}$.

electron and the target molecule. The coordinates of the nuclei are denoted by $\vec{R}_\alpha$, those of the bound (molecular) electrons by $\vec{r}_i$, and the coordinates of the scattering electron by $\vec{r}$.

The next step is to expand the system wavefunction Ψ_E in a complete set of target eigenfunctions ϕ_n, *viz.*

$$\Psi_E(\vec{r}_i\,,\,\vec{r}\,;\,R_\alpha) = A\sum_n^f F_n(\vec{r})\,\phi_n(\vec{r}_i\,;\,R_\alpha) \tag{1.4}$$

The right-hand-side of Eq. (1.4) consists of a completely antisymmetrized sum over discrete states (and an integral over the continuum states) in which the explicit spin dependence has been suppressed. Due to our use of the Born-Oppenheimer and fixed-nuclei approximations, the wavefunctions in Eq. (1.4) have only a parametric dependence on the nuclear coordinates. The ϕ_n are solutions of the (electronic) time-independent Schrödinger equation for the target

$$[\hat{\mathcal{H}}_0 - \epsilon_n]\phi_n(\vec{r}_i\,;R_\alpha) = 0 \tag{1.5}$$

where ϵ_n is the electronic energy for the n^{th} molecular state.

To continue, we substitute Eq. (1.4) into the time-independent Schrödinger equation. If we multiply on the left by $\phi_n{}^*(\vec{r}_i;R_\alpha)$, integrate (sum) over the bound electronic spatial (spin) coordinates, and rearrange terms, we are left with the famous coupled-equations

$$[\nabla_r^2 + k_n^2]F_n(\vec{r}) = 2\sum_{n'}^f [V_{nn'}(\vec{r}) + W_{nn'}(\vec{r})]F_{n'}(\vec{r}) \tag{1.6}$$

where $k_n^2/2 = (E - \epsilon_n)$ is the scattering energy. The "direct" matrix elements are given by

$$V_{nn'}(\vec{r}) = \int \phi_n{}^*(\vec{r}_i)\,V_{e-m}\,\phi_{n'}(\vec{r}_i)\,\mathrm{d}\vec{r}_i \tag{1.7}$$

and the nonlocal exchange matrix elements $W_{nn'}(\vec{r})$ are operators which "pull" the scattering function under an integral and "eject" a bound function in its place.

Since Eq. (1.6) is an infinite set of coupled integro-differential equations, the problem as formulated is somewhat intractable. However, by retaining only the most important terms in the sum, Eq. (1.6) can be greatly simplified. For our study, we will be interested in collisions where the scattering energy is $\lesssim$10 eV and the target is initially—and finally—in the ground electronic state.* Therefore, we truncate the sum in Eq. (1.6) to include only the first term,** *viz.*

$$(\nabla_r^2 - 2[V^{st}(\vec{r}) + V^{ex}(\vec{r})] + k_0^2)F_0(\vec{r}) = 0 \qquad (1.8)$$

where $V^{st}(\vec{r}) \equiv V_{00}(\vec{r})$ and $V^{ex}(\vec{r})\,F_0(\vec{r}) \equiv W_{00}(\vec{r})F_0(\vec{r})$. Some of the consequences of this approximation will be discussed in the next chapter.

The static potential energy, $V^{st}(\vec{r})$, is seen to be the electron-molecule interaction potential energy V_{e-m} "averaged" over the ground electronic state of the molecule. This quantity can be efficiently calculated at the near-Hartree-Fock level of accuracy by existing computer codes.[4,5] The nonlocal energy-dependent exchange interaction is due to the quantum mechanical requirement that the system wavefunction be antisymmetric under pairwise exchange of identical fermions. Careful studies have shown

---

*A scattering energy $\gtrsim$11.36 eV is required to electronically excite the ground-state H_2 molecule.

**This is known as the static-exchange approximation.

that it is possible to include the effects of exchange in an approximate (though accurate) way by the use of a local energy-dependent model exchange potential [see Appendix 1 and references therein]. The use of a local model exchange potential leads to a considerable simplification of Eq. (1.8), although it is currently possible to include the exchange effects in an essentially exact fashion for reasonably simple systems.[6—10] In this study, we have used both exact and approximate treatments of exchange: we generate the model exchange potentials with program EXLAM;[11] calculations in which exchange is treated exactly utilize program ITERSEX.[8]

In order to solve the scattering equation, we incorporate one more expansion, namely

$$F_0(\vec{r}) = \sum_{\ell,m} \frac{1}{r} U_\ell^{(m)}(r)\, Y_\ell^m(\hat{r}) \tag{1.9}$$

where the $U_\ell^{(m)}(r)$ are radial scattering functions and the $Y_\ell^m(\hat{r})$ are the well known spherical harmonics.* Now by substituting Eq. (1.9) into Eq. (1.8), multiplying on the left by $\int d\hat{r}\, Y_{\ell'}^{m'*}(\hat{r})$, and rearranging terms we arrive at the radial coupled-equations

$$\left[\frac{d^2}{dr^2} - \frac{\ell(\ell+1)}{r^2} + k_0^2\right] U_\ell^{(m)}(r) = 2 \sum_{\ell'} V_{\ell\ell'}^{(m)}(r)\, U_{\ell'}^{(m)}(r) \tag{1.10}$$

with the matrix elements $V_{\ell\ell'}^{(m)}(r)$ defined by

$$V_{\ell\ell'}^{(m)}(r) \equiv \int d\hat{r}\, Y_\ell^{m*}(\hat{r})\, [V^{st}(\vec{r}) + V^{ex}(\vec{r})] Y_{\ell'}^m(\hat{r}). \tag{1.11}$$

---

*We use the Condon-Shortley phase convention for the $Y_\ell^m(\hat{r})$. See chapter 1 of reference 12 for definitions and tables.

Due to the cylindrical symmetry (about the internuclear axis) of the static and exchange interactions as well as our use of the fixed-nuclei approximation, the radial equations are not coupled in m. In fact, these equations separate according to the irreducible representations[12] of the electron plus molecule point group, $D_{\infty h}$: Σ_g , Σ_u , Π_u , Π_g , ... These "representations" are defined by the particular values of ℓ and m, *e.g.* ,

$$\Sigma_g : \quad m = 0; \quad \ell = 0, 2, 4, \ldots \tag{1.12a}$$

$$\Sigma_u : \quad m = 0; \quad \ell = 1, 3, 5, \ldots \tag{1.12b}$$

$$\Pi_u : \quad m = 1; \quad \ell = 1, 3, 5, \ldots \tag{1.12c}$$

$$\Pi_g : \quad m = 1; \quad \ell = 2, 4, 6, \ldots \tag{1.12d}$$

The values of ℓ and m represent the orbital angular momentum of the projectile electron and its projection along the internuclear axis, respectively.

To summarize, we have introduced some of the basics of the scattering problem as well as the static and exchange interactions. However, one might well guess that in a thesis purporting to deal with the physics of the polarization interaction, something is missing. We will introduce the "missing" interaction in Chapter II and give a brief survey of its development and use in electron-atom and electron-molecule collisions. The basic theory underlying our approach to the polarization interaction will be developed in Chapter III. We will also describe the manner in which our calculations are carried out and a comparison of our results with other theoretical treatments will be presented. In Chapter IV we will test our polarization potential by using it (together with accurate treatments of the

static and exchange interactions) to calculate scattering results. Again, we will compare our results with those obtained from various experimental measurements as well as with other theoretical results. Finally, in Chapter V we will summarize our findings, present some conclusions, and suggest some future directions for this research.

CHAPTER II

A BRIEF INTRODUCTION TO THE POLARIZATION POTENTIAL IN ELECTRON-ATOM AND ELECTRON-MOLECULE COLLISIONS

2.1 Introduction

In this chapter we will first motivate the need for terms beyond the static-exchange approximation [Eq. (1.8)]. We will then introduce the polarization interaction and briefly survey some of the developments regarding the use of this interaction in electron-atom and electron-molecule collisions. To begin with, we should examine our use of the static-exchange approximation; that is, we need to investigate the consequences of truncating the right-hand-side of Eq. (1.6) (when $n = 0$) to include just the first term. If the results obtained with this approximation accurately reproduce experimental measurements, or better yet, if we can show that the remaining closed-channel (energetically inaccessible) terms make a negligible contribution to the scattering equation, then the static-exchange approximation is valid and we need not introduce any further complications. For electrons scattered from ions or strongly polar molecules, the static-exchange approximation does indeed yield reasonably accurate results; however, for the vast majority of cases involving low-energy electron-atom or electron-molecule collisions, it is necessary to somehow take into account the additional terms in Eq. (1.6).

2.2 The Effects of Closed Channels: Electron-H Scattering, an Example

For the next few sections we will consider the case of electron-H scattering. We have picked this system as an example because of its simplicity, the fact that the hydrogen atom target wavefunctions are well known analytical functions, and because of the large body of research devoted to electron-H collisions. In this chapter, we will assume replacement of the electron-molecule expressions in Chap. I by the appropriate electron-atom forms (*e.g.*, the electron-atom equivalent of Eq. (1.2) is $\hat{\mathcal{H}} = \hat{\mathcal{H}}_0 - \frac{1}{2}\nabla_r^2 + V_{e-a}$ where $\hat{\mathcal{H}}_0$ is the hydrogen atom Hamiltonian and V_{e-a} is the electron-atom interaction potential energy).

We would like to briefly discuss some results which were first worked out by Castillejo *et al.* [13] In what follows, we restrict our treatment to large values of r (where the short-range exchange terms in Eq. (1.6) can be ignored) and we require that the scattering energy be insufficient to excite the hydrogen atom out of its ground-state. Under these assumptions, the boundary conditions on the scattering functions can be written as

$$F_0(\vec{r}) \sim e^{i\vec{k}_0\cdot\vec{r}} + f(\hat{r})\frac{e^{ik_0 r}}{r} \qquad (2.1a)$$

$$rF_n(\vec{r}) \xrightarrow[r\to\infty]{} 0 \quad , \quad \text{for} \quad n \neq 0, \qquad (2.1b)$$

where $f(\hat{r})$ is the scattering amplitude. We are interested in the asymptotic form of the scattering functions because we extract the scattering information in the asymptotic region. The target wavefunctions are given as

$$\phi_n(\vec{r}_1) = \frac{1}{r_1} \; P_{n\ell}(r_1) Y_\ell^m(\hat{r}_1) \qquad (2.2)$$

where the $P_{n\ell}(r_1)$ are the radial wavefunctions of the hydrogen atom.

To investigate the asymptotic behaviour of the coupling matrix elements, $V_{nn'}(\vec{r})$, we utilize a Legendre polynomial expansion of the electron-atom interaction potential energy V_{e-a}

$$V_{e-a} = \frac{1}{|\vec{r} - \vec{r}_1|} - \frac{1}{r} = \sum_{\lambda=0}^{\infty} \frac{r_<^\lambda}{r_>^{\lambda+1}} P_\lambda(\cos\theta) - \frac{1}{r} \tag{2.3}$$

with $\cos\theta = \hat{r} \cdot \hat{r}_1$ and $r_<$ ($r_>$) is the lesser (greater) of (r, r_1). Using the above Castillejo *et al.* showed that the coupling matrix elements $V_{nn'}(\vec{r})$ defined by

$$V_{nn'}(\vec{r}) \equiv \langle \phi_n(\vec{r}_1) | V_{e-a} | \phi_{n'}(\vec{r}_1) \rangle_{d\vec{r}_1} \tag{2.4}$$

go to zero asymptotically at least as fast as r^{-2}. Now, from the boundary conditions listed in Eq. (2.1) we see that (asymptotically) the only important terms on the right-hand-side of Eq. (1.6) are those which couple to the ground state. Therefore, Eq. (1.6) can be rewritten as

$$[\nabla_r^2 + k_n^2] F_n(\vec{r}) = 2V_{n0}(\vec{r}) F_0(\vec{r}) \tag{2.5}$$

for r "large" and $n \neq 0$. For n or n' corresponding to a bound state, $V_{nn'}(\vec{r})$ vanishes exponentially. Thus, we can rearrange Eq. (1.6) for the open channel to give

$$\nabla_r^2 F_0(\vec{r}) \sim -k_0^2 F_0(\vec{r}) + O(r^{-4}). \tag{2.6}$$

This last result allows us to derive

$$F_n(\vec{r}) \sim \frac{V_{n0}(\vec{r}) F_0(\vec{r})}{(\epsilon_0 - \epsilon_n)} \quad , \quad \text{for} \quad n \neq 0, \tag{2.7}$$

which we substitute into the asymptotic form of Eq. (1.6) for the open channel $F_0(\vec{r})$ leaving

$$[\nabla_r^2 + k_0^2]\, F_0\,(\vec{r}) = 2V_{00}(\vec{r})F_0(\vec{r}) - 2\sum_{n'\neq 0} \frac{|V_{0n'}(\vec{r})|^2 F_0(\vec{r})}{\epsilon_{n'} - \epsilon_0}\,. \qquad (2.8)$$

For large values of r, we have

$$\sum_{n'\neq 0} \frac{|V_{0n'}(\vec{r})|^2}{\epsilon_{n'} - \epsilon_0} \sim \frac{\alpha_d}{2r^4} \qquad (2.9)$$

where α_d is defined by

$$\alpha_d \equiv \frac{2}{3}\sum_{n'\neq 0} \frac{|\langle P_{01}(r_1)|r_1|P_{n'1}(r_1)\rangle_{dr_1}|^2}{\epsilon_{n'} - \epsilon_0}\,. \qquad (2.10)$$

We can use the above results to write a simplified version of Eq. (2.8) which is valid in the asymptotic region, *viz.*

$$[\nabla_r^2 - 2(V^{st}(\vec{r}) - \frac{\alpha_d}{2r^4}) + k_0^2]F_0(\vec{r}) = 0\,. \qquad (2.11)$$

So far our analysis shows that including the closed channels gives rise to an additional term in the scattering equation which varies asymptotically like r^{-4}. This is a very important result and we will discuss it further in the next section.

2.3 The Asymptotic Polarization Potential via Time Independent Perturbation Theory

In the previous section we were concerned with the consequences of including the closed channels or *virtual excitations* in Eq. (1.6). We will take a more "physical" approach in this section. The static-exchange

approximation is equivalent to truncating the expansion of the system wavefunction Ψ_E in Eq. (1.4) to include only the first term. For the electron-H system this gives

$$\Psi_E(\vec{r}_1, \vec{r}) = F_0(\vec{r})\,\phi_0(\vec{r}_1) \tag{2.12}$$

which is just the antisymmetrized product of the scattering function and the ground-state wavefunction of the hydrogen atom. But we know that the atom will distort in the presence of a perturbing electric field, *e.g.*, the field of the scattering electron. This "polarization" of the target charge density gives an additional contribution to the system energy E, which is known (not surprisingly) as the polarization potential.

To investigate this phenomenon we will *fix* the position of the scattering electron at a large distance from the target atom and utilize time independent perturbation theory (see Chapter 4 of reference 1) to calculate a correction to the system energy. We begin by writing the system Hamiltonian as

$$\hat{\mathcal{H}} = \hat{\mathcal{H}}_0 + V_{e-a} \tag{2.13}$$

where $\hat{\mathcal{H}}_0$ is the Hamiltonian for the hydrogen atom. Here we will treat V_{e-a} as the perturbation. Now, using Eq. (2.4) to define the matrix elements $V_{nn'}(\vec{r})$, we can write the perturbed hydrogen atom wavefunctions correct to first-order as

$$\phi_0'(\vec{r}_1; \vec{r}) = \phi_0(\vec{r}_1) + \sum_{n' \neq 0} \frac{V_{n'0}(\vec{r})\phi_{n'}(\vec{r}_1)}{\epsilon_0 - \epsilon_{n'}}. \tag{2.14}$$

From these perturbed wavefunctions, we can calculate the energy correct

to second-order, *viz.*

$$E = \epsilon_0 + V_{00}(\vec{r}) + \sum_{n' \neq 0} \frac{|V_{0n'}(\vec{r})|^2}{\epsilon_0 - \epsilon_{n'}} \tag{2.15}$$

where we make the following identifications for the terms on the right-hand-side of Eq. (2.15): the first term is the ground-state energy of the unperturbed hydrogen atom; the second term is the first-order correction to the energy which we recognize as the static potential $V^{st}(\vec{r})$; and the third term (which is due to the induced distortion of the target) is the second-order correction to the energy which we will call the polarization potential $V^{\rm pol}(\vec{r})$. A quick comparison with the previous section reveals that the correction represented by $V^{\rm pol}(\vec{r})$ is exactly the same result that we obtained by including the closed channels. Thus we can use Eq. (2.9) to immediately write

$$V^{\rm pol}(\vec{r}) \sim \frac{-\alpha_d}{2r^4} \tag{2.16}$$

where α_d is known as the dipole polarizability. For the hydrogen atom $\alpha_d = 4.5a_0^3$; Castillejo *et al.* [13] found that 65.8% of this value comes from the $2p$ states, an additional 15.6% comes from all the rest of the discrete (bound) states, and the remaining 18.6% comes from the continuum states.

Now we have the very interesting result that — at least for large values of r — the more intuitive approach utilizing a polarization potential accounts for the effects of closed channels. In fact, most treatments which go beyond the static-exchange approximation do so by incorporating a polarization potential of some sort. However, we have only derived $V^{\rm pol}(\vec{r})$ for a stationary electron at large distances from the target. In the next

section we will look at some of the implications associated with these assumptions and discuss some means for going beyond them.

2.4 The Importance of Being Nonadiabatic

We have found that the long-range form of $V^{\rm pol}(\vec{r})$ for a stationary electron is given by Eq. (2.16). However, the scattering electron is certainly not stationary and it is not always "far" from the target. In this section we will examine the correction introduced when we take the motion of the scattering electron into account. First, we will look at the large-r region, and then we will briefly discuss some of the methods which have been developed to extend the polarization potential into the small-r region.

The polarization potential derived in the previous section will be correct whenever the *adiabatic* approximation is valid. In this approximation, the target is assumed to respond adiabatically to the motion of the projectile electron; that is, the molecular charge cloud is assumed to immediately readjust to the instantaneous position of the scattering electron. For slow (low-energy) collisions, one might expect the adiabatic approximation to be good, or alternatively, that the nonadiabatic corrections will be small. To see whether or not this is so, we can use the perturbed target wavefunctions in Eq. (2.14) to calculate nonadiabatic correction terms in the limit of large r.

First, we *renormalize* the $\phi_0'(\vec{r}_1;\vec{r})$ of Eq. (2.14); this step is important, and if not performed, we will miss the lowest-order correction. Now, if we take the kinetic energy operator of the projectile electron, $-\frac{1}{2}\nabla_r^2$, as a perturbation on the system Hamiltonian in Eq. (2.13), we

can write the "first-order" nonadiabatic correction as

$$\Delta^{\rm na}(\vec{r}) = \overline{\langle\phi_0'(\vec{r}_1,\vec{r})|} - \frac{1}{2}\nabla_r^2\,\overline{|\phi_0'(\vec{r}_1,\vec{r})\rangle_{d\vec{r}_1}} \tag{2.17}$$

where the overbar indicates renormalization. We can write

$$\overline{\phi_0'(\vec{r}_1,\vec{r})} = N(\vec{r})\,\phi_0'(\vec{r}_1;\vec{r}) \tag{2.18}$$

where the r-dependent normalization has the asymptotic form

$$N(\vec{r}) \sim 1 - \frac{1}{2}\frac{\beta_1}{r^4} \tag{2.19}$$

with β_1 defined by

$$\beta_1 \equiv \sum_{n\neq 0} \frac{|\langle\phi_0(\vec{r}_1)|r_1 P_1(\cos\theta)|\phi_n(\vec{r}_1)\rangle_{d\vec{r}_1}|^2}{(\epsilon_n - \epsilon_0)^2}. \tag{2.20}$$

Notice that the $\phi_n(\vec{r}_1)$ and ϵ_n in Eq. (2.20) are the *unperturbed* hydrogen atom wavefunctions and energies.

By substituting the above results back into Eq. (2.17) and keeping terms to lowest order, we can write the "first nonadiabatic correction" as

$$\Delta^{\rm na} \sim \frac{3\beta_1}{r^6}, \tag{2.21}$$

which is independent of the scattering energy. Combining this result with Eq. (2.16) we can write

$$V^{\rm pol}(\vec{r}) \sim \frac{-\alpha_d}{2r^4} + \frac{3\beta_1}{r^6}. \tag{2.22}$$

From Eq. (2.20) we can see that β_1 is a positive quantity; therefore the nonadiabatic correction acts to cancel some of the adiabatic polarization potential. However, there are higher-order terms in both the adiabatic

polarization potential and the nonadiabatic correction which are not negligible. In fact, Drachman[14] has recently shown that the asymptotic form of the polarization potential correct through r^{-7} is given by

$$V^{\rm pol}(\vec{r}) \sim \frac{-\alpha_d}{2r^4} + \frac{(-\alpha_q + 6\beta_1 + 24\gamma k_0^2)}{2r^6} + \frac{\delta}{2r^7} \qquad (2.23)$$

where the numerical values (in atomic units) of the coefficients in Eq. (2.23) are given as: $\alpha_d = 4.5$; $\alpha_q = 15$; $\beta_1 = 43/8$; $\gamma = 319/48$; and $\delta = 213/2$. We note that this potential is energy-dependent since $k_0^2/2$ is the scattering energy. To ensure elastic collisions, we require that $k_0^2 < 0.75\,\mathrm{Ry}$. For the purpose of illustration we assume that the higher-order terms represent an energy- and r-dependent correction to the dipole polarizability; we can rewrite Eq. (2.23) as

$$V^{\rm pol}(\vec{r}) \sim \frac{-\alpha_d(k_0^2\,,\,r)}{2r^4} \qquad (2.24)$$

with $\alpha_d(k_0^2\,,\,r)$ defined by

$$\alpha_d(k_0^2\,,\,r) \equiv \alpha_d - \frac{(-\alpha_q + 6\beta_1 + 24\gamma k_0^2)}{r^2} - \frac{\delta}{r^3}\,. \qquad (2.25)$$

In Table 1 we present calculated values of $\alpha_d(k_0^2\,,\,r)$ for three values of k_0^2 and r. We should mention that Eq. (2.23) and hence Eq. (2.25) are valid only in the limit of large r; our use of these expressions for the particular values of r in Table 1 involves some approximation. At any rate, it appears that the nonadiabatic corrections are small for $r \gtrsim 15\,a_0$, therefore the adiabatic approximation, Eq. (2.16), is valid in this region.

Table 1.

Values of the "corrected" hydrogen atom dipole polarizability $\alpha_d(k_0^2, r)$ in units of a_0^3.

k_0^2(Ry) \ $r(a_0)$	10.0	15.0	20.0
0.00	4.2	4.4	4.4
0.30	3.7	4.2	4.3
0.75	3.0	3.9	4.1

For a local exchange potential, we can write the total scattering potential as

$$V(\vec{r}) = V^{st}(\vec{r}) + V^{ex}(\vec{r}) + V^{\text{pol}}(\vec{r}). \tag{2.26}$$

To use this potential in scattering calculations we must be able to accurately calculate $V^{\text{pol}}(\vec{r})$ when the scattering electron is near the target. Although the adiabatic approximation is valid in the large-r region, as the scattering electron approaches the target it experiences more of the attractive static-exchange potential, thereby gaining a "local kinetic energy" comparable to that of the bound electron. The approximation that the target relaxes adiabatically in the field of a stationary scattering electron becomes less valid

as the distance between the projectile electron and the target decreases.[15] Thus the nonadiabatic effects must somehow be included when the scattering electron is near the target. The number of divers and wonderful schemes that have been employed in previous investigations testifies to the difficulty of this problem. However, we shall briefly list some of the major categories of treatments.

One can attack the coupled-equations directly by attempting to include a tractable number of additional states specifically chosen as to allow for polarization. This is the basic idea behind pseudostate treatments.[16—18]

A large class of reasonably successful treatments based on the polarized orbital method of Temkin[19] and Temkin and Lamkin[20] has been reviewed by Drachman and Temkin[21] and by Callaway.[22] These treatments utilize the perturbed target wavefunctions discussed previously and usually include nonadiabatic effects in an approximate way.

It is also possible to calculate an approximate correction to the adiabatic polarization potential [as in Eq. (2.17)] for all values of r. Callaway *et al.* [23] utilized polarization potentials generated in this fashion to perform scattering calculations for electron-H and electron-He collisions. Their study concluded that this method of treating the polarization interaction worked well for the electron-He system, but over corrected for the electron-H system (the hydrogen atom is approximately three times more "polarizable" than the helium atom). This method is also difficult to extend to more complicated systems. (For further discussion of polarization poten-

tials and their use in electron-atom scattering, see Chapter 5 of reference 24.)

2.5 The Polarization Potential for Electron-Molecule Collisions

In the previous sections we have introduced some of the physics of polarization potentials which occur in electron-atom collisions. This was done to take advantage of the relative simplicity of electron-atom systems, and because most of the techniques used to calculate electron-molecule polarization potentials have their basis (*sic*) in work done on electron-atom systems. Due to their aspherical nature, the electron-molecule interaction potential is somewhat more complicated than the corresponding electron-atom potential. For example, the simple scalar polarizability of Eq. (2.16) becomes a tensor of rank 2 for the general electron-molecule case. Fortunately, for homonuclear-diatomic molecules we can represent the polarizability by $\alpha_{\|}$, the parallel polarizability, and $\alpha_{\perp}$, the perpendicular polarizability. The quantities $\alpha_{\|}$ and $\alpha_{\perp}$ represent the "distortability" of the molecule in a uniform electric field oriented along—or perpendicular to—the internuclear axis, respectively.

The asymptotic form of the adiabatic polarization potential [*cf.*, Eq. (2.16)] can be written as

$$V^{\mathrm{pol}}(\vec{r}) \sim \frac{-\alpha_0}{2r^4} - \frac{\alpha_2 P_2(\cos\theta)}{2r^4} \tag{2.27}$$

where $P_2(\cos\theta)$ is a Legendre polynomial and θ is the angle from the internuclear axis to the scattering electron in our body-fixed reference frame of Chapter I. The spherical polarizability α_0 is given by

$$\alpha_0 = \frac{1}{3} \quad [2\alpha_\perp + \alpha_\parallel] \tag{2.28}$$

while the nonspherical polarizability α_2 is given by

$$\alpha_2 = \frac{2}{3} \quad [\alpha_\parallel - \alpha_\perp] \,. \tag{2.29}$$

As was the case in the previous section, nonadiabatic effects must be included when the projectile is near the target.

Polarization effects have often been represented by a semi-empirical approximation based on the known asymptotic form in Eq. (2.27). The semi-empirical potential takes the form

$$V^{\text{pol}}(\vec{r}) = C(r)\left(\frac{-\alpha_0}{2r^4} - \frac{\alpha_2 P_2(\cos\theta)}{2r^4}\right) \tag{2.30}$$

where $C(r)$ is usually written as

$$C(r) = 1 - \exp\left(-\left(\frac{r}{r_c}\right)^p\right). \tag{2.31}$$

This potential mocks nonadiabatic effects by cutting off the asymptotic form of the adiabatic polarization potential for values of $r \lesssim r_c$. The cutoff radius r_c is an adjustable parameter which can be "tuned"[25] to bring calculated cross sections into agreement with some experimentally-determined feature of the scattering (*e.g.*, a shape resonance). Alternatively, r_c may be chosen to coincide with the approximate radius of the molecular charge cloud. Some of the inaccuracies associated with the semi-empirical potential were demonstrated by Morrison and Hay[26] and Truhlar *et al.* [27] Their studies utilized molecular structure codes to calculate accurate *ab initio*

(though fully adiabatic) polarization potentials. Although the *ab initio* treatments were accurate over a larger region of space than the semi-empirical potential, neglect of the nonadiabatic effects led to unphysically strong potentials near the target.

Polarization potentials including approximate nonadiabatic effects have been generated by Lane and Henry[28] and Hara.[29] In order to obtain the proper asymptotic behaviour, both of these potentials had to be scaled, thereby introducing some uncertainty into the short- and intermediate-range regions.[3] More recently, Schneider,[30] using a pseudostate approach, and Klonover and Kaldor,[31] using a second-order optical potential, have calculated scattering results in which nonadiabatic effects were included at various levels of approximation. Very recently, Schneider and Collins[32] have reported some preliminary calculations in which an optical potential approach was used to include nonadiabatic effects.

In the next chapter we will (finally) develop our treatment of the polarization interaction potential and present the results of some calculations.

CHAPTER III

A PARAMETER-FREE NONADIABATIC POLARIZATION POTENTIAL FOR ELECTRON-H_2 SCATTERING

3.1 Introduction

In the previous chapter we introduced the need for terms beyond the static-exchange approximation and showed that an approach based on our intuitive ideas about how the target should distort in the presence of a charged particle could account for these terms. We also discussed the need to include nonadiabatic effects in the polarization potential. Finally, we briefly introduced some of the methods that have been used to go beyond the static-exchange approximation for electron-atom and electron-molecule collisions.

In this chapter we will present our treatment of the polarization interaction for e-H_2 collisions. To begin with, we will discuss the use of molecular structure codes to calculate adiabatic polarization potentials. Then we will introduce a procedure which allows us to include approximate nonadiabatic effects in our structure code calculations. We will describe some of the numerical techniques used to implement this nonadiabatic procedure. Polarization potentials obtained from this treatment will be presented and a comparison with the results of other calculations will be made.

3.2 On the Use of Structure Codes to Calculate the Adiabatic Polarization Potential

In this section we will discuss the use of a molecular structure code to calculate the adiabatic polarization potential (*cf.*, references 26 and 27). Central to this approach is the idea of treating the scattering electron as an additional (bogus) nucleus of charge $-e$. The additional nucleus is fixed at position $\vec{C}$ with respect to the origin of coordinates (see Figure 1) and the energy of this system is calculated by a molecular structure code. For our calculation we use the POLYATOM[33] computer programs. These codes perform analytic restricted-Hartree-Fock calculations. To endow the jargon in the previous sentence with a little more meaning, we will briefly describe these calculations for the isolated H_2 molecule.

We begin by writing the ground-state electronic H_2 wavefunction as a single Slater determinant (see Chapter 8 of reference 1), *viz.*

$$\phi_0(\vec{r}_i\,;R) = \frac{1}{\sqrt{2}} \begin{vmatrix} \psi_0(\vec{r}_1\,;R)\,\alpha_1 & \psi_0(\vec{r}_1\,;R)\,\beta_1 \\ \psi_0(\vec{r}_2\,;R)\,\alpha_2 & \psi_0(\vec{r}_2\,;R)\,\beta_2 \end{vmatrix} \tag{3.1}$$

where the α (β) are spin up (down) functions and the ψ_0 are molecular orbitals for the ground-state configuration. Our goal is to find the molecular orbitals which minimize the system energy $E_0^0(R)$

$$E_0^0(R) = \langle\, \phi_0(\vec{r}_i\,;R)\, |\hat{\mathcal{H}}_0|\, \phi_0(\vec{r}_i\,;R)\,\rangle_{d\vec{r}_i} + V_n(R) \tag{3.2}$$

where $\hat{\mathcal{H}}_0$ is the complete electronic Hamiltonian for the molecule and $V_n(R)$ is the potential energy of the nucleus-nucleus interactions

$$V_n(R) = \frac{1}{|\vec{A}-\vec{B}|} = \frac{1}{R} \tag{3.3}$$

The molecular orbitals satisfy the Hartree-Fock equations

$$\hat{\mathcal{H}}_{HF}\,\psi_0 = \epsilon_0\,\psi_0 \tag{3.4}$$

where ϵ_0 is the orbital energy and the Hartree-Fock Hamiltonian for bound electron 1 is written as

$$\hat{\mathcal{H}}_{HF}\,(1) = \hat{\mathcal{H}}_0(1) + \langle \psi_0\,(\vec{r}_2\,;R)\,|\frac{1}{|\vec{r}_1 - \vec{r}_2|}|\,\psi_0(\vec{r}_2\,;R)\rangle_{d\vec{r}_2}\,. \tag{3.5}$$

Here, $\hat{\mathcal{H}}_0\,(1)$ is defined by

$$\hat{\mathcal{H}}_0\,(1) \equiv\; -\frac{1}{2}\nabla^2_{\vec{r}_1} - \frac{1}{|\vec{r}_1 - \vec{A}|} - \frac{1}{|\vec{r}_1 - \vec{B}|}\,. \tag{3.6}$$

Since the molecular orbitals are normalized ($\langle\psi_0|\psi_0\rangle = 1$), we can rearrange Eq. (3.4) and multiply on the left by $\int d\vec{r}_1\;\psi_0{}^*(\vec{r}_1;R)$ leaving

$$\langle\psi_0(\vec{r}_1;R)|\hat{\mathcal{H}}_{HF}(1) - \epsilon_0|\psi_0(\vec{r}_1;R)\rangle_{d\vec{r}_1} = 0\,. \tag{3.7}$$

To solve this equation we will use a linear combination of atomic orbitals to form the molecular orbitals: This approach was introduced by Roothaan[34] and is known as the LCAO:MO method (see Chapter 15 of reference 1 and Chapter 25 of reference 12). Thus we write

$$\psi_0(\vec{r}_1;R) = \sum_{k=1}^{M} C_k(R)\eta_k(\vec{r}_1) \tag{3.8}$$

where the η_k are a basis of "atomic" functions and the C_k are coefficients which we have to determine. For a given set of basis functions, we can find the C_k which minimize the energy by the linear variational method (see Chapter 4 of reference 1).

First, we substitute the molecular orbital of Eq. (3.8) into Eq. (3.7) leaving

$$\sum_{\ell}\sum_{k} C_{\ell}^{*}(R)C_{k}(R)[H_{\ell k} - \epsilon_0 S_{\ell k}] = 0 \tag{3.9}$$

where the Hamiltonian matrix elements are defined by

$$H_{\ell k} \equiv \langle \eta_{\ell}(\vec{r}_1)|\hat{\mathcal{H}}_{HF}(1)|\eta_k(\vec{r}_1)\rangle_{d\vec{r}_1} \tag{3.10}$$

and the overlap matrix elements are defined by

$$S_{\ell k} \equiv \langle \eta_{\ell}(\vec{r}_1)|\eta_k(\vec{r}_1)\rangle_{d\vec{r}_1} \tag{3.11}$$

To minimize the energy with respect to the linear coefficients, we take $\frac{\partial}{\partial C_k}$ onto both sides of Eq. (3.9) leaving

$$\sum_{\ell} C_{\ell}^{*}(R)[H_{\ell k} - \epsilon_0 S_{\ell k}] = 0 \tag{3.12}$$

Using the Hermiticity of the Hamiltonian matrix ($H_{\ell k} = H_{k\ell}^{*}$), we can rewrite Eq. (3.12) as

$$\sum_{\ell} C_{\ell}(R)[H_{k\ell} - \epsilon_0 S_{k\ell}] = 0 \tag{3.13}$$

These are known as the secular equations. Now, given a set of basis functions, POLYATOM solves the secular equations for the C_{ℓ} and calculates the variationally minimized energy $E_0^0(R)$.

If we introduce the scattering electron as an additional nucleus at $\vec{C}$, we can write the energy of this system as

$$E_0^P(\vec{C},R) = \langle \phi_0^P(\vec{r}_i;\vec{C};R)|\hat{\mathcal{H}}_0'|\phi_0^P(\vec{r}_i;\vec{C};R)\rangle_{d\vec{r}_i} + V_n'(\vec{C},R). \tag{3.14}$$

Using the $\hat{\mathcal{H}}_0$ and V_n of Eq. (3.2) and Eq. (3.3) we can write

$$\hat{\mathcal{H}}'_0 = \hat{\mathcal{H}}_0 + \frac{1}{|\vec{r}_1 - \vec{C}|} + \frac{1}{|\vec{r}_2 - \vec{C}|} \tag{3.15}$$

and

$$V'_n(\vec{C}, R) = V_n(R) - \frac{1}{|\vec{A} - \vec{C}|} - \frac{1}{|\vec{B} - \vec{C}|}. \tag{3.16}$$

The electronic wavefunction ϕ_0^P is formed from the distorted (polarized) orbitals

$$\psi_0^P(\vec{r}_1\,;\,\vec{C}\,;\,R) = \sum_{k=1}^{M} C_k^P(\vec{C}, R)\eta_k(\vec{r}_1) \tag{3.17}$$

where we have used the same set of basis functions as in Eq. (3.8). The C_k^P are found by solving

$$\sum_{\ell} C_\ell^P(\vec{C}, R)[H'_{k\ell} - \epsilon'_0 S_{k\ell}] = 0 \tag{3.18}$$

where

$$H'_{k\ell} = \langle \eta_k(\vec{r}_1) | \hat{\mathcal{H}}'_{HF}(1) | \eta_\ell(\vec{r}_1) \rangle_{d\vec{r}_1} \tag{3.19}$$

and, using the $\hat{\mathcal{H}}'_{HF}(1)$ of Eq. (3.5), we have

$$\hat{\mathcal{H}}'_{HF}(1) = \hat{\mathcal{H}}_{HF}(1) + \frac{1}{|\vec{r}_1 - \vec{C}|} \tag{3.20}$$

Therefore, the only difference between Eq. (3.18) and Eq. (3.13) is a term in the Hamiltonian matrix. For a given k and ℓ we write

$$H'_{k\ell} - H_{k\ell} = \langle \eta_k(\vec{r}_1) | \frac{1}{|\vec{r}_1 - \vec{C}|} | \eta_\ell(\vec{r}_1) \rangle_{d\vec{r}_1}. \tag{3.21}$$

This term is responsible for the C_k^P being different from the C_k.

Now, we define the adiabatic polarization potential as the difference in the system energy due to distortions induced in the target by a projectile electron fixed at $\vec{C}$, therefore we can write

$$V^{\rm pol}(\vec{C},R) \equiv E_0^P(\vec{C},R) - E_0^U(\vec{C},R) \tag{3.22}$$

where $E_0^U(\vec{C},R)$ is defined by

$$E_0^U(\vec{C},R) \equiv \langle \phi_0(\vec{r}_i,R) | \hat{\mathcal{H}}_0' | \phi_0(\vec{r}_i;R) \rangle_{d\vec{r}_s} + V_n'(\vec{C},R)\,. \tag{3.23}$$

Here, $\hat{\mathcal{H}}_0'$ and V_n' are the same as in Eq. (3.14). The target wavefunction ϕ_0 is formed from the *undistorted* orbitals in Eq. (3.8), that is, the ϕ_0 in Eq. (3.23) is just the ground-state wavefunction for the isolated H_2 molecule.

An interesting result can be obtained if we "rearrange" Eq. (3.23) slightly. Since $V_n'(\vec{C},R)$ does not depend on the bound-electron coordinates $\vec{r}_i$, we can "pull" $V_n'(\vec{C},R)$ inside the matrix element in Eq. (3.23). Using $\hat{\mathcal{H}}_0'$ and V_n' as given in Eqs. (3.15–3.16) and replacing $\vec{C}$ with $\vec{r}$, we can write

$$\hat{\mathcal{H}}_0' + V_n'(\vec{r},R) = \hat{\mathcal{H}}_0 + V_{e-m} + V_n(R) \tag{3.24}$$

with V_{e-m} given by Eq. (1.3). Thus, we are left with

$$E_0^U(\vec{r},R) = E_0^0(R) + V^{St}(\vec{r}) \tag{3.25}$$

which we recognize (*cf.*, section 2.3) as the system energy correct to first-order in V_{e-m}. However, E_0^P is obtained by a variational treatment and — in some sense — contains higher than second-order terms in V_{e-m}. We will return to this point in a later section.

In this section we have shown how the adiabatic polarization potential can be calculated by using a molecular structure program (POLYATOM) to solve for the relevant quantities on the right-hand-side of Eq. (3.22). These codes are very efficient, and provided a sufficiently flexible set of basis functions is used, very accurate results are possible. In the next section we will examine a procedure which allows for the inclusion of approximate nonadiabatic effects in this formulation.

3.3 The Inclusion of Nonadiabatic Effects

In this section we will introduce a cutoff procedure which includes nonadiabatic effects in an approximate way; afterwards, we will discuss some of the details involved in the implementation of this procedure. In one of his early studies on electron-atom scattering,[19] Temkin suggested that the scattering-bound electron interaction should be set to zero via a step-function whenever the scattering electron was inside the radius of the bound electron. For $r < r_1$, this effectively cut off the interaction responsible for distorting the atomic orbitals and led to a weaker polarization potential near the target. Physically, this seems to say that once the scattering electron experiences approximately the same potential as the bound electron we should stop allowing the target to relax adiabatically. This is consistent with our argument in section 2.4 where we maintained that nonadiabatic effects would be most important when the "local kinetic energy" of the scattering electron was comparable to that of the bound electrons, and the target charge cloud could no longer "follow" the instantaneous field of the projectile. The cutoff procedure has been used with

considerable success for various electron-atom systems (see references 21 and 22).

Lane and Henry[28] used a linear variational approach to calculate electron-H_2 polarization potentials. Their method involved the use of a trial function of the form

$$\phi_0^P(\vec{r}_i;\vec{r};R_{\rm eq}) = \phi_0(\vec{r}_i;R_{\rm eq})\sum_{\alpha,\beta} C_{\alpha,\beta}(\vec{r},R_{\rm eq})[x_1+x_2]^\alpha[z_1+z_2]^\beta \quad (3.26)$$

where $R_{\rm eq}$ denotes the equilibrium internuclear separation and $\phi_0(\vec{r}_i;R_{\rm eq})$ is the isolated ground-state H_2 wavefunction of Joy and Parr.[35] The energy of the electron-H_2 system was minimized with respect to the $C_{\alpha,\beta}$ and the equivalent of Eq. (3.22) was used to calculate the polarization potential. Hara[29] calculated electron-H_2 polarization potentials in a two-center formulation by using a variation-perturbation approach. A standard linear variational treatment was used to form the secular equations which were then expanded in orders of V_{e-m}, and only terms of first- and second-order were retained. In addition, Hara included only the dipole contribution to the polarization potential. We will discuss the dipole approximation later. Both Lane and Henry and Hara calculated polarization potentials which utilized the Temkin cutoff (non-penetrating) procedure to approximate nonadiabatic effects. In order to obtain the proper asymptotic behaviour, both of these potentials had to be scaled, thereby introducing some uncertainty into the short- and intermediate-range regions. The disagreement with the known long-range values was probably due to a lack of flexibility in the trial functions used in these treatments.

In our study of the polarization interaction, approximate nonadiabatic effects are included by the non-penetrating (cutoff) procedure described above. The actual implementation of this procedure affects the calculation of the integrals on the right-hand-side of Eq. (3.21), *viz.*

$$\langle \eta'(\vec{r}_1) | \frac{1}{|\vec{r}_1 - \vec{C}|} | \eta(\vec{r}_1) \rangle_{d\vec{r}_1} . \tag{3.27}$$

The "atomic" basis functions which appear in these integrals need not be true solutions of an atomic Hamiltonian but are usually chosen for flexibility and ease of computation. The POLYATOM codes utilize basis sets of nucleus-centered Cartesian Gaussian-type-orbitals. A given member of the basis can consist of a linear combination of Gaussian "primitives" contracted into a single basis function. For a Gaussian primitive on nucleus A we have the general form

$$\eta(\vec{r}_1) = N_{qrs}(x_A)^q (y_A)^r (z_A)^s e^{-\alpha_t r_A^2} \tag{3.28}$$

where N_{qrs} is a normalization constant, α_t is the exponential coefficient, and the remaining terms are defined in Table 2. We can write a similar expression for a primitive on nucleus B. The particular values of qrs define the "type" of Gaussian function, *e.g.*,

$q = r = s = 0$; s-type function (3.29a)

$q = 1, r = s = 0$; p_x-type function (3.29b)

$r = 1, q = s = 0$; p_y-type function (3.29c)

$s = 1, q = r = 0$; p_z-type function (3.29d)

These are the only types of functions which we will use for our electron-H_2 calculations. In Table 3 we list the relationships between the various types of functions used and linear combinations of spherical harmonics. These relationships are very useful in the actual evaluation of integrals.

Table 2

Definitions of the terms appearing in Gaussian primitives (*c.f.*, Figure 1).

For a Gaussian primitive on nucleus A

$$x_A \equiv x_1 - A_x = x_1 = r_1 \sin\theta_1 \cos\phi_1$$
$$y_A \equiv y_1 - A_y = y_1 = r_1 \sin\theta_1 \sin\phi_1$$
$$z_A \equiv z_1 - A_z = r_1 \cos\theta_1 + |A_z|$$
$$r_A^2 \equiv r_1^2 + A_z^2 + 2r_1|A_z| \cos\theta_1$$

For a Gaussian primitive on nucleus B

$$x_B \equiv x_1 - B_x = x_1 = r_1 \sin\theta_1 \cos\phi_1$$
$$y_B \equiv y_1 - B_y = y_1 = r_1 \sin\theta_1 \sin\phi_1$$
$$z_B \equiv z_1 - B_z = r_1 \cos\theta_1 - |B_z|$$
$$r_B^2 \equiv r_1^2 + B_z^2 - 2r_1|B_z| \cos\theta_1$$

Table 3

Relationships between the types of basis functions used and the spherical harmonics. (For a more extensive table see p. 6 of reference 12.)

Notation	Coordinates	Spherical Harmonics
S	1	$\sqrt{4\pi}\, Y_0^0(\hat{r}_1)$
p_x	$x_1 = r_1 \sin\theta_1 \cos\phi_1$	$\sqrt{\frac{2\pi}{3}}\,[Y_1^{-1}(\hat{r}_1) - Y_1^1(\hat{r}_1)]r_1$
p_y	$y_1 = r_1 \sin\theta_1 \sin\phi_1$	$\sqrt{=\frac{2\pi}{3}}\,[Y_1^{-1}(\hat{r}_1) + Y_1^1(\hat{r}_1)]r_1$
p_z	$z_1 = r_1 \cos\theta_1$	$\sqrt{\frac{4\pi}{3}}\, Y_1^0(\hat{r}_1) r_1$

The POLYATOM codes use analytic forms[36] to evaluate the integrals in Eq.(3.27). Unfortunately, the cutoff procedure restricts the radial component of the integrals such that these analytic forms are no longer valid. Instead, we have chosen to evaluate these integrals numerically by a method which we will now describe. To incorporate the non-penetrating procedure we employ the following expansion

$$\frac{1}{|\vec{r}_1 - \vec{C}|} = \begin{cases} \sum_\lambda \sum_{\mu=-\lambda}^{\lambda} \left(\frac{4\pi}{2\lambda+1}\right) \frac{r_1^\lambda}{C^{\lambda+1}} Y_\lambda^\mu(\hat{r}_1)^* \, Y_\lambda^\mu(\hat{C}), & r_1 \leq C \qquad (3.30a) \\ 0, & r_1 > C \qquad (3.30b) \end{cases}$$

which effectively cuts off the scattering-bound electron interaction for $r_1 > C$. The Gaussian primitives are expanded in a series of spherical harmonics, *viz.*

$$\eta(\vec{r}_1) = \sum_i \sum_{j=-i}^{i} \frac{1}{r_1} a_i^j(r_1) \, Y_i^j(\hat{r}_1) \qquad (3.31)$$

where the a_i^j are given as

$$a_i^j(r_1) = r_1 \int d\hat{r}_1 \, Y_i^j(\hat{r}_1)^* \, \eta(\vec{r}_1) \, . \qquad (3.32)$$

Analytic expressions for these coefficients can be derived by methods discussed in Appendix 2. Now, substituting the expansions in Eqs.(3.30 and 3.31) into Eq.(3.27) and using the Gaunt formula for the integral over three spherical harmonics (see Chapter 1 of reference 12) we have

$$\langle \eta'(\vec{r}_1)|\frac{1}{|\vec{r}_1-\vec{C}|}|\eta(\vec{r}_1)\rangle_{d\vec{r}_1} = \sum_{\lambda ik}\sum_{j=-i}^{i}\sum_{\ell=-k}^{k}$$
$$\cdot\left\{(-1)^{\ell}Y_{\lambda}^{\ell-j}(\hat{C})\left[\frac{4\pi(2i+1)(2k+1)}{2\lambda+1}\right]^{1/2}\right.$$
$$\cdot\begin{pmatrix}\lambda & i & k\\ 0 & 0 & 0\end{pmatrix}\begin{pmatrix}\lambda & i & k\\ j-\ell & -j & \ell\end{pmatrix}\frac{1}{C^{\lambda+1}}\int_0^C$$
$$\left.\cdot\, dr_1\, a_i^{j*}(r_1)\, r_1^{\lambda}\, a_k^{\ell}(r_1)\right\} \qquad (3.33)$$

The Wigner 3-J coefficients vanish unless

$$\lambda + i + k = \text{even integer} \qquad (3.34a)$$

$$|i-k| \leq \lambda \leq i+k \qquad (3.34b)$$

and the sums in Eq.(3.33) are further restricted by the allowed values of i and j for the expansion coefficients a_i^j. The remaining radial integrals in Eq.(3.33) will be evaluated numerically.

At this point we should mention something about the "great multipole mystery". We have used a multipole expansion of the scattering-bound electron interaction potential [Eq.(3.30)] where λ labels the multipole components, *e.g.*, $\lambda = 0$ is the monopole term, $\lambda = 1$ is the dipole term, and $\lambda = 2$ is the quadrupole term. In principle there are an infinite number of these terms which should be included; in practice we need only include enough terms to converge our integral to some specified accuracy. However, a number of earlier investigations[21,22,37] have found that retention of the monopole term often leads to "unphysically" strong potentials.

As a correction, some treatments simply exclude the monopole ($\lambda = 0$) contribution while others keep only the dipole ($\lambda = 1$) contribution to the polarization potential. In section 3.5 we present polarization potentials calculated with various multipole contributions. To see whether or not the monopole term will give rise to a problem in our treatment, consider the following. We can replace $\vec{C}$ with $\vec{r}$ and use Eq.(3.24) to rewrite Eqs.(3.14 and 3.23) as

$$E_0^P(\vec{r},R) = \langle \phi_0^P(\vec{r}_i;\vec{r};R)|\hat{\mathcal{H}}_0 + V_{e-m} + V_n(R)|\phi_0^P(\vec{r}_i;\vec{r};R)\rangle_{d\vec{r}_i} \qquad (3.35)$$

and

$$E_0^U(\vec{r},R) = \langle \phi_0(\vec{r}_i;R)|\hat{\mathcal{H}}_0 + V_{e-m} + V_n(R)|\phi_0(\vec{r}_i;R)\rangle_{d\vec{r}_i}. \qquad (3.36)$$

In the non-penetrating approximation, we can make the following multipole expansion of V_{e-m} [Eq.(1.3)]

$$V_{e-m} = \sum_n \left(\frac{r_1^n}{r^{n+1}}P_n(\hat{r}_1\cdot\hat{r}) + \frac{r_2^n}{r^{n+1}}P_n(\hat{r}_2\cdot\hat{r}) - \left[\frac{(-R_<)^n + (R_<)^n}{R_>^{n+1}}\right]P_n(\hat{r}\cdot\hat{z})\right) \qquad (3.37)$$

where $R_<$ is the lesser of $(r, \frac{R}{2})$ and $R_>$ is the greater of $(r, \frac{R}{2})$. We are only interested in the monopole ($n = 0$) term here, which we can write as

$$V_{e-m}^0 = \frac{2}{r} - \frac{2}{R_>}. \qquad (3.38)$$

The first term on the right-hand-side is from the scattering-bound electron interaction and the second term is due to the interaction between the scattering electron and the nuclei. For the equilibrium internuclear separation of H_2, $R = 1.4a_0$ and $R_> = r$ for $r \geq 0.7a_0$. Thus, the monopole component of the electron-molecule interaction potential vanishes for $r \geq 0.7a_0$ and should make no contribution to the polarization potential. However,

as we shall show in section 3.5, including the $\lambda = 0$ term in Eq.(3.33) has a very significant (and unwanted) effect on the polarization potential. The reason for this "mishandling" of the monopole term is due to the way that the structure code calculates the system energy and our use of the cutoff procedure in evaluating the integrals of Eq.(3.33). For the isolated H_2 molecule, the ground-state energy can be written as (see Chapter 25 of reference 12)

$$E_0^0(R) = 2\langle\psi_0(\vec{r}_1;R)|\hat{\mathcal{H}}_{HF}(1)|\psi_0(\vec{r}_1;R)\rangle_{d\vec{r}_1} + V_n(R) \qquad (3.39)$$

which is equivalent to Eq.(3.2). The POLYATOM codes actually calculate the system energy based on Eq.(3.39) rather than the form given in Eq.(3.2). We can also write

$$E_0^P(\vec{r},R) = 2\langle\psi_0^P(\vec{r}_1;\vec{r};R)|\hat{\mathcal{H}}'_{HF}(1)|\psi_0^P(\vec{r}_1;\vec{r};R)\rangle_{d\vec{r}_1} + V'_n(\vec{r},R) \qquad (3.40)$$

and

$$E_0^U(\vec{r},R) = 2\langle\psi_0(\vec{r}_1;R)|\hat{\mathcal{H}}'_{HF}(1)|\psi_0(\vec{r}_1;R)\rangle_{d\vec{r}_1} + V'_n(\vec{r},R)\,. \qquad (3.41)$$

The terms involving V_{e-m} in Eq.(3.40) can be written as

$$2\langle\psi_0^P(\vec{r}_1;\vec{r};R)|\frac{1}{|\vec{r}_1-\vec{r}|}|\psi_0^P(\vec{r}_1;\vec{r};R)\rangle_{d\vec{r}_1} - \frac{1}{|\vec{r}+\vec{R}/2|} - \frac{1}{|\vec{r}-\vec{R}/2|} \qquad (3.42)$$

and for Eq.(3.41) we have

$$2\langle\psi_0(\vec{r}_1;R)|\frac{1}{|\vec{r}_1-\vec{r}|}|\psi_0(\vec{r}_1;R)\rangle_{d\vec{r}_1} - \frac{1}{|\vec{r}+\vec{R}/2|} - \frac{1}{|\vec{r}-\vec{R}/2|}\,. \qquad (3.43)$$

If we substitute the multipole expansion of Eq.(3.37) into Eqs.(3.42 and 3.43) and keep only the monopole term, we are left with

$$\langle\psi_0^P(\vec{r}_1;\vec{r};R)\,|\,\frac{2}{r}\,|\,\psi_0^P(\vec{r}_1;\vec{r};R)\rangle_{d\vec{r}_1} - \frac{2}{R_>} \tag{3.44}$$

and

$$\langle\psi_0(\vec{r}_1;R)|\frac{2}{r}|\psi_0(\vec{r}_1;R)\rangle_{d\vec{r}_1} - \frac{2}{R_>}\,. \tag{3.45}$$

Although $\langle\psi_0^P|\psi_0^P\rangle = \langle\psi_0|\psi_0\rangle = 1$, in our cutoff procedure we have restricted the radial integrals such that we are left with

$$\frac{2}{r}\Big(\int d\hat{r}_1 \int_0^r r_1^2\, dr_1 |\psi_0^P(\vec{r}_1;\vec{r};R)|^2\Big) - \frac{2}{R_>} \tag{3.46}$$

for Eq.(3.44) and

$$\frac{2}{r}\Big(\int d\hat{r}_1 \int_0^r r_1^2\, dr_1 |\psi_0(\vec{r}_1;R)|^2\Big) - \frac{2}{R_>} \tag{3.47}$$

for Eq.(3.45). Since the integrals in these equations are not in general unity, the monopole terms in this formulation do *not* cancel when $R_> = r$. To remedy this situation, we remove the monopole component of the scattering-bound electron interaction in $\hat{\mathcal{H}}'_{HF}(1)$ and add it to $V'_n(\vec{r},R)$ for all values of r in Eqs.(3.40 and 3.41). This rearrangement is certainly valid for $r \geq \frac{R}{2}$, and in order to avoid a significant discontinuity in the polarization potential, we do the same for $r < \frac{R}{2}$ as well. Now, $V^{\rm pol} = E_0^P - E_0^U$, therefore the net effect of our machinations is to remove the monopole contribution to $V^{\rm pol}$. This procedure can be readily implemented by requiring that $\lambda > 0$ in Eq.(3.33).

3.4 Numerical Procedures

In this section we will discuss some of the computational details involved in implementing the non-penetrating procedure of the previous section. To begin with, it was necessary to modify the POLYATOM codes so that the integrals of Eq.(3.33) would be used instead of the regular analytic forms. This was accomplished by including some additional options in subroutine VINTS which are controlled by the value of an input parameter NPOPT (for non-penetrating option). The options corresponding to the particular values of this parameter are the following:

NPOPT= 0	Normal operation of the structure code.
NPOPT= 1	Normal operation of the structure code plus the production of a disk (or tape) file containing a list of the parameters which uniquely specifies each of the integrals involving the bogus nucleus [cf., Eq.(3.27)].
NPOPT= 2	The structure code reads a file of evaluated integrals corresponding to the file produced when NPOPT = 1. These values are substituted for those normally calculated in VINTS.

Since we are trying to calculate a better-than-adiabatic (BTA) polarization potential by using the cutoff procedure described in the previous section, we need a code to evaluate the modified integrals involved in our approximation. Such a code (BTAINTS by name) has been developed and tested during the course of this study. Essentially, this program

reads the file produced by POLYATOM when NPOPT = 1 and evaluates the integrals one at a time using Eq.(3.33); the evaluated integrals are then written into a disk (or tape) file for subsequent use in POLYATOM when NPOPT = 2.

The file produced by POLYATOM when NPOPT = 1 contains all of the information necessary to specify the two Gaussian primitives $\eta'(\vec{r}_1)$ and $\eta(\vec{r}_1)$ for each integral involving the bogus nucleus. This information includes which of the real nuclei the primitive is centered on and the location of that nucleus. Due to the way POLYATOM discards integrals which are zero by symmetry, the particular list of integrals produced will depend on the point group to which the nuclear framework (including the bogus nucleus) belongs. For the electron-H_2 system, we need only consider the following point groups:

$C_{\infty v}$	When the scattering electron is located along the internuclear axis.
C_{2v}	When the scattering electron is located along a perpendicular bisector of the internuclear axis.
C_s	When the scattering electron is located anywhere else.

Also, for a given internuclear separation R, the list of integrals to be evaluated is produced only once for each point group.

The sums over i and k in Eq.(3.33) are truncated at the values IMAX and KMAX, respectively. These values (usually IMAX = KMAX) are chosen such that the system energy E_0^P is converged to some specified

tolerance. For a given pair of primitives, all of the required expansion coefficients a_i^j and a_k^ℓ are generated and stored for use in the radial integrals which are then performed by a fixed step-size trapezoidal quadrature scheme. If the scattering electron is sufficiently far from the target, the integrals calculated from Eq.(3.33) should approach the values obtained from the analytic forms used in POLYATOM. In Table 4 we show the convergence properties of E_0^P with respect to IMAX and the step-size RSTEP used in the trapezoidal quadratures. For these calculations, the scattering electron was fixed at $C_z = 10.0a_0$ and the equilibrium internuclear separation $R = 1.4a_0$ was used. Additional convergence studies for smaller values of C indicate that one should choose a value of RSTEP which requires at least 25–30 steps in the trapezoidal quadratures. The value of IMAX for a given calculation depends on which multipoles are included; *e.g.* , IMAX = 16 is necessary if the monopole term in Eq.(3.33) is included, whereas IMAX = 12 is sufficient if no monopole contribution is allowed.

Table 4.

Convergence characteristics of $E_0^P(\vec{C}, R)$ [in Hartrees] with respect to IMAX and RSTEP. Here, the scattering electron is fixed at $C_z = 10.0a_0$ and the equilibrium internuclear separation $R = 1.4a_0$ is used. The value obtained when the analytic integrals in POLYATOM are used is $E_0^P = -1.133694792E_h$.

IMAX \ RSTEP(a_0)	0.4	0.2	0.1
10	−1.133658147	−1.133696309	−1.133695047
12	−1.133657861	−1.133696123	−1.133694856
14	−1.133657775	−1.133696072	−1.133694805
16		−1.133696060	−1.133694794
18		−1.133696057	−1.133694791

All of our calculations involving the polarization potential have been performed in double-precision on an IBM 370/158 computer. In the BTAINTS code we have exploited the axial symmetry of the electron-H_2 interaction potential so that only real quantities are handled numerically. This is accomplished by restricting the position of the scattering electron to the xz-plane ($\phi_C = 0$, see Figure 1). Currently, the BTAINTS code can perform integrals for s- and p-type Gaussian primitives. However, it should be straightforward to augment the program so that it can handle d-type functions as well. It should also be possible to make the BTAINTS code more efficient; most of the computer time used in calculating the polarization potential is spent in this program.

3.5 Calculation of the Polarization Potential

In this section we will describe the general procedure involved in calculating a polarization potential and then present the various potentials. The first step is to obtain a good set of basis functions for the H_2 target. We start with a [5S2P/3S2P] set of Gaussian basis functions. The exponents and contraction coefficients for this basis set are those given by Huzinaga.[38] This set is augmented with diffuse s- and p-type Gaussian functions to form a [6S3P/4S3P] basis set. The diffuse Gaussians give the target wavefunction added flexibility; *i.e.*, they allow for greater distortion of the target charge cloud. The exponents for the diffuse functions were obtained by continuing the sequence of exponents in the original set as a geometric series. A list of the exponents and contraction coefficients for the [6S3P/4S3P] basis set is given in Table 5.

Table 5

Exponents and contraction coefficients for the [6S3P/4S3P] Gaussian basis set used in calculating the polarization potential.

* * GAUSSIAN FUNCTION SPECIFICATIONS * *

NUMBER OF PRIMITIVE GAUSSIANS = 30
NUMBER OF BASIS FUNCTIONS = 26

GAUSSIAN	FUNCTION	COMPONENT	CENTER	TYPE	EXPONENT	COEFFICIENT
1	1	1	H1	S	33.6444000	0.0253740
2	1	2	H1	S	5.0579600	0.1896830
3	1	3	H1	S	1.1468000	0.8529300
4	2	1	H1	S	0.3211440	1.0000000
5	3	1	H1	S	0.1013090	1.0000000
6	4	1	H1	S	0.0300000	1.0000000
7	5	1	H1	X	1.1142000	1.0000000
8	6	1	H1	X	0.2592000	1.0000000
9	7	1	H1	X	0.0600000	1.0000000
10	8	1	H1	Y	1.1142000	1.0000000
11	9	1	H1	Y	0.2592000	1.0000000
12	10	1	H1	Y	0.0600000	1.0000000
13	11	1	H1	Z	1.1142000	1.0000000
14	12	1	H1	Z	0.2592000	1.0000000
15	13	1	H1	Z	0.0600000	1.0000000
16	14	1	H2	S	33.6444000	0.0253740
17	14	2	H2	S	5.0579600	0.1896830
18	14	3	H2	S	1.1468000	0.8529300
19	15	1	H2	S	0.3211440	1.0000000
20	16	1	H2	S	0.1013090	1.0000000
21	17	1	H2	S	0.0300000	1.0000000
22	18	1	H2	X	1.1142000	1.0000000
23	19	1	H2	X	0.2592000	1.0000000
24	20	1	H2	X	0.0600000	1.0000000
25	21	1	H2	Y	1.1142000	1.0000000
26	22	1	H2	Y	0.2592000	1.0000000
27	23	1	H2	Y	0.0600000	1.0000000
28	24	1	H2	Z	1.1142000	1.0000000
29	25	1	H2	Z	0.2592000	1.0000000
30	26	1	H2	Z	0.0600000	1.0000000

Now, using our augmented basis we obtain the energy of the unperturbed molecule $E_0^0(R)$ and the coefficients $C_k(R)$ of Eq.(3.8). These coefficients will be used in the calculation of $E_0^U(\vec{C},R)$ when the scattering electron is introduced as an additional nucleus. For $R = 1.4a_0$, we obtain $E_0^0 = -1.13295E_h$ using the augmented basis set. This can be compared with the Hartree-Fock limit value, $E_0^0 = -1.13363E_h$, calculated by Kolos and Roothaan[39] and the very accurate configuration-interaction (CI) value of Kolos and Wolniewicz[40] $E_0^0 = -1.17447E_h$.

A better indication of how "good" our basis is for the calculation of polarization potentials can be obtained by calculating the polarizabilities $\alpha_\parallel$ and $\alpha_\perp$. To calculate $\alpha_\parallel$ we place the scattering electron far from the target along the z-axis ($C = C_z \geq 10.0a_0$), then $\alpha_\parallel$ is given as

$$\alpha_\parallel = -2\,V^{\rm pol}(C_z,R)\cdot C_z^4\,. \tag{3.48}$$

For $\alpha_\perp$ we place the scattering electron far from the target along the x-axis ($C = C_x \geq 10.0a_0$), with $\alpha_\perp$ given as

$$\alpha_\perp = -2\,V^{\rm pol}(C_x,R)\cdot C_x^4\,. \tag{3.49}$$

In Table 6 we present calculated values of $\alpha_\parallel$ and $\alpha_\perp$ for various values of C and R. For comparison, we include the CI results of Rychlewski.[41] Because the field of the scattering electron is directed radially from the charge instead of uniformly along the x- or z-axis, the calculated polarizabilities have a C-dependence. As the scattering electron is placed farther away the molecule "sees" a more nearly uniform field, and the calculated polarizabilities approach their true C-independent values.[42]

Table 6.

Calculated values of $\alpha_{\parallel}$ and $\alpha_{\perp}$ (in a_0^3) for various values of C and R. The values of $\alpha_{\perp}$ are listed in parentheses below the corresponding values of $\alpha_{\parallel}$. The column labeled CI contains the configuration-interaction results of Rychlewski.[41]

$R(a_0)$	$C(a_0)$				
	10.0	15.0	20.0	30.0	CI
1.2	5.266	5.212	5.189	5.171	5.152
	(3.851)	(3.865)	(3.867)	(3.867)	(3.947)
1.4	6.635	6.558	6.525	6.499	6.387
	(4.512)	(4.534)	(4.539)	(4.541)	(4.579)
1.8	10.172	10.022	9.957	9.906	9.332
	(5.955)	(6.002)	(6.014)	(6.020)	(5.879)

In order to avoid confusion, we will establish some nomenclature for the various polarization potentials. Potentials calculated in the adiabatic approximation are referred to as adiabatic (AD) or penetrating (P). Any potential which is calculated using the modified integrals of Eq.(3.33) will contain a BTA in its name. The various BTA potentials depend on which multipole contributions are retained. We have calculated the following cases:

Name of potential	Values of λ retained in Eq.(3.33)
BTA	$\lambda = 0 - 32$
BTAD	$\lambda = 1$
BTADP2	$\lambda = 1 - 3$
BTADP23	$\lambda = 1 - 24$

Other calculations which employ the cutoff procedure will be referred to as non-penetrating (NP) along with whatever other descriptive qualifiers seem appropriate; *e.g.* , we will refer to the scaled non-penetrating calculation of Lane and Henry[28] as the SNP potential and the scaled non-penetrating dipole treatment of Hara[29] as the SNPD potential.

For the electron-H_2 system we assume that (for a given R) the polarization potential can be written as

$$V^{\rm pol}(\vec{r}) = v_0^{\rm pol}(r) + v_2^{\rm pol}(r) P_2(\cos\theta) \tag{3.50}$$

where $v_0^{\rm pol}(r)$ is given by

$$v_0^{\rm pol}(r) = \frac{1}{3}\left[2V_\perp^{\rm pol}(r) + V_\parallel^{\rm pol}(r)\right] \tag{3.51}$$

and $v_2^{\rm pol}(r)$ is given by

$$v_2^{\rm pol}(r) = \frac{2}{3}\left[V_{\parallel}^{\rm pol}(r) - V_{\perp}^{\rm pol}(r)\right]. \tag{3.52}$$

Provided Eq.(3.50) is valid, we need only calculate $V_{\parallel}^{\rm pol}(r) = V^{\rm pol}(C_z, R)$ and $V_{\perp}^{\rm pol}(r) = V^{\rm pol}(C_x, R)$—here, we are again using $\vec{r}$ and $\vec{C}$ as interchangeable labels for the position of the scattering electron. The polarization potentials $V_{\parallel}^{\rm pol}(r)$ and $V_{\perp}^{\rm pol}(r)$ are calculated on a mesh of 23 r-values for $0 \leq r \leq 10.0a_0$. For use in scattering calculations, we need the polarization potential on a much denser mesh of r-values. These values are provided via a cubic-spline fit of the 23 calculated values. Once we have $V_{\parallel}^{\rm pol}(r)$ and $V_{\perp}^{\rm pol}(r)$ on the appropriate r-mesh, $v_0^{\rm pol}(r)$ and $v_2^{\rm pol}(r)$ are generated using Eqs. (3.51 and 3.52).

To test the validity of Eq. (3.50), direct calculations of $V^{\rm pol}(\vec{C}, R)$ for $\theta_C = \frac{\pi}{4}$ were compared to the predicted values. We find agreement to within 5% for $r < 1.0a_0$, and within 2% for $r > 1.5a_0$ for the BTA potential. Lane and Henry[28] found similar agreement for their SNP potential. For the BTAD potential, we find agreement to within 0.2% for all values of r considered.

For $r > 10.0a_0$, we use a simple fit based on the long-range form of the adiabatic potential, *viz.* ,

$$v_0^{\rm pol}(r) = \frac{-\alpha_0}{2r^4} \tag{3.53}$$

and

$$v_2^{\rm pol}(r) = \frac{-\alpha_2}{2(r^2+b^2)^2} \tag{3.54}$$

with α_0 and α_2 given by Eqs. (2.28 and 2.29). The value of b depends on the particular potential being fit, *e.g.* , $b = 1.0a_0$ for the BTAD potential when $R = 1.4a_0$.

In Figures 2 and 3 we present various $V_{\parallel}^{\rm pol}(r)$ [$\theta = 0$] and $V_{\perp}^{\rm pol}(r)$ [$\theta = \frac{\pi}{2}$]; unless otherwise specified, all of these results are for $R = 1.4a_0$. Included in these figures are the AD, BTA, BTADP23, and BTAD potentials. The most striking feature in these figures is the difference between the BTA potential and the other two potentials in which nonadiabatic effects have been included. This difference is due to the (improper) inclusion of the monopole contribution and is similar to the findings of Weatherford *et al.* [37] In fact, we see that the BTA potential is more attractive than the full AD potential for $r \gtrsim 1.2a_0$.

In Figures 4 and 5 we present the BTAD, BTADP2, and BTADP23 potentials. These results show that — at least for the electron-H_2 system — the polarization potential converges rapidly in λ [*cf.*, Eq. (3.33)] and is reasonably well represented by keeping only the dipole ($\lambda = 1$) contribution. To see how these differences affect $v_0^{\rm pol}(r)$ and $v_2^{\rm pol}(r)$, we show results for the BTAD and BTADP23 potentials in Figure 6. Inclusion of the higher multipoles makes very little difference for $v_0^{\rm pol}(r)$, although a more substantive difference is noted for $v_2^{\rm pol}(r)$.

A comparison of our AD and BTAD potentials with the SNPD calculations of Hara[29] is shown in Figures 7 and 8. By spline-fitting Hara's $V_{\parallel}^{\rm pol}(r)$ and $V_{\perp}^{\rm pol}(r)$ potentials and using Eqs. (3.51 and 3.52) we can compare results for $v_0^{\rm pol}(r)$ and $v_2^{\rm pol}(r)$. These comparisons are shown

in Figures 9 and 10. Some of the small-r repulsion in Hara's results is due to "overshoot" in the cubic-spline fit.

In order to explicitly calculate vibrational excitation cross sections, one needs to know how the potentials depend on internuclear separation. In Figures 11 and 12 we show BTAD potentials for $R = 1.2a_0$, $R = 1.4a_0$, and $R = 1.8a_0$. All of these potentials were calculated with the [6S3P/4S3P] basis set of Table 5.

In section 3.3 we mentioned that our variational calculations included higher than second-order terms in V_{e-m}. If our polarization potentials were calculated to second-order in V_{e-m}, changing the sign of the projectile's charge would make no difference. However, in our structure code treatment we find that replacing the electron by a positron results in a considerably different polarization potential. Adiabatic potentials for the electron (AD) and positron (ADPOS) cases are presented in Figures 13-16. We also show the first three coefficients in a spherical harmonic $[Y_L^M(\hat{r}_1)]$ expansion of the AD and ADPOS polarized orbitals in Figures 17-19. These results were obtained when the bogus nucleus (electron or positron) was located at $C_z = 2.5a_0$; for these orbitals, $M = 0$. For comparison, we show the expansion coefficients of the unperturbed (NEUTRAL) orbital.

Finally, for use in other scattering calculations, an analytic fit to the $R = 1.4a_0$ BTAD potential was performed, *viz.*,

$$v_0^{\rm pol}(r) = \begin{cases} \frac{-4.0}{2(r^2+b_0r+r_0^2)^2}\left(1-\exp\left(-(\frac{r}{1.1})^{2.6}\right)\right) & r < 10a_0 \qquad (3.55a) \\ \frac{-\alpha_0}{2r^4} & r > 10a_0 \qquad (3.55b) \end{cases}$$

where $b_0 = -2.036a_0$, $r_0 = 2.79a_0$, and the spherical polarizability $\alpha_0 = 5.2a_0^3$;

$$v_2^{\rm pol}(r) = \begin{cases} \frac{-1}{2(r^2+b_1 r+r_1^2)^2}\left(1-\exp\left(-(\frac{r}{0.9})^{5.8}\right)\right) & r < 4a_0 \qquad (3.56a) \\ \frac{-1.32}{2(r^2+b_2 r+r_2^2)^2} & 4a_0 < r < 10a_0 \qquad (3.56b) \\ \frac{-\alpha_2}{2(r^2+1)^2} & r > 10a_0 \qquad (3.56c) \end{cases}$$

with $b_1 = -1.82a_0$, $r_1 = 2.42a_0$, $b_2 = 0.03365a_0$, $r_2 = 0.767a_0$, and the nonspherical polarizability $\alpha_2 = 1.32a_0^3$. Our spherical and nonspherical polarizabilities were obtained from the values of $\alpha_\parallel$ and $\alpha_\perp$ when $C = 20.0a_0$ and $R = 1.4a_0$ (see Table 6). The corresponding experimentally determined values are $\alpha_0 = 5.44a_0^3$ [43] and $\alpha_2 = 1.37a_0^3$. [44] A comparison of the analytic fit with the numerical potential is shown in Figure 20.

In the next chapter we will test our potentials in scattering calculations.

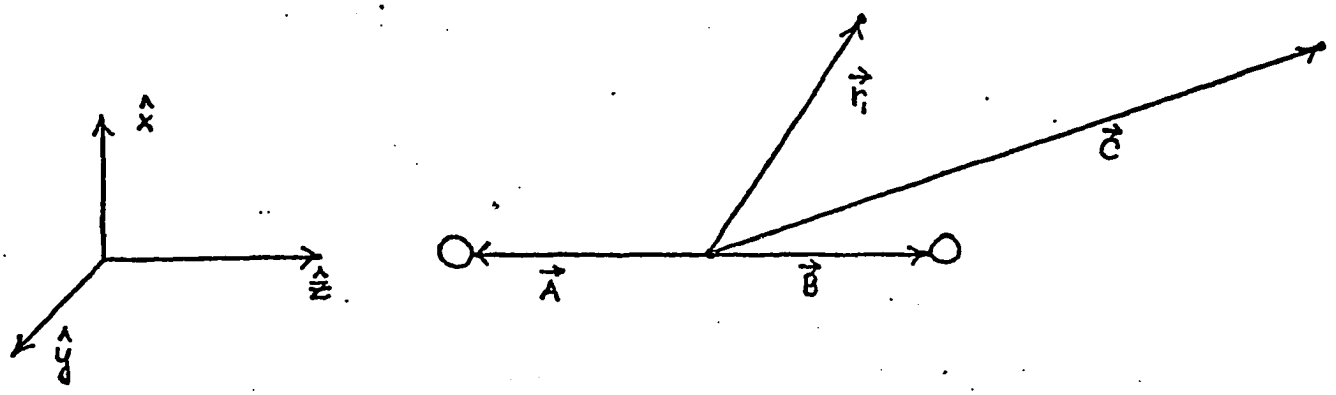


Figure 1. The coordinates used for the electron-H_2 system. Here, the positions of the nuclei are represented by $\vec{A}$, $\vec{B}$, and (for the bogus nucleus) $\vec{C}$; $\vec{r}_1$ is the coordinate of a bound electron.

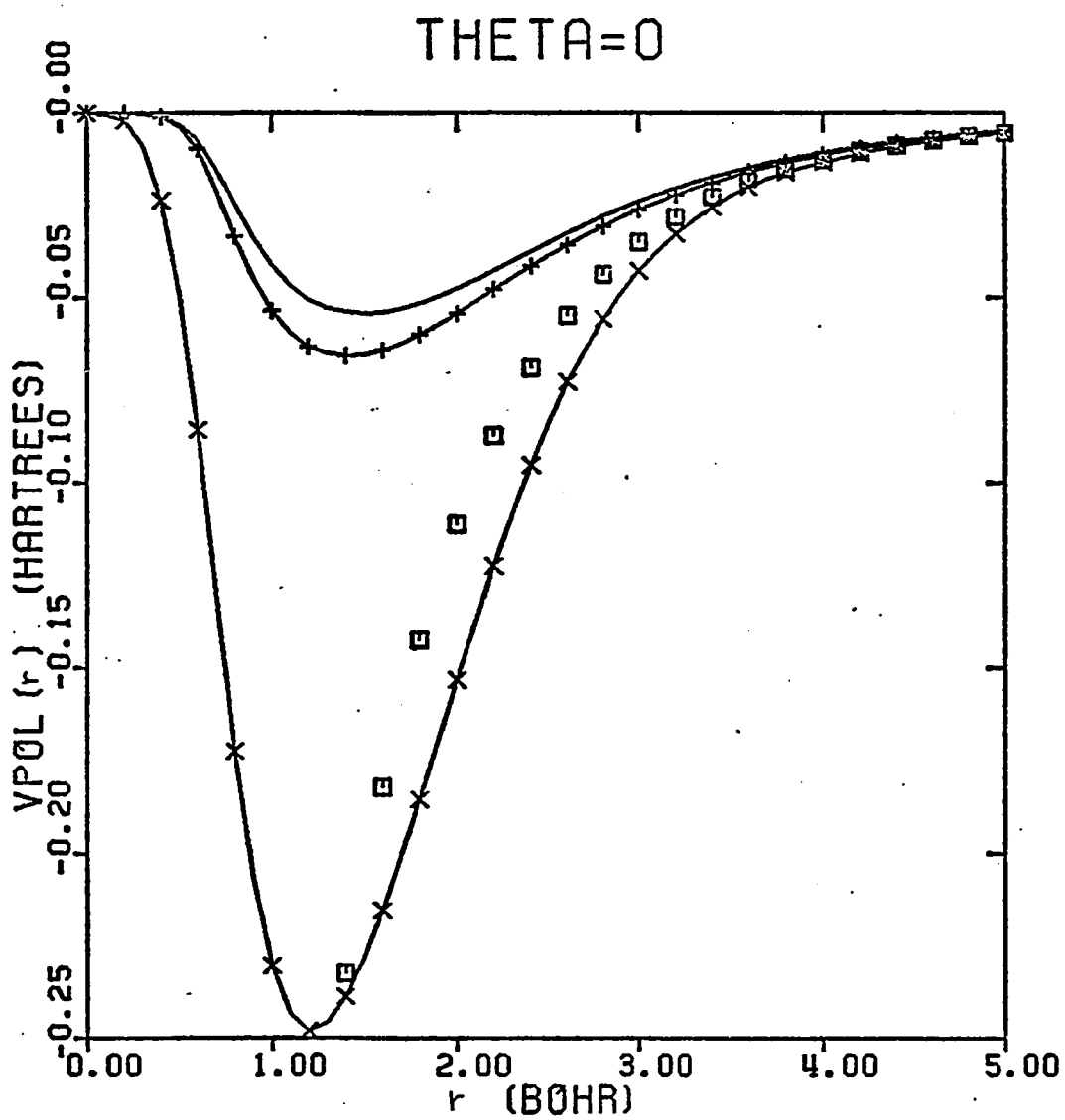


Figure 2. Polarization potentials obtained when the scattering electron is located along the z-axis ($\theta = 0$). The following potentials are shown:
—, BTAD; +, BTADP23; □, AD; ×, BTA.

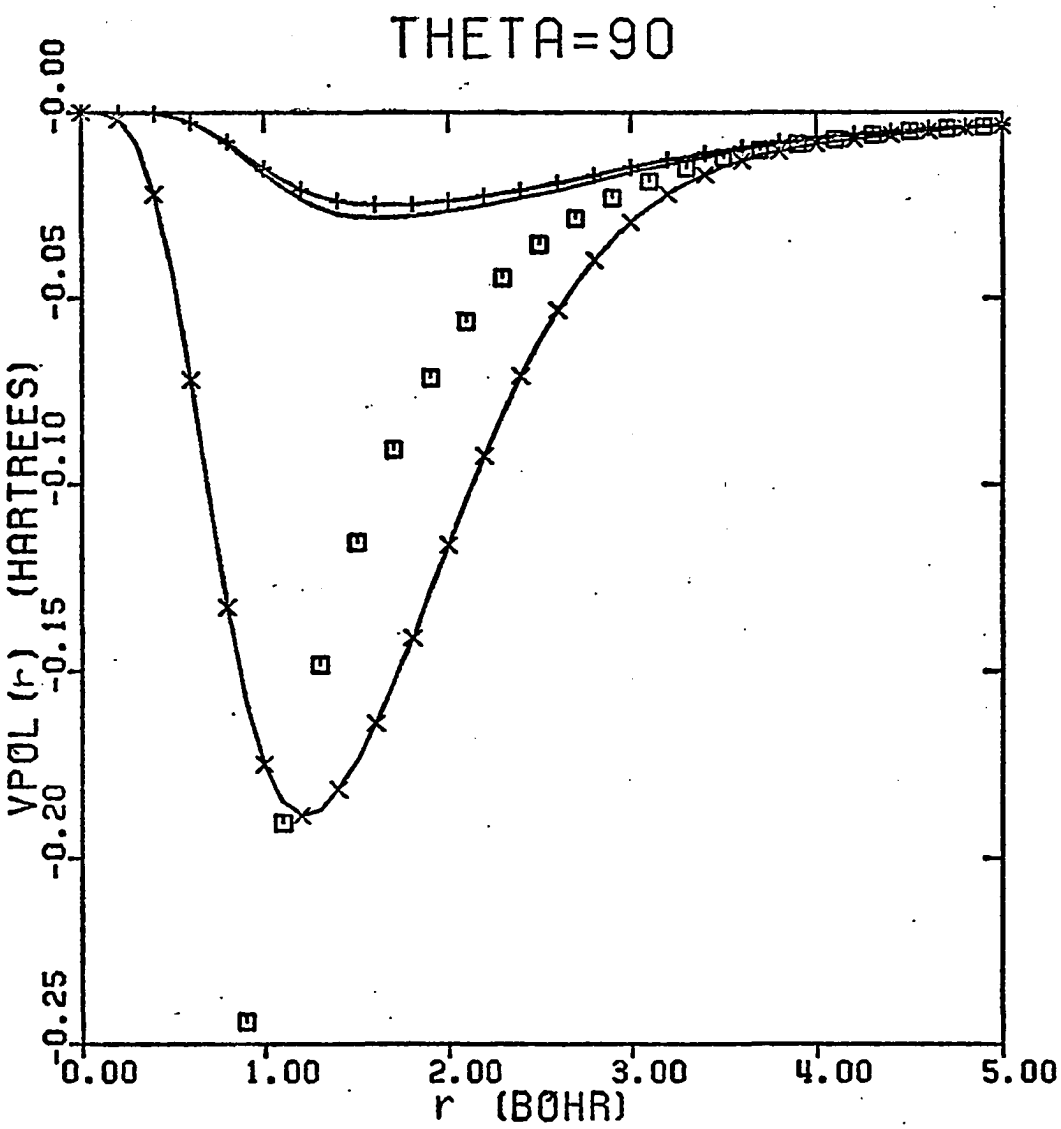


Figure 3. Polarization potentials obtained when the scattering electron is located along the x-axis ($\theta = \pi/2$); curves labelled as in Figure 2.

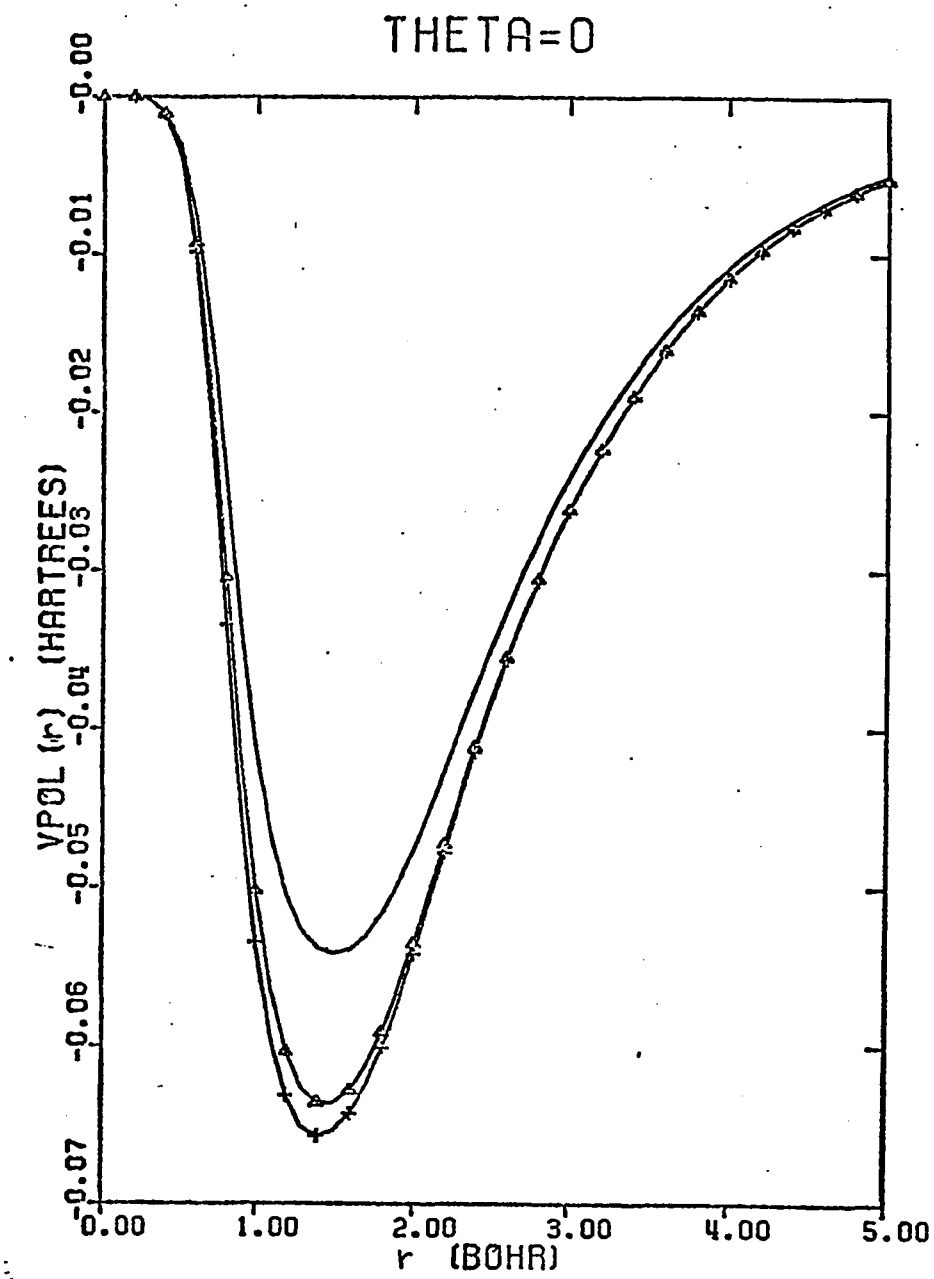


Figure 4. Polarization potentials for $\theta = 0$. The curves shown include the BTAD (—), BTADP2 (Δ), and BTADP23 (+) potentials.

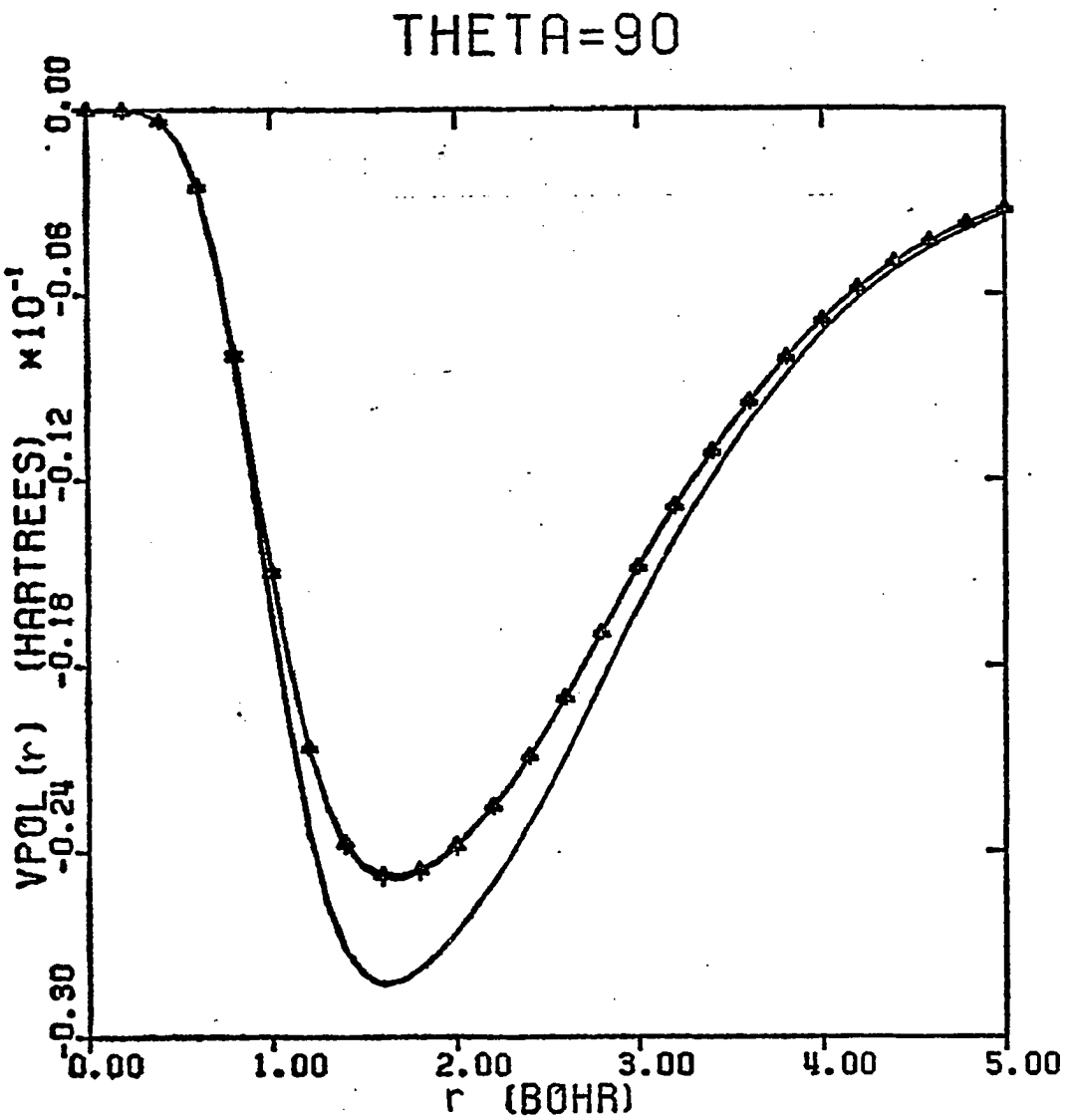


Figure 5. Polarization potentials for $\theta = \pi/2$; symbols as in Figure 4.

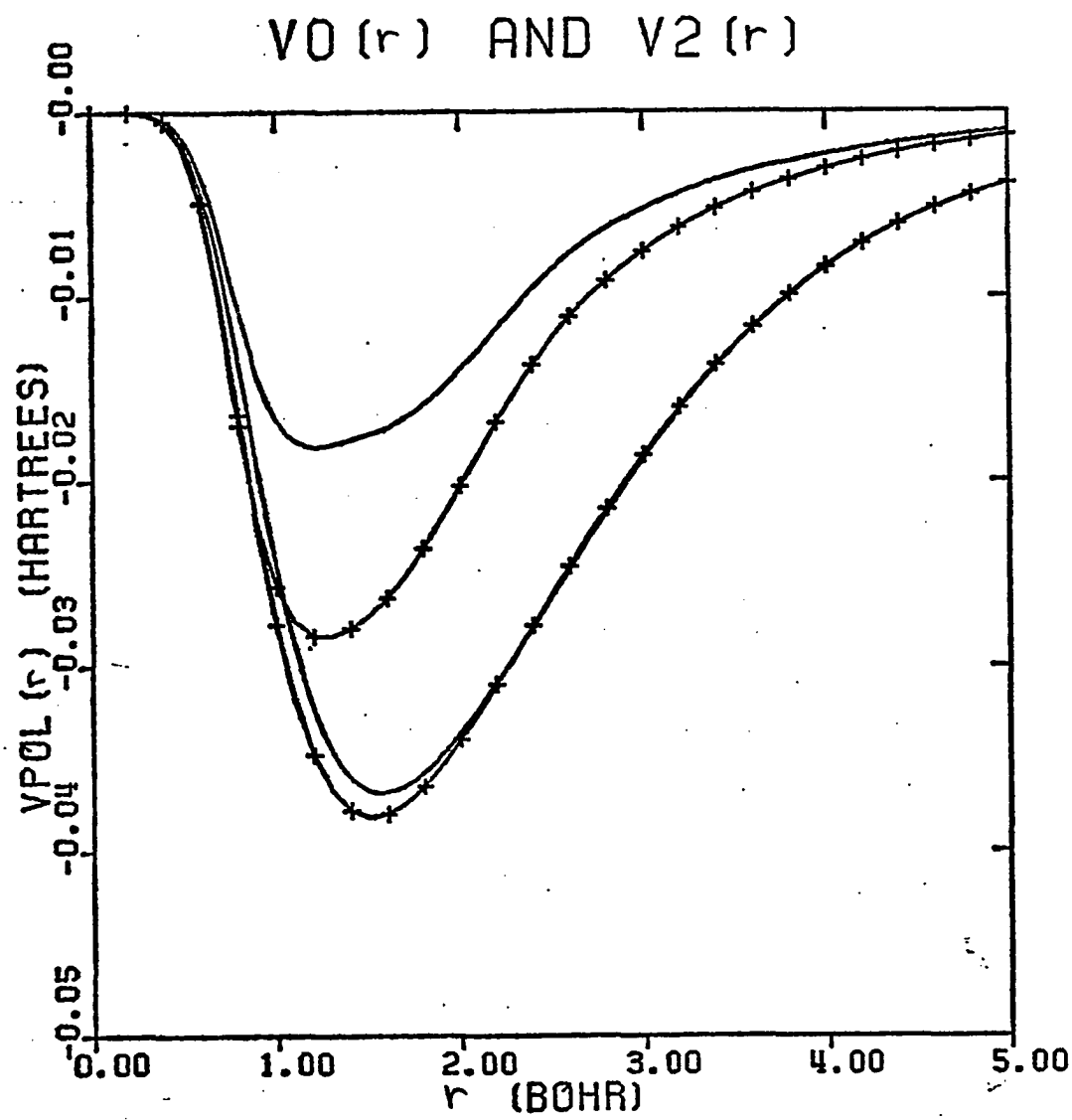


Figure 6. The spherical (lower curves) and non-spherical (upper curves) components of the BTAD (—) and BTADP23 (+) polarization potentials.

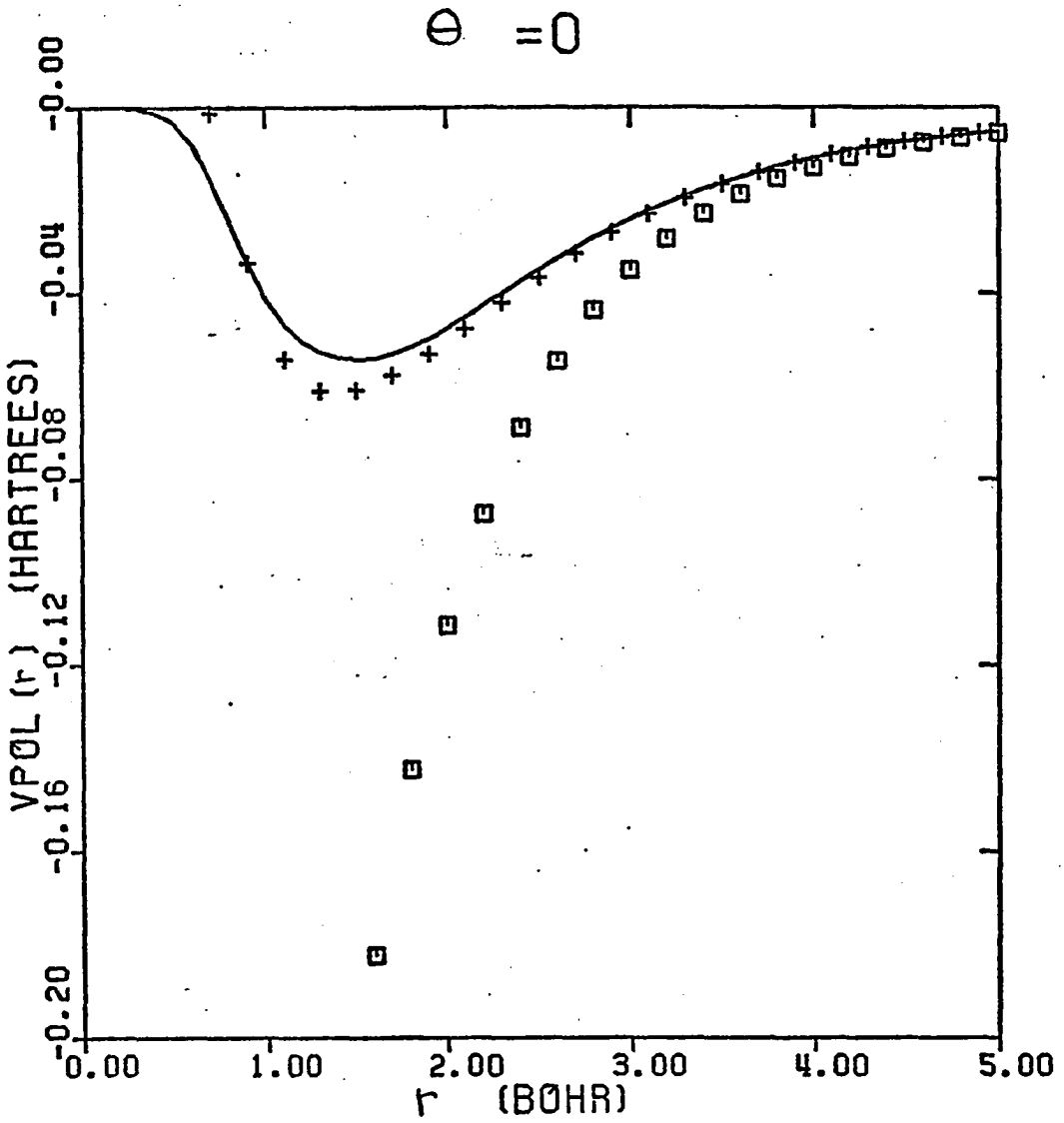


Figure 7. Polarization potentials for $\theta = 0$. The following potentials are presented: —, BTAD; +, SNPD; □, AD.

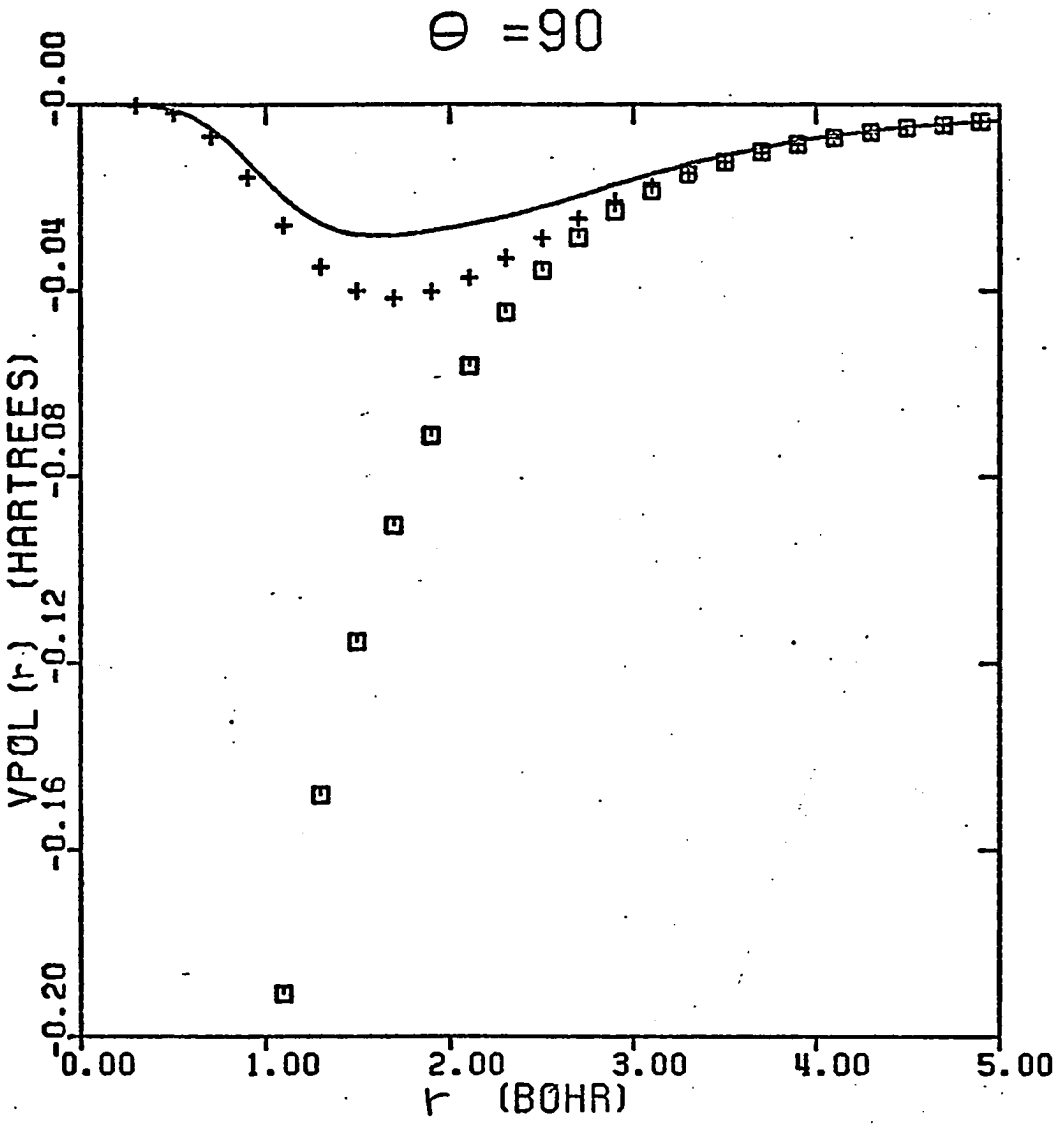


Figure 8. Polarization potentials for $\theta = \pi/2$; symbols as in Figure 7.

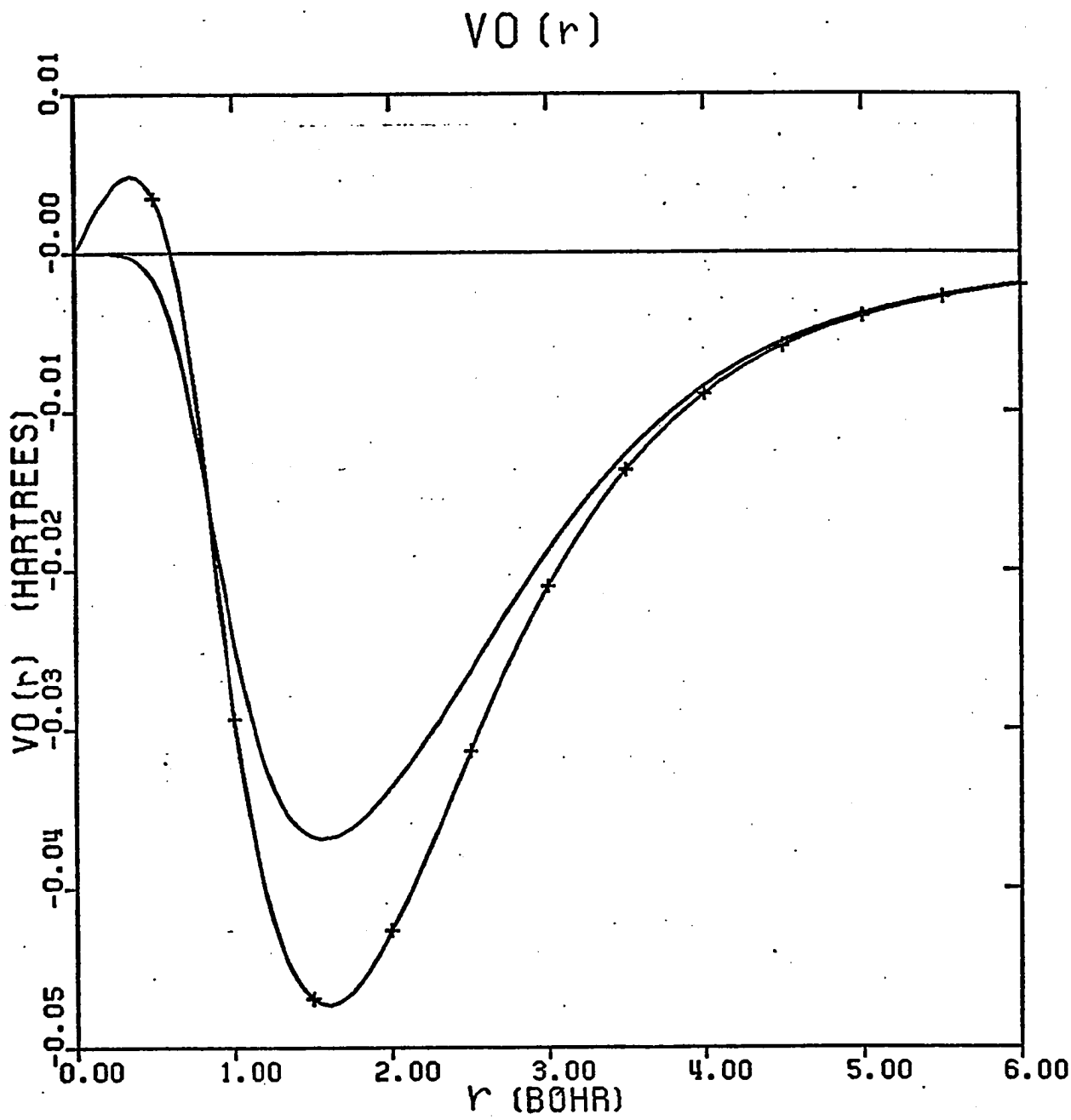


Figure 9. The spherical component of the BTAD (—) and SNPD (+) polarization potentials.

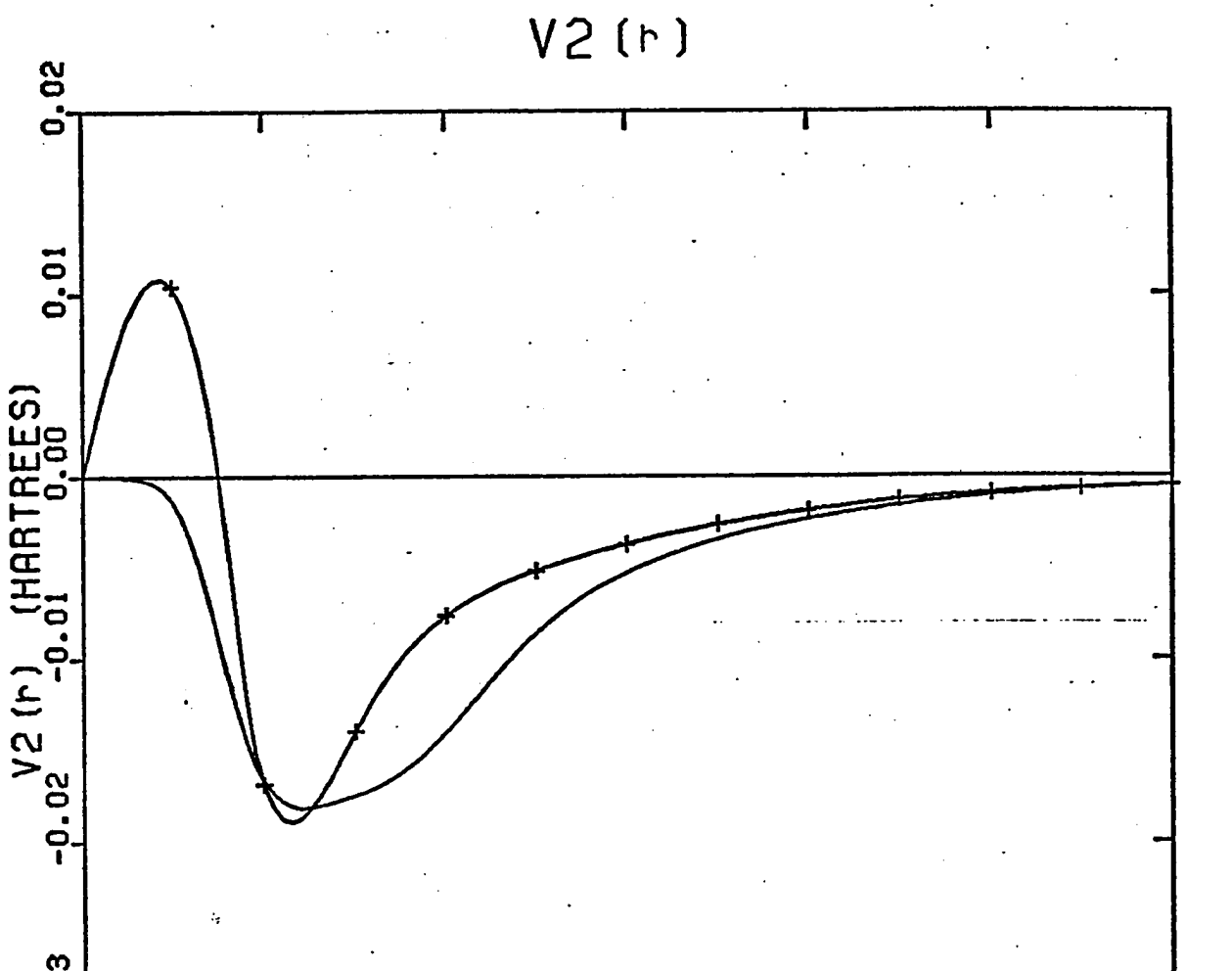


Figure 10. The non-spherical components of the BTAD (—) and SNPD (+) potentials.

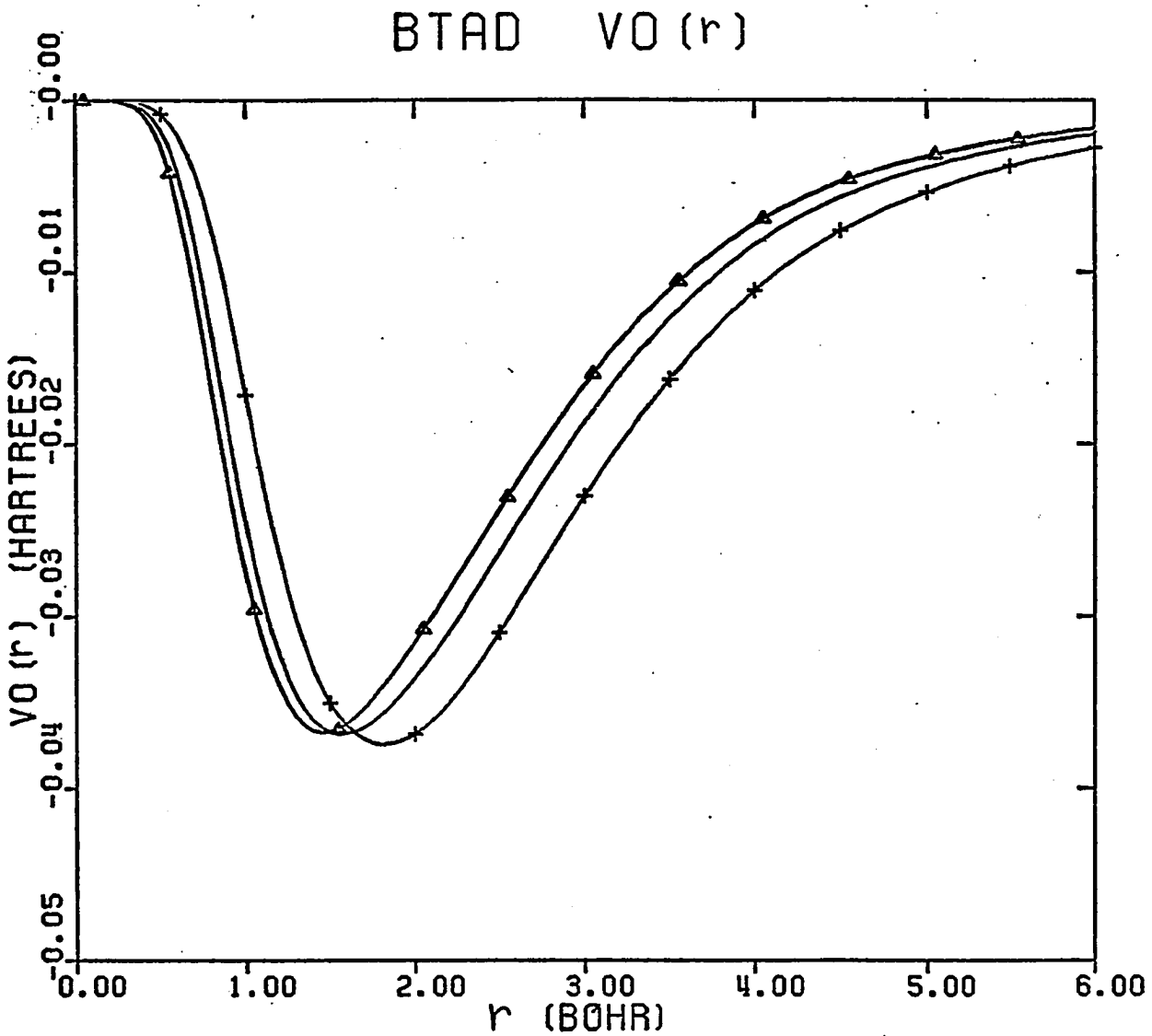


Figure 11. The spherical component of the BTAD polarization potential for the following internuclear separations: Δ , $R = 1.2\,a_0$; — , $R = 1.4\,a_0$; + , $R = 1.8\,a_0$.

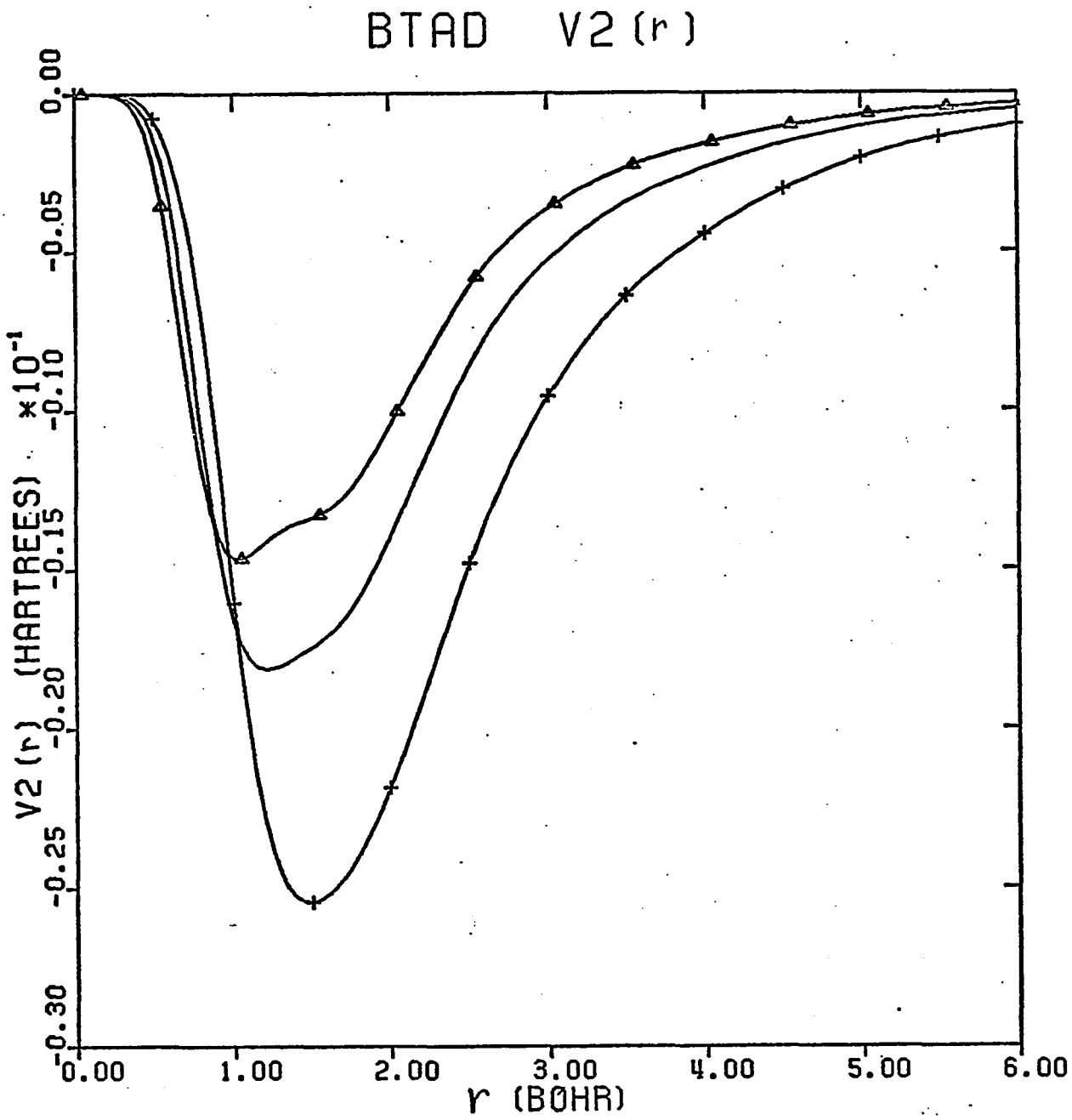


Figure 12. The non-spherical component of the BTAD polarization potential; curves labelled as in Figure 11.

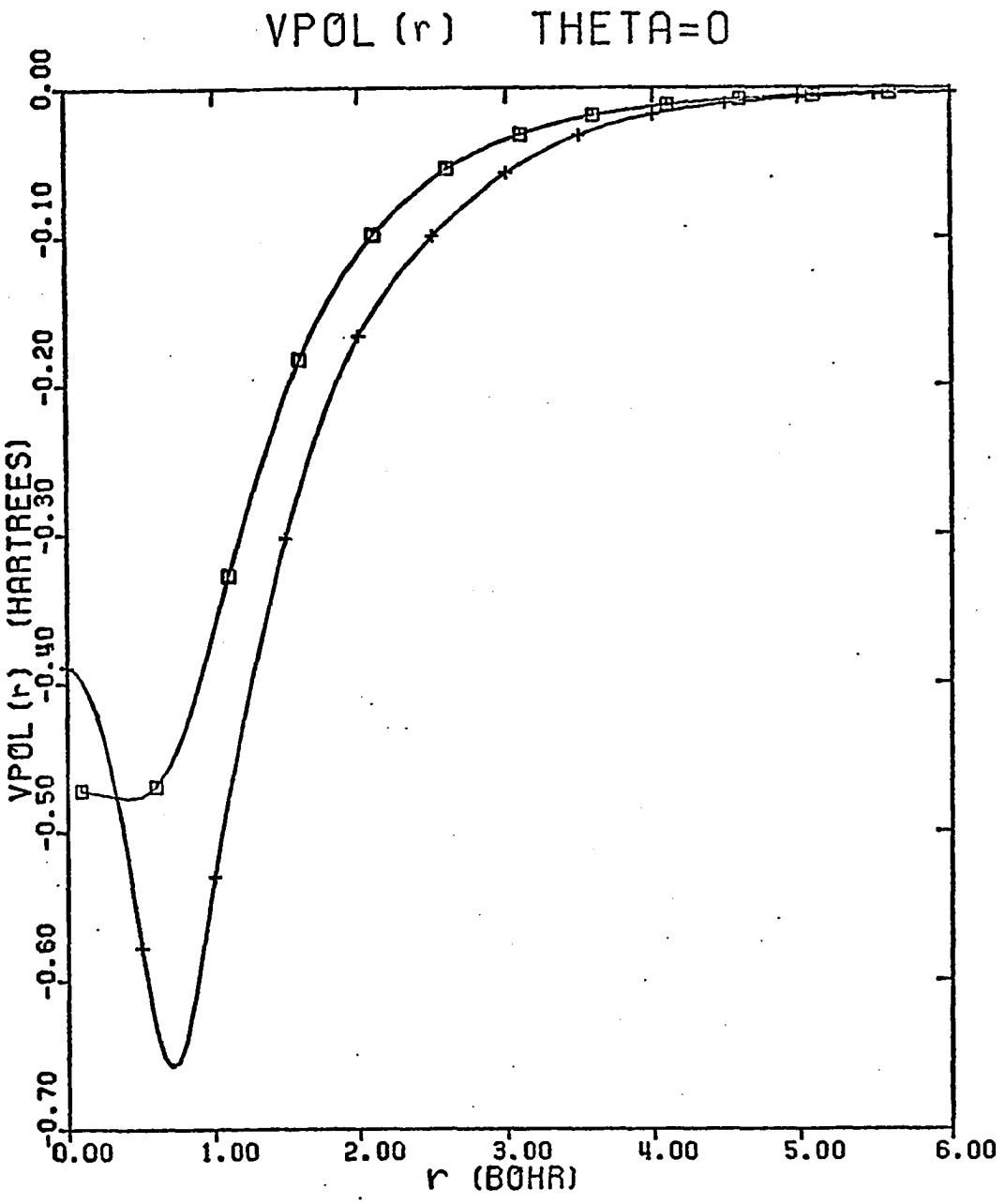


Figure 13. Adiabatic polarization potentials for $\theta = 0$. The curves presented are the AD (□) and ADPOS (+) potentials.

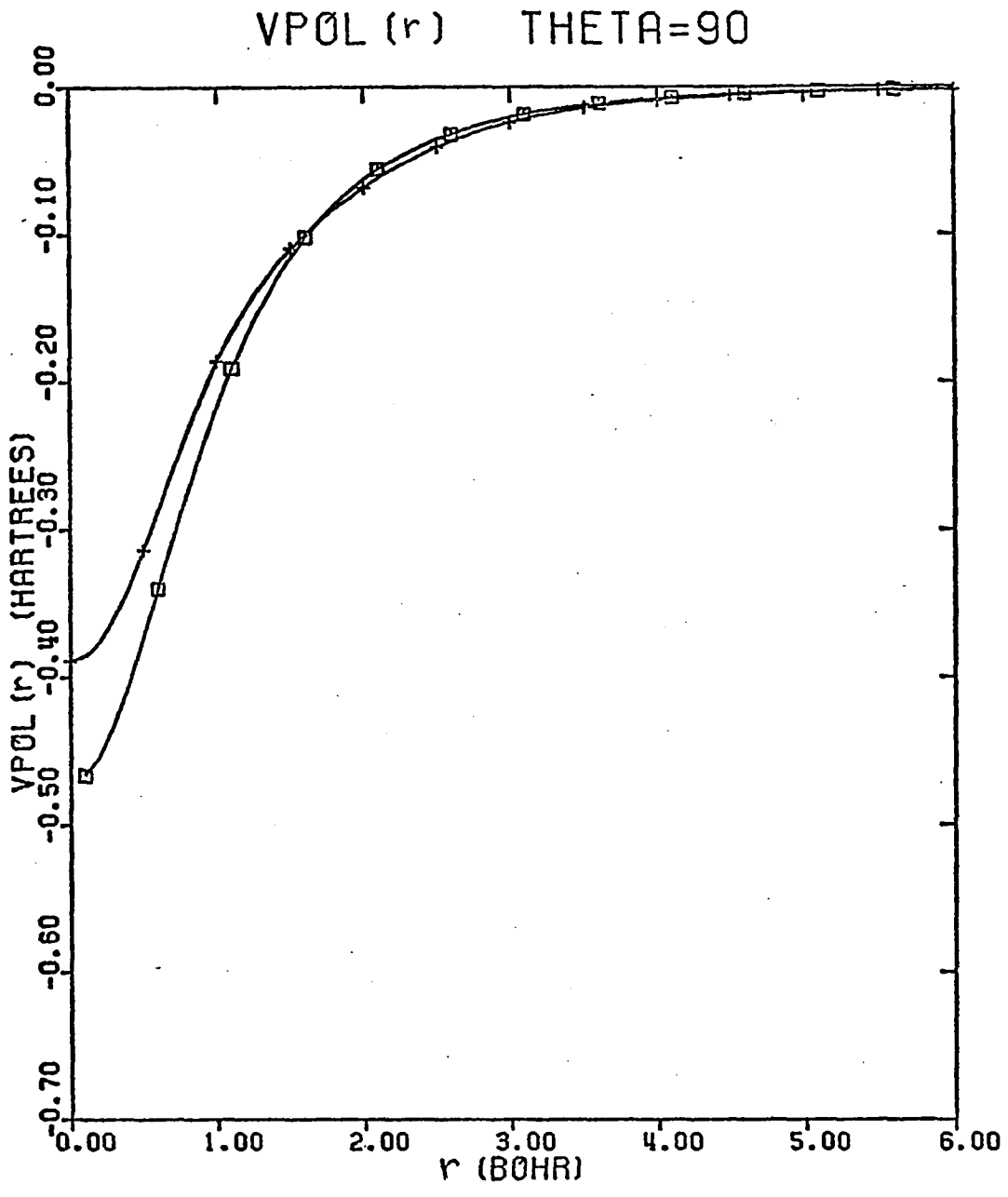


Figure 14. Adiabatic polarization potentials for $\theta = \pi/2$; the symbols used are the same as in Figure 13.

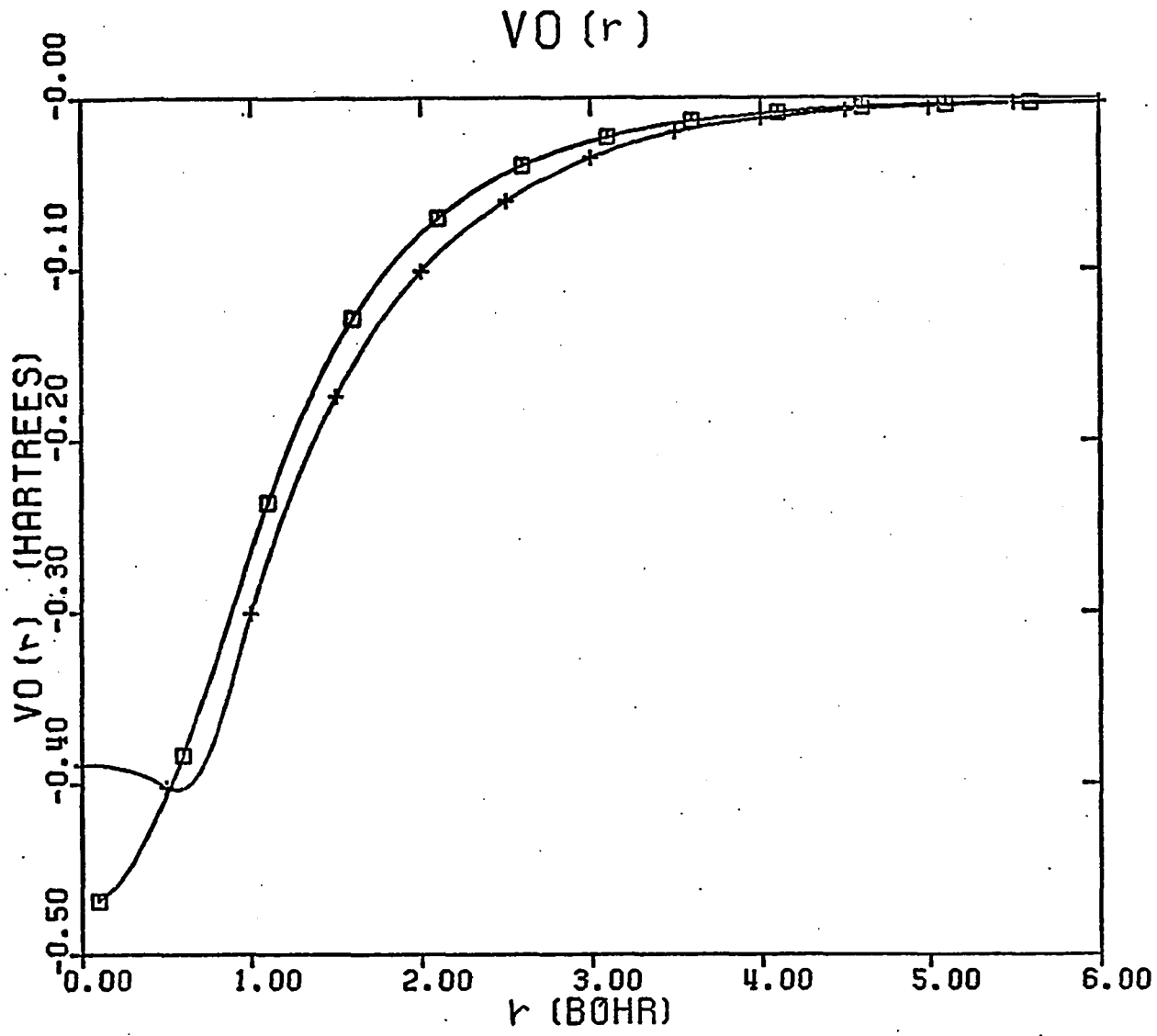


Figure 15. The spherical components of the AD (□) and ADPOS (+) polarization potential.

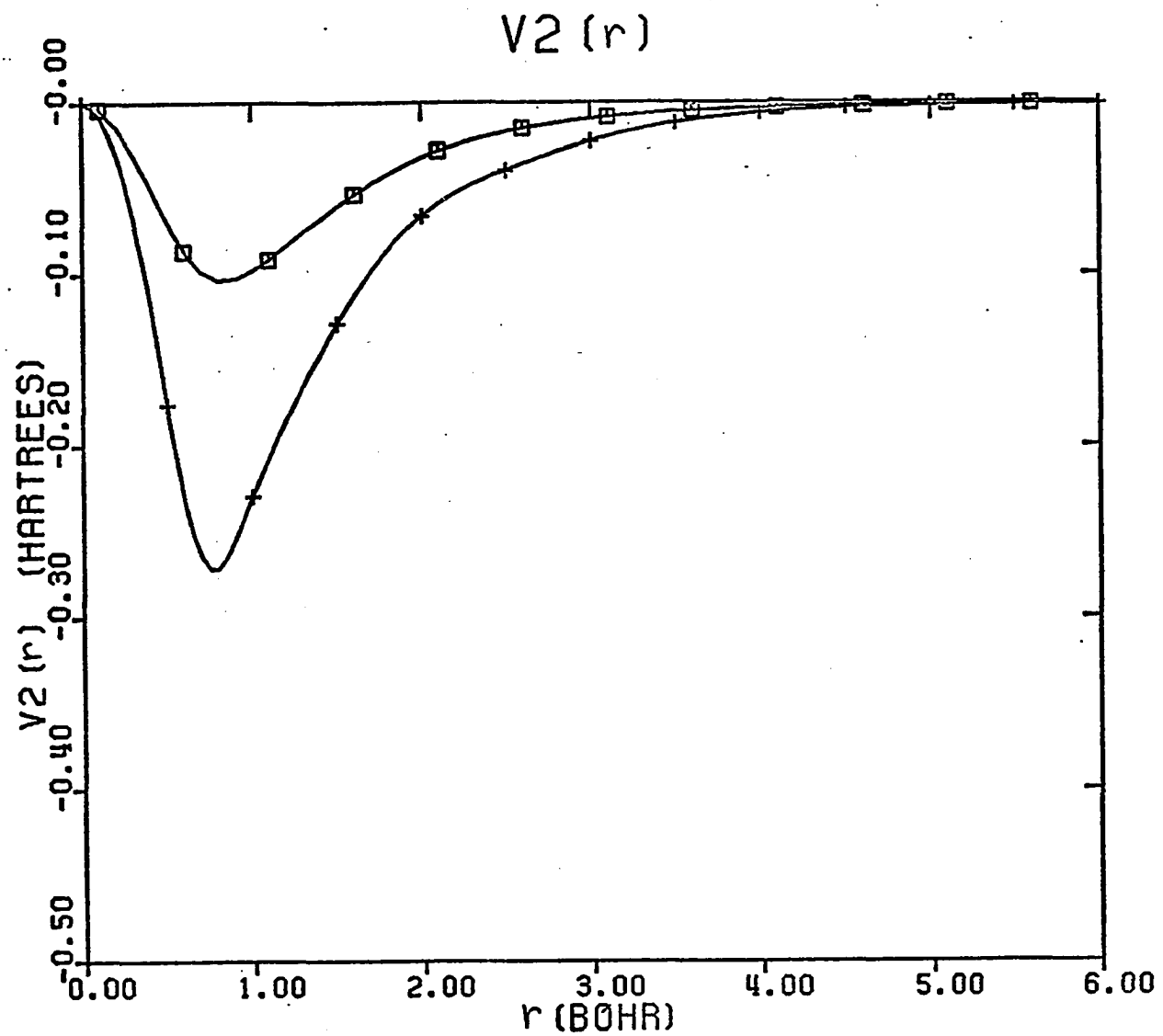


Figure 16. The non-spherical components of the AD (□) and ADPOS (+) polarization potentials.

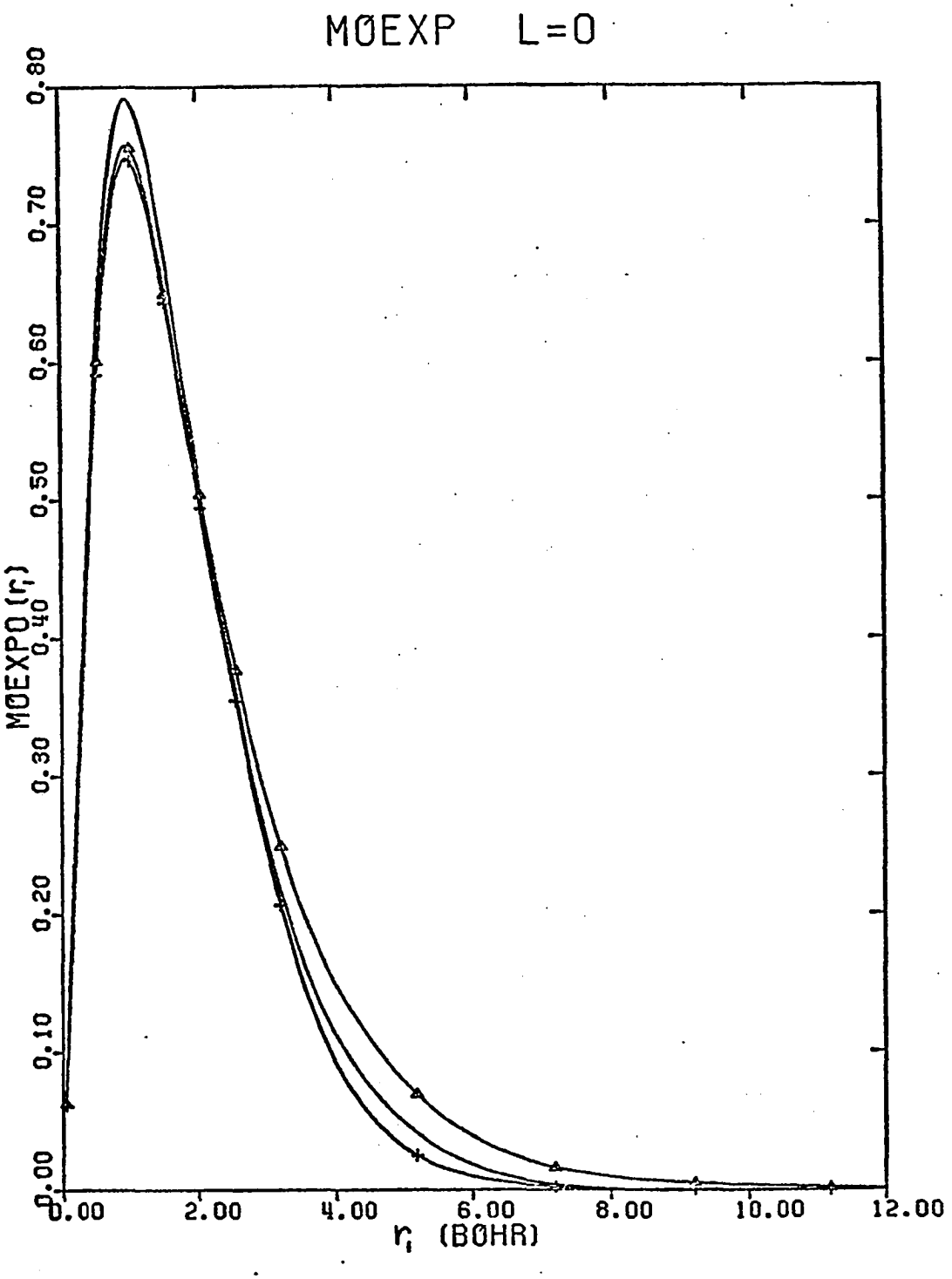


Figure 17. The $L = 0$ molecular orbital expansion (MOEXP) coefficients from a spherical harmonic ($Y_L^M(\hat{r}_1)$) expansion of the following orbitals: — , NEUTRAL; Δ , AD; $+$, ADPOS. For the AD(ADPOS) curves the scattering electron (positron) was located at $C_z = 2.5\, a_0$.

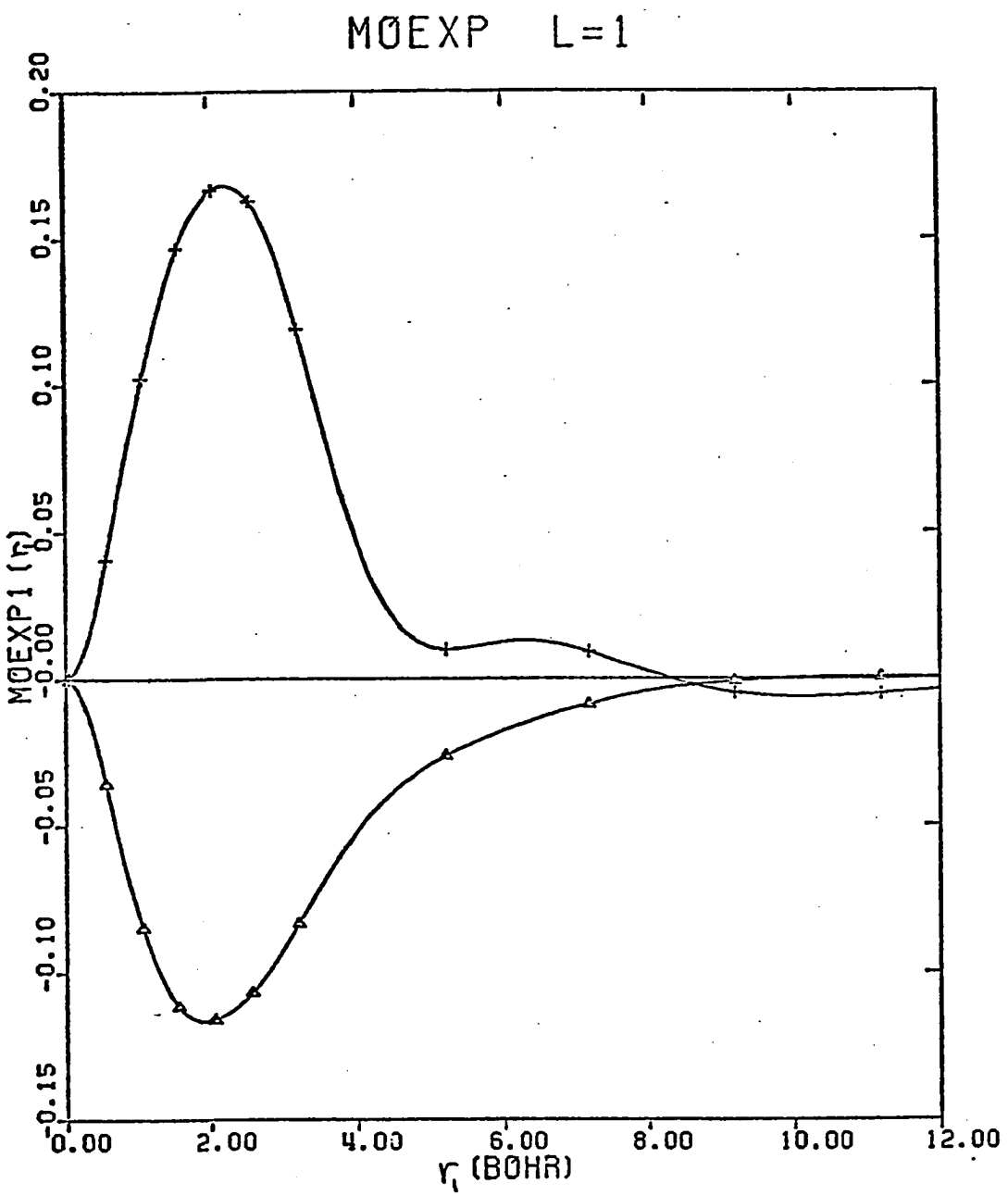


Figure 18. The $L = 1$ expansion coefficients; curves labelled as in Fig. 17.

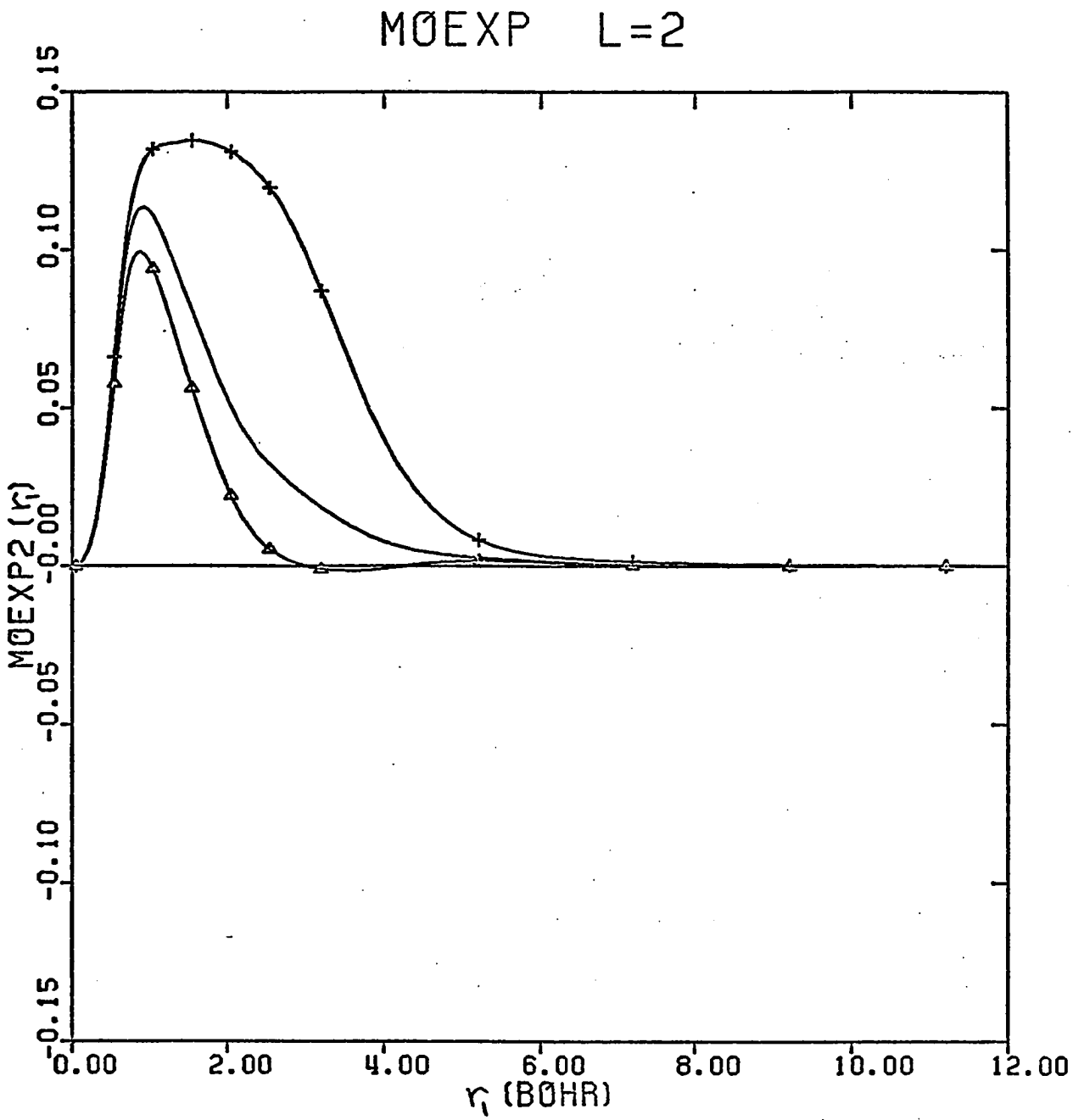


Figure 19. The $L = 2$ expansion coefficients; curves labelled as in Fig. 17.

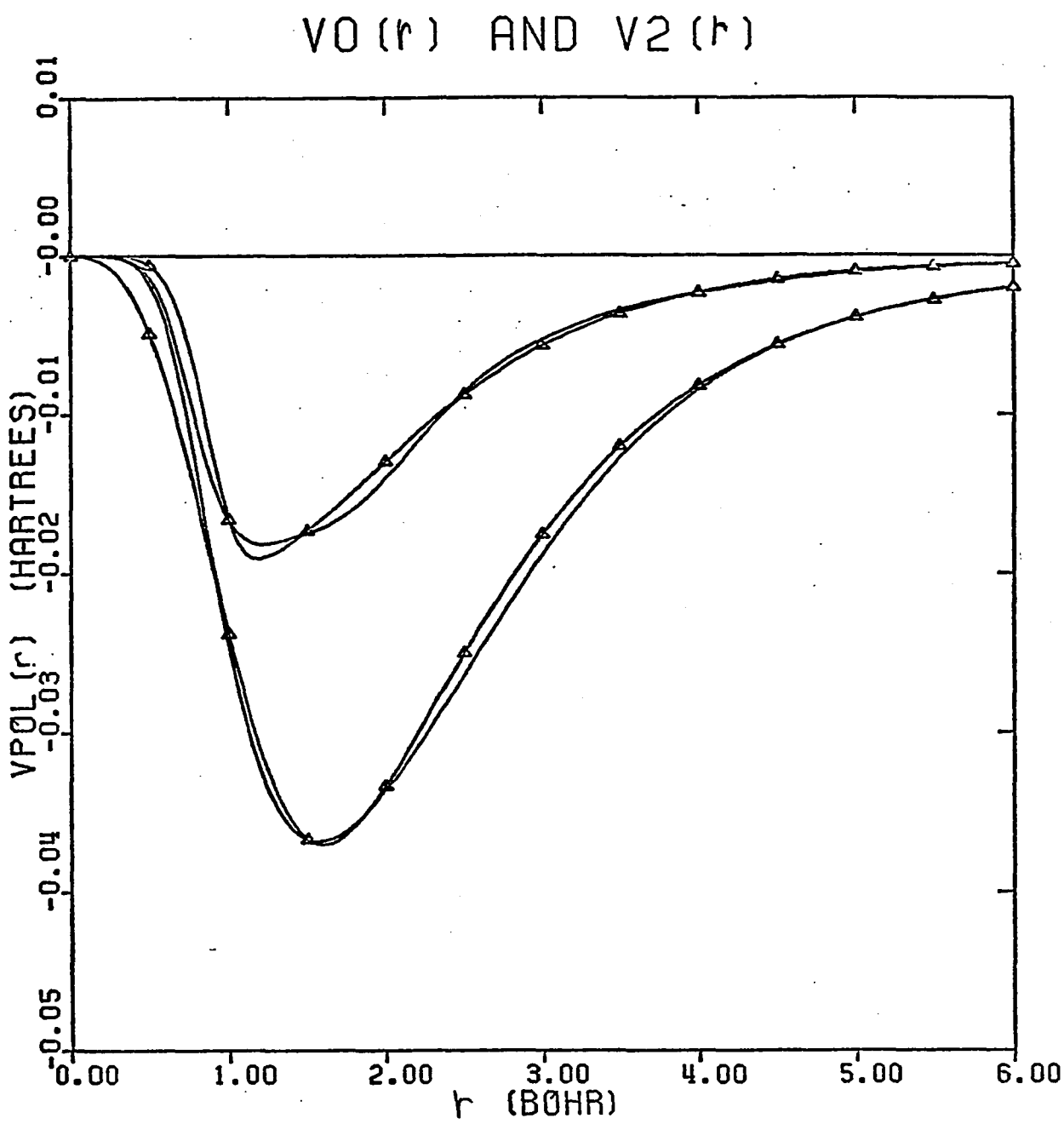


Figure 20. The spherical (lower curves) and non-spherical (upper curves) components of the BTAD (—) and ANALYTIC FIT (△) potentials.

CHAPTER IV

ELECTRON-H_2 SCATTERING RESULTS

In the previous chapter we presented various polarization potentials in which approximate nonadiabatic effects were included. In this chapter we will test our treatment of the polarization interaction in scattering calculations; our scattering results will be compared to experimental measurements and other theoretical values.

Two basic types of scattering calculation have been performed. The first type uses the body-frame fixed-nuclei (BF) formulation described in Chapter I. In the second type of calculation, the rotation of the nuclear framework (for fixed R) is explicitly taken into account by a laboratory-frame close-coupling (LF) formulation.[3,45] A numerical procedure based on an integral-equations algorithm[46,47] is used to solve the relevant scattering equations in both formulations.

To determine cross sections for electron-H_2 collisions, we calculated an *ab initio* static potential[4,5] using the near-Hartree-Fock H_2 $X^1\Sigma_g^+$ wavefunction of Feldt and Morrison.[48] The Feldt and Morrison wavefunction is derived from the unaugmented [5S2P/3S2P] set† of Gaussian basis

†The exponents for the p-type functions in this set are larger by a factor of 2 than the ones in the basis set used for the polarization potential.

functions that we started with for the polarization calculation (*cf.*, section 3.5). This same H_2 wavefunction was used to incorporate approximate exchange effects via the tuned free-electron-gas model-exchange potential (see Appendix I and references therein); a value of 2.27 eV was determined for the "tuned ionization potential".

The static and exchange potentials are expanded in a Legendre polynomial series, *viz.*,

$$V^{st(ex)}(\vec{r}) = \sum_{\lambda=0}^{\lambda_{max}} v_\lambda^{st(ex)}(r) P_\lambda(\cos\theta) \tag{4.1}$$

with $\lambda_{max} = 8$. Thus, the static model exchange polarization (SMEP) potential can be written as

$$V(\vec{r}) = V^{st}(\vec{r}) + V^{ex}(\vec{r}) + V^{pol}(\vec{r}) \tag{4.2}$$

where V^{st} and V^{ex} are given by Eq.(4.1) and V^{pol} is given by Eq.(3.50).

In the BF formulation we can perform scattering calculations in which exchange effects are included exactly.[8] However, we can not currently perform exact static-exchange-polarization (ESEP) calculations in the LF formulation. For BF calculations we include five channels per symmetry for the Σ_g, Σ_u, Π_g, Π_u, and Δ_g symmetries, but only three channels for the Δ_u symmetry [see Eq.(1.12)]. The total angular momentum $\vec{J}$ in the LF formulation is restricted to $J \leq 4$, and we retain four rotor-states in the close-coupling expansion.

Using the different formulations and interaction potentials described above, we have calculated total (elastic plus rotational-excitation) cross sections. In order to keep the results of the various treatments from getting too

confused, we shall establish some more nomenclature. The name of a given calculation will indicate which of the two scattering formulations was employed, whether exact or model exchange was used, and which of the various polarization potentials was incorporated; *e.g.*, SMEP cross sections calculated in the LF formulation using the BTAD polarization potential are referred to as LFSMEP(BTAD) results.

In Figure 21 we show BFSMEP(BTAD), BFSMEP(BTADP2), and BFSMEP(BTADP23) integrated total cross sections. We find agreement between the BFSMEP total cross sections and the corresponding LFSMEP results (not shown) to within better than 1% for the lowest scattering energies considered ($E \approx 0.020$eV) and to within much better than 1% for larger energies. Since the scattering results obtained with the different polarization potentials in Figure 21 are so similar,[†] we consider only the BTAD potential for further scattering calculations.

Total integrated cross sections for very low-energy ($E \leq 0.5$eV) collisions are presented in Figure 22. Here, we compare our LFSMEP(BTAD)

[†]The LFSMEP(BTAD) and LFSMEP(BTADP23) integrated rotational-excitation cross sections do not agree as well as the total cross sections in Figure 21. Also, scattering results obtained with the BTA potential are so thunderously bad that we do not present them here.

and BFESEP(BTAD) results to the measured values of Ferch *et al.* [49] and the LFESEP(SNP) cross sections of Henry and Lane.[50] A modified-effective-range theory[51] fit to our LFSMEP(BTAD) total cross sections (which are globally converged to better than 1%) produces a scattering length $A = 1.26a_0$. This value is in excellent agreement with that reported by Chang,[52] who obtained $A = 1.27 \pm 0.01a_0$ by fitting the experimentally-determined results of Crompton *et al.* [53] and those of Ferch *et al.* [49] Cross sections for higher energies are presented in Figures 23 and 24, where we compare our results with the measured values of Golden *et al.* ,[54] Dalba *et al.* ,[55] and Jones.[56] Also shown in Figure 23 are the following theoretical cross sections: the LFESEP(SNP) results of Henry and Lane;[50] the BFESEP(SNPD) results of Hara;[57] and the BFESEP(DPS)† results of Klonover and Kaldor.[58] All of the theoretical results presented in these figures were calculated with a fixed internuclear separation; Klonover and Kaldor[59] have shown that explicit integration over R can lead to a small increase in the total cross section and a significant increase in the rotational-excitation cross section. The disparity between our LFSMEP(BTAD) and BFESEP(BTAD) curves in Figure 24 is almost entirely due to the different treatments of the exchange interaction.

In Table 7 we compare our integrated rotational-excitation cross sections for $j = 0$ to $j' = 2$ with those of Henry and Lane[50] and with the

---

†Klonover and Kaldor[58] incorporated nonadiabatic polarization effects via a diagrammatic perturbation series (DPS).

swarm measurements of Crompton *et al.* [53] Additional cross sections for this excitation are shown in Figure 25. The BFESEP(BTAD) rotational-excitation cross sections were calculated in the scaled adiabatic-nuclear-rotation (SANR) approximation of Feldt and Morrison.[60] This scaling procedure corrects most of the known deficiencies[48] in the results obtained from adiabatic-nuclear-rotation theory. Rotational-excitation results for $j = 1$ to $j' = 3$ are shown in Figure 26, where our results are compared with those of Henry and Lane,[50] Hara,[61] and the experimentally-determined values of Linder and Schmidt.[62]

Finally, in Figures 27–30 we present a comparison of our BFESEP(BTAD) results with the BFESEP(OPT)† calculations of Schneider and Collins.[63] In their preliminary study, these authors have considered only the Σ_g and Σ_u symmetries for the electron-H_2 system. Given the difference in the way polarization (closed-channel) effects are included in these calculations, the observed agreement between our results and those of Schneider and Collins is particularly gratifying.

---

†Schneider and Collins have included (in principle) all closed-channel effects via an approximate optical (OPT) potential.

Table 7

Integrated cross sections (in 10^{-16}cm^2) for the $j = 0$ to $j' = 2$ transition in e-H_2 scattering.

Energy (eV)	CGM[a]	HL[b]	LFSMEP(BTAD)
0.05	0.027	0.024	0.023
0.07	0.053	0.052	0.048
0.10	0.074	0.074	0.069
0.15	0.099	——	0.096
0.20	0.120	0.119	0.120
0.30	0.160	0.161	0.169
0.40	0.210	——	0.222
0.50	0.263	0.254	0.280

[a]Crompton *et al.* [53]

[b]Henry and Lane[50]

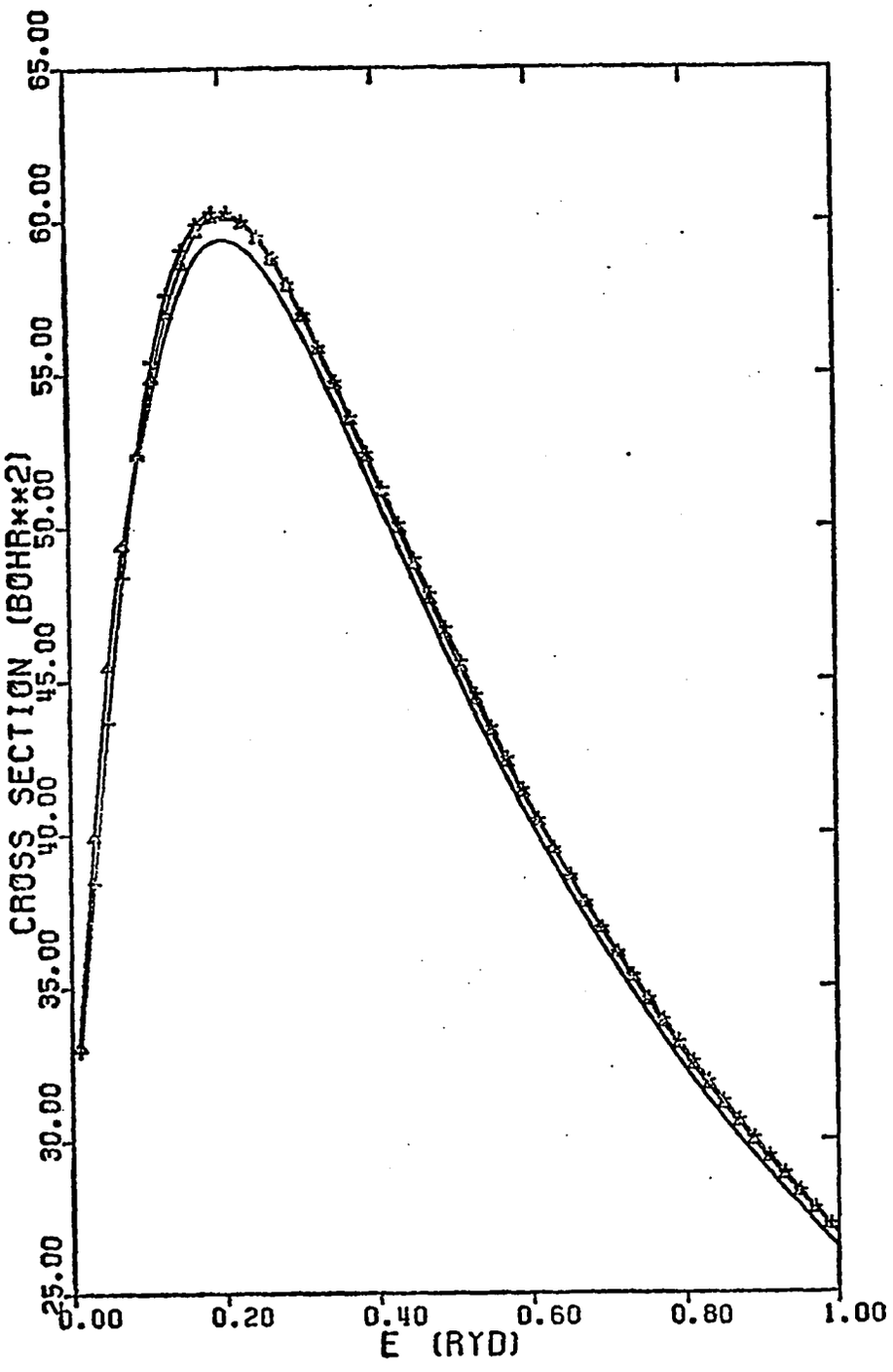


Figure 21. Total (elastic plus rotational-excitation) integrated cross sections for the following: — , BFSMEP(BTAD); △ , BFSMEP(BTADP2); + , BFSMEP(BTADP23).

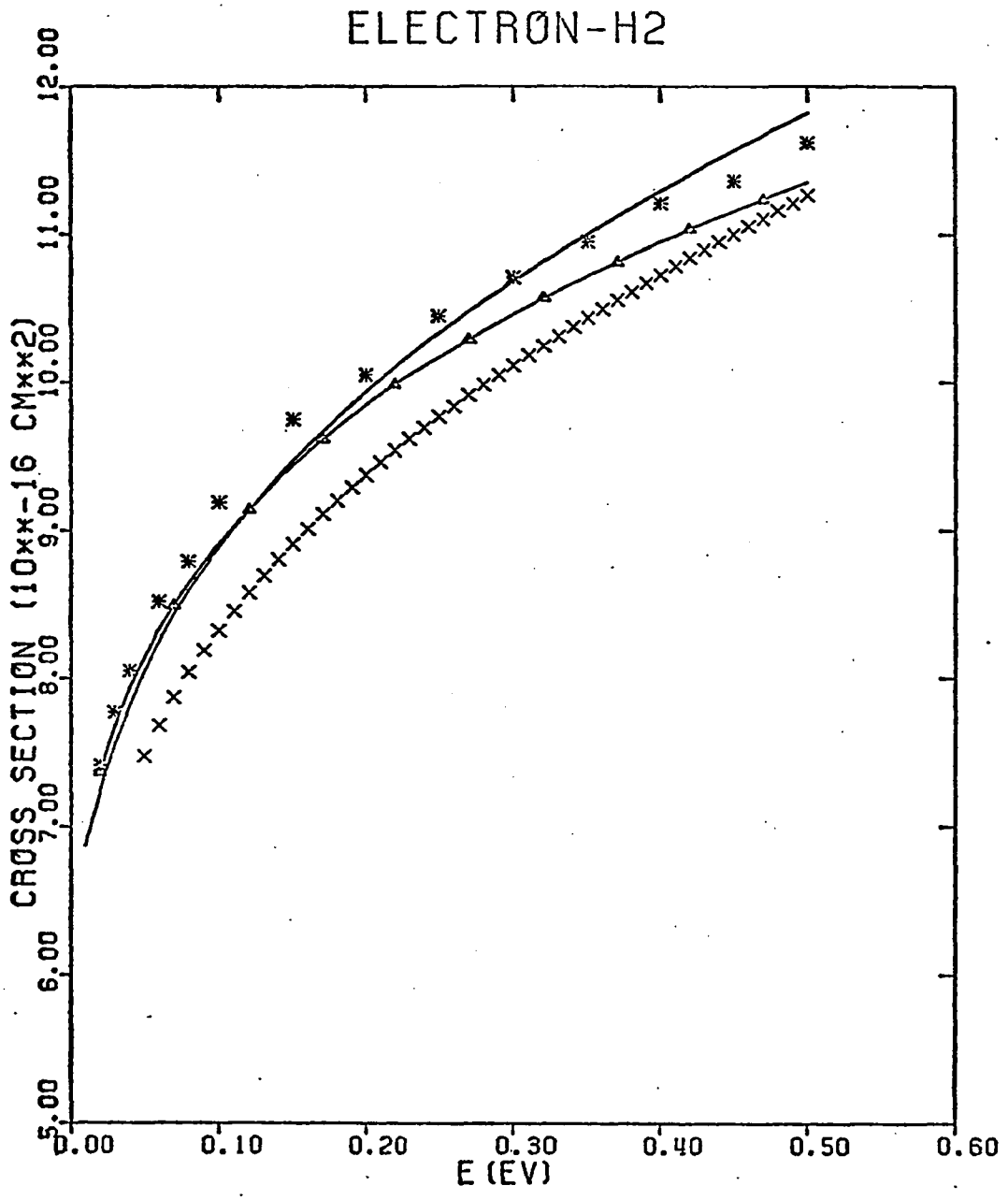


Figure 22. Total integrated cross sections for very low-energy electron-H_2 scattering: — , LFSMEP(BTAD); △ , BFESEP(BTAD); ✳ , the measured values of Ferch *et al.*;[49] × , theoretical results of Henry and Lane.[50]

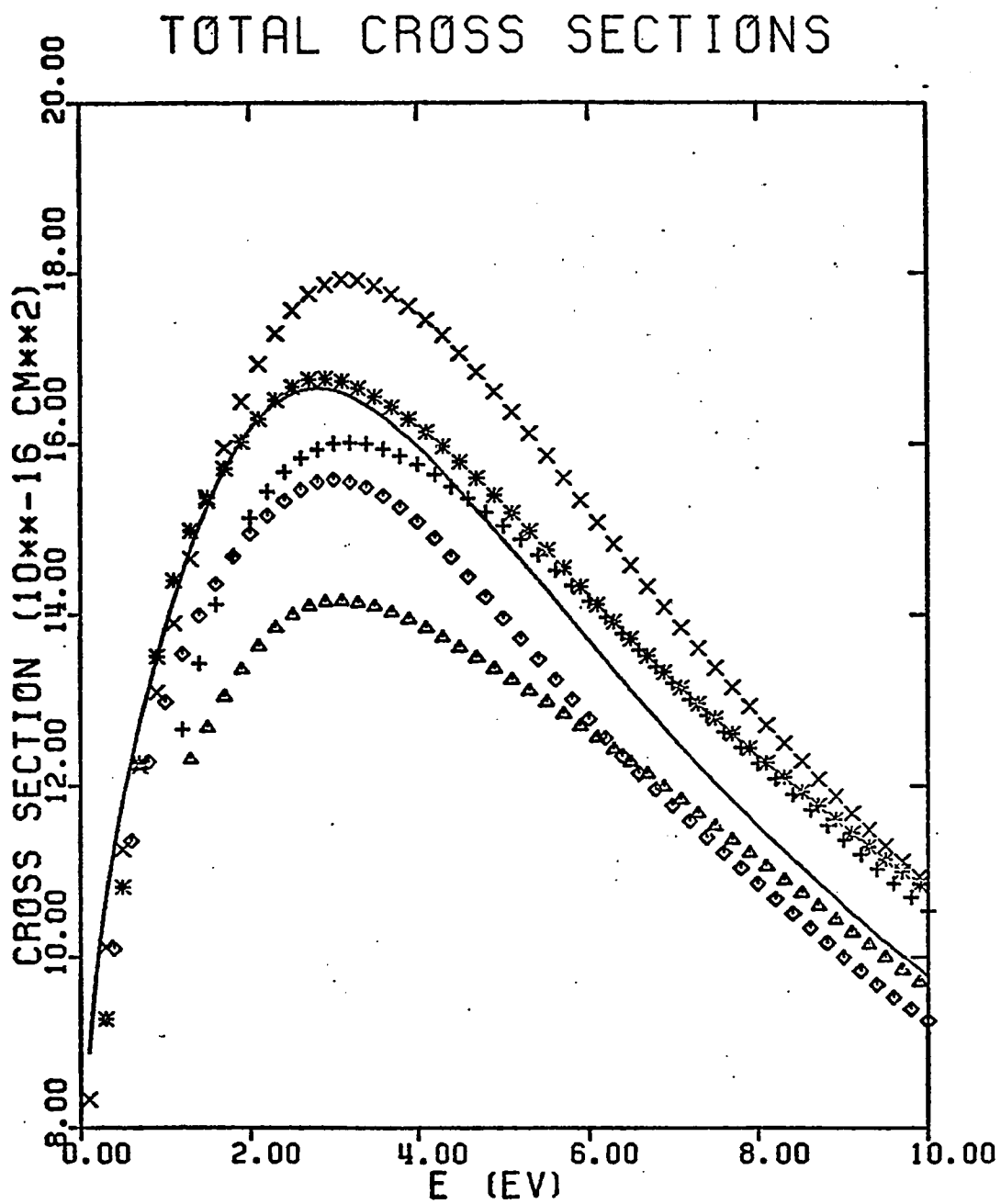


Figure 23. Total integrated cross sections for e-H_2 scattering. Theoretical curves presented: —, LFSMEP(BTAD); × , Henry and Lane;[50] + , Hara;[57] △ , Klonover and Kaldor.[58] Experimental curves shown: ✳ , Dalba *et al.*;[55] ◇ , Golden *et al.*[54]

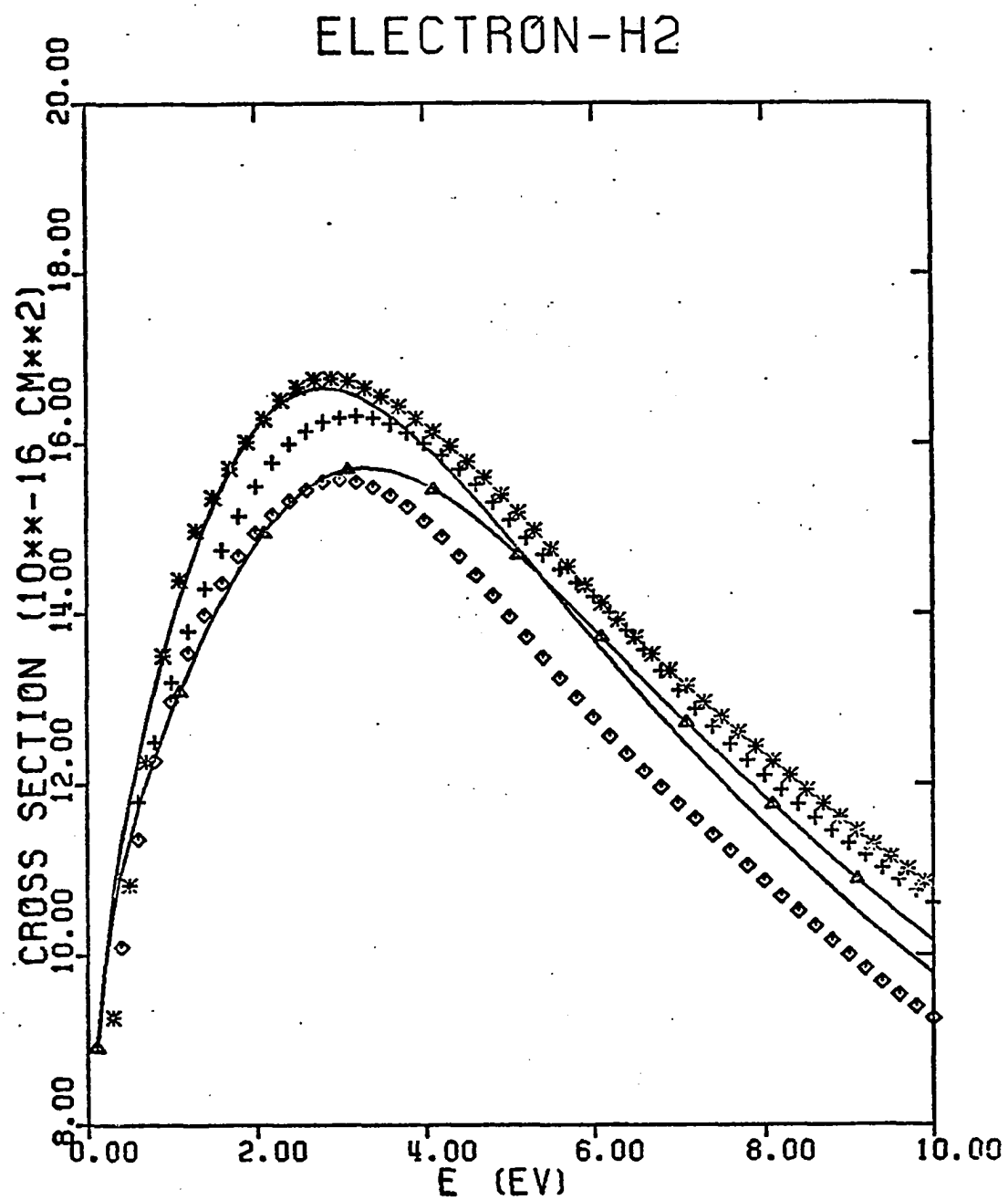


Figure 24. Total integrated cross sections for e-H_2 collisions. Theoretical curves presented: —, LFSMEP(BTAD); △, BFESEP(BTAD). Experimental curves shown: ✳, Dalba *et al.*;[55] ◇, Golden *et al.*;[54] +, Jones.[56]

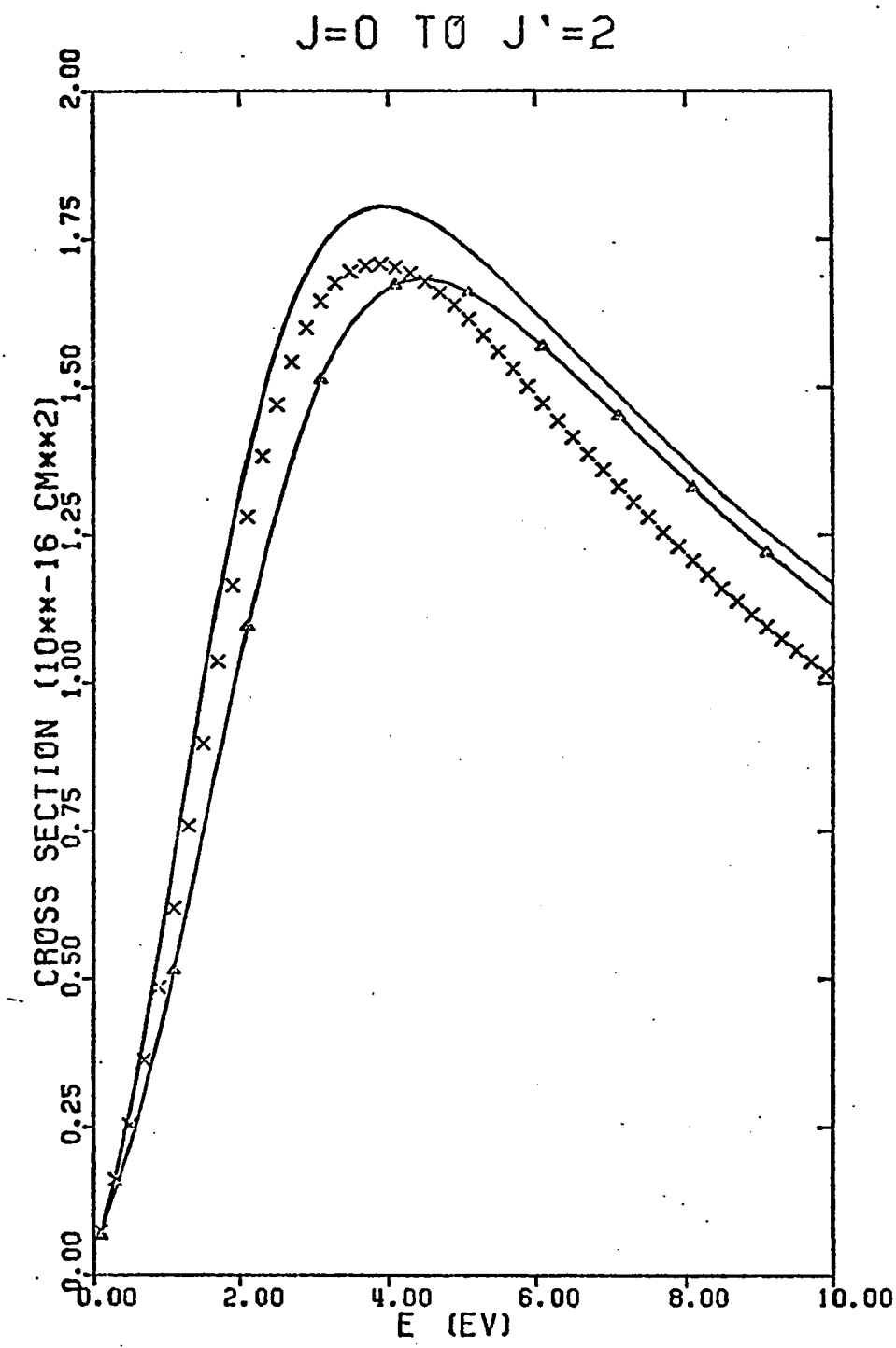


Figure 25. Integrated cross sections for the $j = 0$ to $j' = 2$ transition in electron-H_2 scattering: —, LFSMEP(BTAD); △, BFESEP(BTAD); ×, Henry and Lane.[50]

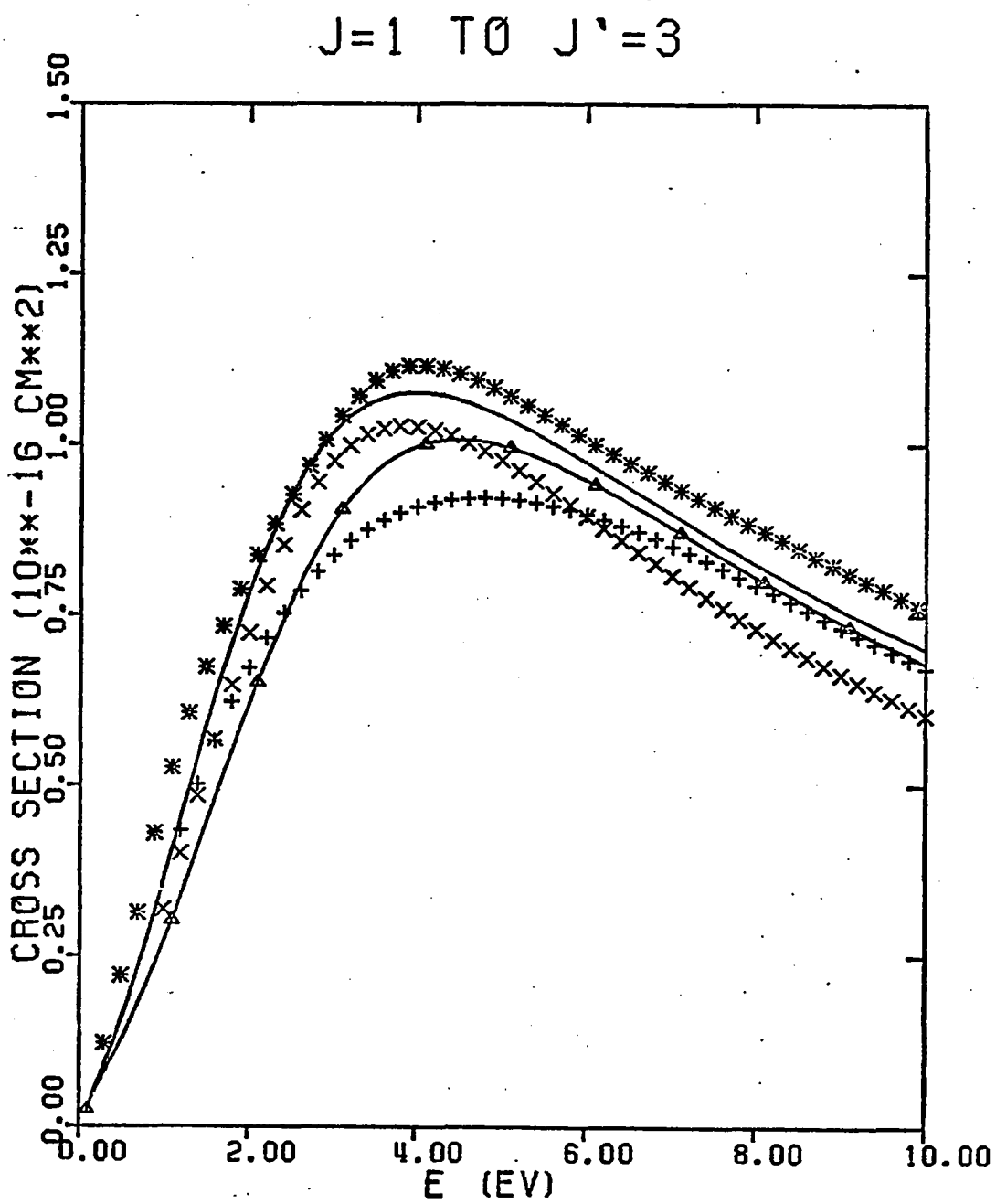


Figure 26. Integrated cross sections for the $j = 1$ to $j' = 3$ transition in electron-H_2 scattering: —, LFSMEP(BTAD); △, BFESEP(BTAD); ×, Henry and Lane;[50] +, Hara;[61] ✳, the measurements of Linder and Schmidt.[62]

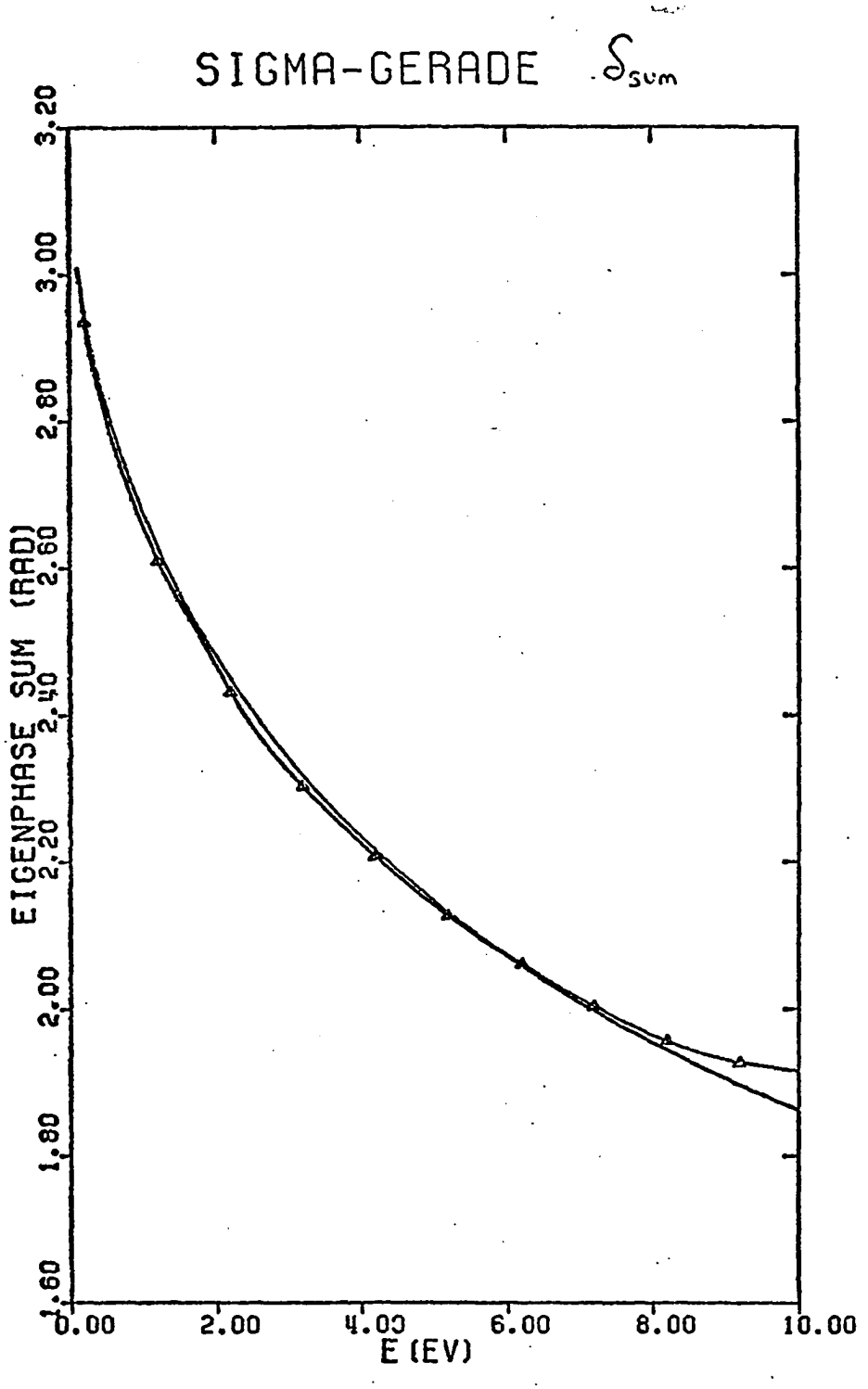


Figure 27. Eigenphase sums for the Σ_g symmetry: —, BFESEP(BTAD); Δ , Schneider and Collins.[63]

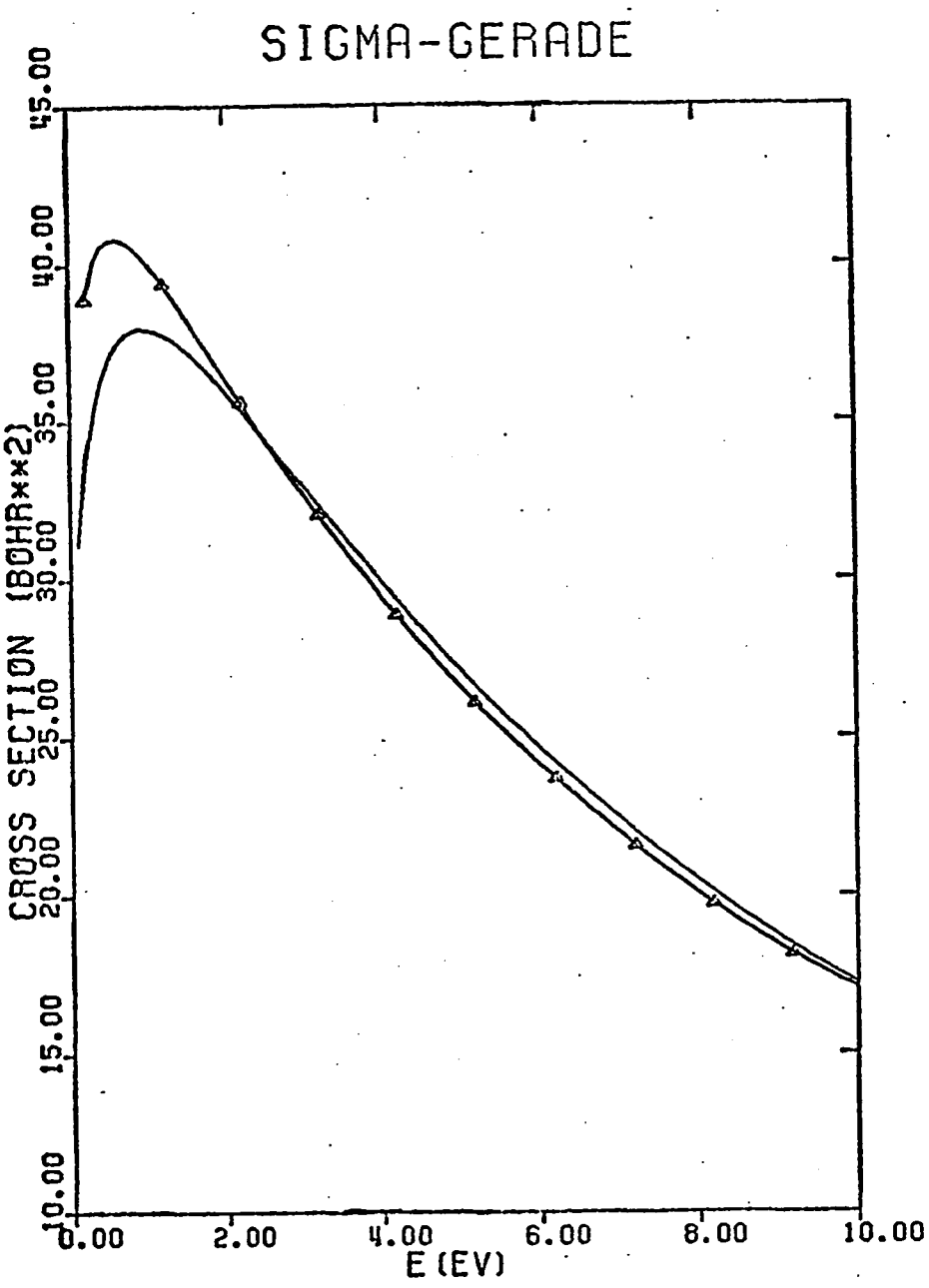


Figure 28. Integrated cross sections for the Σ_g symmetry; symbols as in Figure 27.

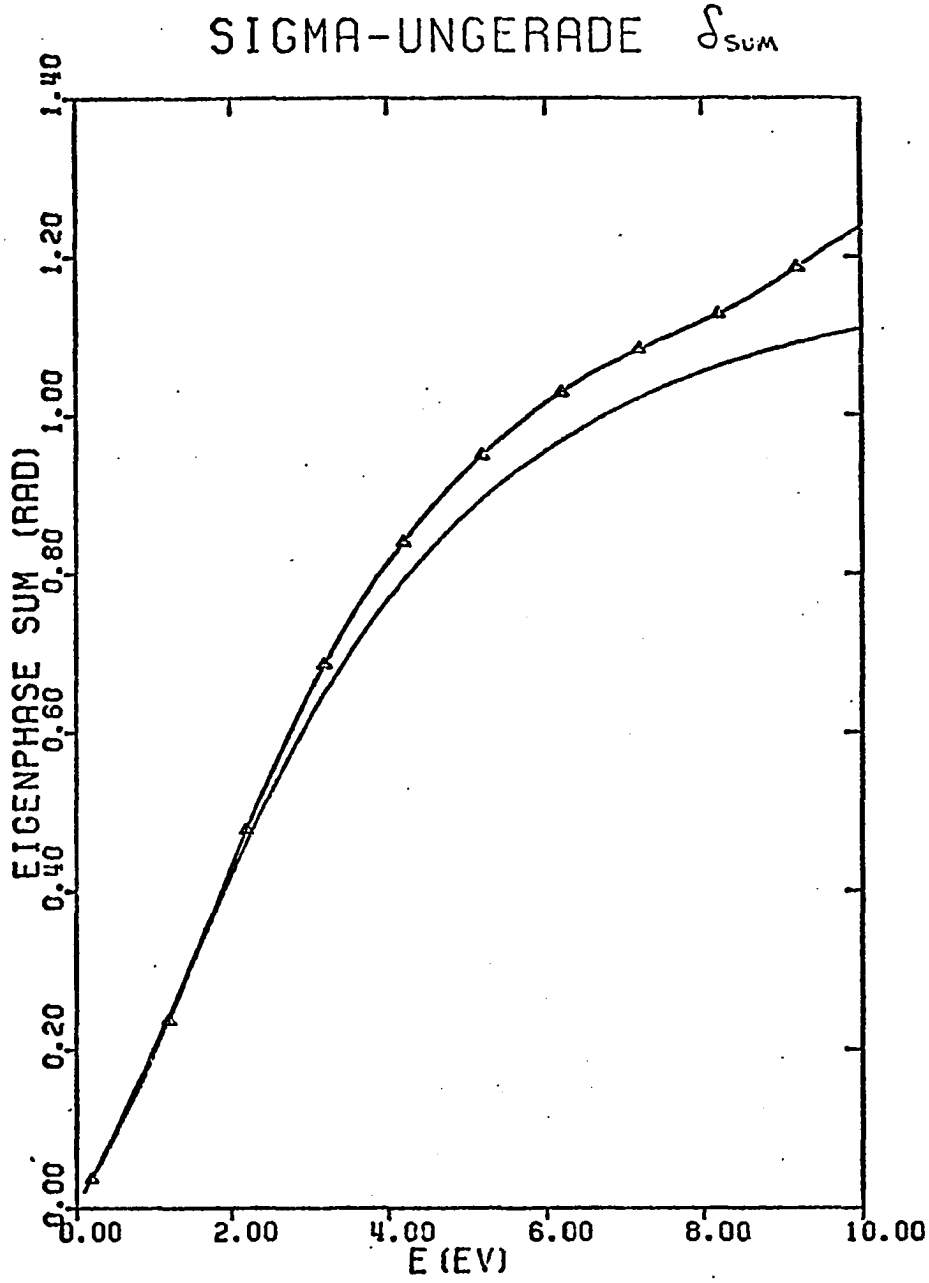


Figure 29. Eigenphase sums for the Σ_u symmetry; curves labelled as in Figure 27.

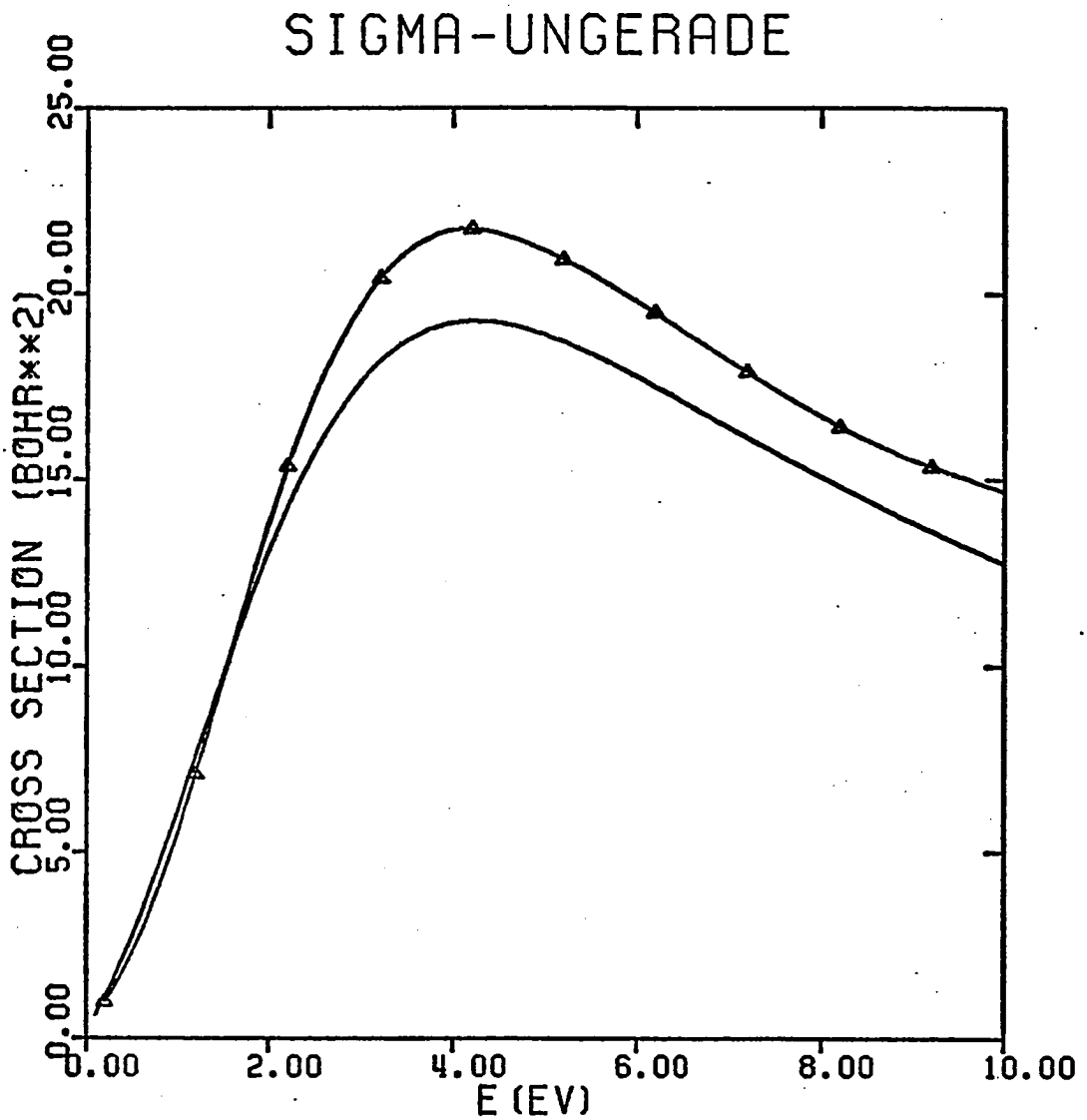


Figure 30. Integrated cross sections for the Σ_u symmetry; symbols as in Figure 27.

CHAPTER V
CONCLUSIONS

In this final chapter we will briefly summarize our study and then present some conclusions and future directions for this research. We began this study by considering ways to go beyond the static-exchange approximation. A physical approach in which a polarization potential is used to include closed-channel effects was selected, and the importance of nonadiabatic contributions was investigated. We discussed the use of a molecular structure code to calculate polarization potentials and described the procedures that were developed to incorporate nonadiabatic effects. Polarization potentials which included various multipole contributions were presented and compared with each other. Finally, scattering calculations in which the polarization interaction was represented by our calculated potentials were performed and found to be in very good agreement with a variety of recent exprimental measurements.

The observed agreement between our scattering results and the experimental measurements indicates that, for the calculation of electron-H_2 total cross sections from 0.02 to 10.0 eV scattering energy, the BTAD potential provides a good representation of the polarization interaction. Also, since our polarization potential is energy-independent, it appears that

an explicit energy-dependence (*c.f.*, section 2.4) is not necessary for the low-energy collisions considered here.

In principle, one should retain all of the higher multipole contributions to the polarization potential. However, including the additional multipoles "costs" more — sometimes considerably more — in terms of the computer-time required to evaluate the modified integrals in program BTAINTS. For the electron-H_2 system, the BTADP2 potential contains essentially all of the important multipole contributions (see Figures 4 and 5) and for a given value of $\vec{r}$ does not require substantially more time to compute than the BTAD potential. Although the total cross sections in Figure 21 agree quite well, rotational-excitation cross sections obtained when polarization is represented by the BTAD potential can be significantly different from those obtained when the BTADP2 potential is used; *e.g.* , we find that the 0.5 eV LFSMEP(BTAD) cross section for the $j = 0$ to $j' = 2$ excitation is 7% smaller than the corresponding LFSMEP(BTADP2) result. The rotational-excitation cross sections are also sensitive to the way in which the exchange interaction is incorporated (see Figures 25 and 26) and to explicit inclusion of vibrational effects. Klonover and Kaldor[59] have found that explicit integration over the R-dependence can increase rotational-excitation cross sections from 8–40% depending on the scattering energy. To adequately represent the R-dependence, potentials for several values of the internuclear separation must be determined; given these circumstances, the BTAD polarization potential seems to present the best compromise between cost and accuracy.

The *ab initio* treatment of the polarization interaction that we have utilized in this study has several advantages. First, our use of a molecular structure code allows us to generate $V^{\rm pol}(\vec{r},R)$ to better than second-order in V_{e-m} for all required values of $\vec{r}$ and R. In addition, near-Hartree-Fock wavefunctions determined from the same basis set can be used to compute all components of the electron-H_2 interaction potential, thereby assuring internal consistency. Although nonadiabatic effects are included in an approximate way, our polarization potentials require no scaling and contain no adjustable parameters.

Perhaps the best feature of this treatment is its extensibility to more complicated systems. The POLYATOM codes are already quite general, and with relatively minor additions to the BTAINTS code, non-adiabatic polarization potentials for larger targets (*e.g.*, N_2) can be generated. The major computational limitation on the complexity of the system considered is the amount of computer-time required by the BTAINTS code; this code can probably be made significantly more efficient. We should point out that the success of our polarization potentials in determining electron-H_2 scattering results by no means guarantees that similar results will be obtained for more complicated systems. However, we also have no reason to believe otherwise, and less successful results — or even spectacular failure — can still tell us a great deal about the validity of our approximations and the underlying physics involved.

REFERENCES

1. M. A. Morrison, T. L. Estle, and N. F. Lane, *Quantum States of Atoms, Molecules, and Solids* (Prentice-Hall, Englewood Cliffs, N.J., 1976), Chap. 12.
2. D. E. Golden, N. F. Lane, A. Temkin, and E. Gurjuoy, *Rev. Mod. Phys.* **43**, 642 (1971), section 4.
3. N. F. Lane, *Rev. Mod. Phys.* **52**, 29 (1980)
4. M. A. Morrison, "ALAM, A Program for the Calculation and Expansion of Molecular Charge Densities," *Comput. Phys. Commun.* **21**, 63 (1980)
5. L. A. Collins, D. W. Norcross, and G. B. Schmid, "VLAM, A Program for Computing the Electron-Molecule Static Interaction Potential from a Legendre Expansion of the Molecular Charge Density," *Comput. Phys. Commun.* **21**, 79 (1980)
6. M. A. Morrison and B. I. Schneider, *Phys. Rev. A* **16**, 1003 (1977)
7. D. K. Watson and V. McKoy, *Phys. Rev. A* **20**, 1474 (1979)
8. L. A. Collins, W. D. Robb, and M. A. Morrison, *Phys. Rev. A* **21**, 488 (1980)
9. A. E. Orel and T. N. Rescigno, *Phys. Rev. A* **24**, 1267 (1981)
10. L. A. Collins and B. I. Schneider, *Phys. Rev. A* **24**, 2387 (1981)

11. W. F. Weitzel, T. L. Gibson, and M. A. Morrison, "EXLAM, A Program for the Calculation and Expansion of Local Model Exchange Potentials," *Comput. Phys. Commun.* (accepted for publication).

12. M. Weissbluth, *Atoms and Molecules* (Academic Press, New York, 1978), Chaps. 3–5.

13. L. Castillejo, I. C. Percival, and M. J. Seaton, *Proc. Roy. Soc. (London)* **A 254,** 259 (1960).

14. R. J. Drachman, *J. Phys. B* **12,** L699 (1979)

15. V. M. Martin, M. J. Seaton, and J.B.C. Wallace, *Proc. Phys. Soc.* (London) **72,** 701 (1958)

16. B. H. Bransden and M.R.C. McDowell, *Phys. Rep.* **30,** 207 (1977)

17. S. Geltman, *Physics of Electronic and Atomic Collisions,* VII ICPEAC (North-Holland, London, 1972), 216

18. P. W. Coulter, *Phys. Rev. A* **22,** 372 (1980)

19. A. Temkin, *Phys. Rev.* **107,** 1004 (1957)

20. A. Temkin and J. C. Lamkin, *Phys. Rev.* **121,** 788 (1961)

21. R. J. Drachman and A. Temkin, *Case Studies in Atomic Collision Physics II* (North-Holland, London, 1972), Chap. 6

22. J. Callaway, *Comput. Phys. Commun.* **6,** 265 (1974)

23. J. Callaway, R. W. LaBahn, R. T. Pu, and W. M. Duxler, *Phys. Rev.* **168,** 12 (1968)

24. B. H. Bransden, *Atomic Collision Theory* (W. A. Benjamin, New York, 1970), Chap. 5

25. M. A. Morrison, N. F. Lane, and L. A. Collins, *Phys. Rev. A* **15**, 2186 (1977)

26. M. A. Morrison and P. J. Hay, *Phys. Rev. A* **20**, 740 (1979)

27. D. G. Truhlar, D. A. Dixon, and R. A. Eades, *J. Phys. B* **12**, 1913 (1979)

28. N. F. Lane and R.J.W. Henry, *Phys. Rev.* **173**, 183 (1968)

29. S. Hara, *J. Phys. Soc. Japan* **27**, 1262 (1969)

30. B. I. Schneider, *Chem. Phys. Lett.* **51**, 578 (1977)

31. A. Klonover and U. Kaldor, *J. Phys. B* **11**, 1623 (1978)

32. B. I. Schneider and L. A. Collins, *J. Phys. B* (submitted)

33. J. M. Moskowitz and L. C. Snyder, in *Methods in Electronic Structure Theory,* edited by H. F. Schaefer III (Plenum, New York, 1977), p. 387

34. C.C.J. Roothaan, *Rev. Mod. Phys.* **23**, 69 (1951)

35. H. W. Joy and R. G. Parr, *J. Chem. Phys.* **28**, 444 (1958)

36. H. Taketa, S. Huzinaga and K. O-Ohata, *J. Phys. Soc. Japan* **21**, 2313 (1966)

37. C. A. Weatherford, R.J.W. Henry and M. C. Bruels, *Proc. Ind. Nat. Sci. Acad.* A **39**, 437 (1973)

38. S. Huzinaga, *J. Chem. Phys.* **42**, 1293 (1965)

39. W. Kolos and C.C.J. Roothaan, *Rev. Mod. Phys.* **32**, 219 (1960)

40. W. Kolos and L. Wolniewicz, *J. Chem. Phys.* **43**, 2429 (1965)

41. J. Rychlewski, *Mol. Phys.* **41**, 833 (1980)

42. M. A. Morrison and P. J. Hay, *J. Chem. Phys.* **70**, 4034 (1979)

43. See W. Kolos and L. Wolniewicz, *J. Chem. Phys.* **46**, 1426 (1967) and H. Schüler and K. L. Wolf, *Z. Physik* **34**, 343 (1925)

44. K. B. MacAdam and N. F. Ramsey, *Phys. Rev. A* **6**, 898 (1972). For a recent review see T. M. Miller and B. Bederson, *Adv. At. Mol. Phys.* **13**, 1 (1978)

45. A. M. Arthurs and A. Dalgarno, *Proc. Roy. Soc. (London) A* **256**, 540 (1960)

46. W. N. Sams and D. J. Kouri, *J. Chem. Phys.* **51**, 4809 (1969)

47. M. A. Morrison, *Electron-Molecule and Photon-Molecule Collisions*, eds. T. N. Rescigno, V. McKoy, and B. I. Schneider (New York: Plenum) pp 15-50

48. A. N. Feldt and M. A. Morrison, *J. Phys. B* **15**, 301 (1982)

49. J. Ferch, W. Raith, and K. Schröder, *J. Phys. B* **13**, 1481 (1980). The values presented in Figure 22 are from a table provided by Dr. Ferch.

50. R. J. W. Henry and N. F. Lane, *Phys. Rev.* **183**, 221 (1969). A very complete table of scattering results was provided by Dr. N. F. Lane.

51. T. F. O'Malley, L. Rosenberg, and L. Spruch, *Phys. Rev.* **125**, 1300 (1962)

52. E. S. Chang, *J. Phys. B* **14**, 893 (1981)

53. R. W. Crompton, D. K. Gibson, and A. I. McIntosh, *Austr. J. Phys.* **22**, 715 (1969)

54. D. E. Golden, H. W. Bandel, and J. A. Salerno, *Phys. Rev.* **146**, 40

(1966)

55. G. Dalba, P. Fornasini, I. Lazzizzera, G. Ranieri, and A. Zecca, *J. Phys. B* **13**, 2839 (1980)

56. R. Jones (to be published). A table of measured cross sections was provided by Dr. R. Bonham.

57. S. Hara, *J. Phys. Soc. Japan* **27**, 1009 (1969)

58. A. Klonover and U. Kaldor, *J. Phys. B* **11**, 1623 (1978). Dr. U. Kaldor kindly provided a table of scattering cross sections.

59. A. Klonover and U. Kaldor, *J. Phys. B* **12**, L61 (1979)

60. A. N. Feldt and M. A. Morrison (to be published)

61. S. Hara, *J. Phys. Soc. Japan* **27**, 1592 (1969)

62. F. Linder and H. Schmidt, *Z. Naturf.* **26a**, 1603 (1971)

63. B. I. Schneider and L. A. Collins, *J. Phys. B* (submitted). A table of results was provided by Dr. L. A. Collins.

64. For definitions and numerical compilations of the special functions of Mathematical Physics, see M. Abramowitz and I. A. Stegun, *Handbook of Mathematical Functions* (Washington: NPS, 1964).

APPENDIX I

COMPARISON OF MODEL EXCHANGE POTENTIALS FOR LOW-ENERGY e-H_2 COLLISIONS WITH AND WITHOUT POLARIZATION EFFECTS

J. Phys. B 14, 727 (1981)

Thomas L. Gibson and Michael A. Morrison

J. Phys. B: At. Mol. Phys. 14 (1981) 727–739. Printed in Great Britain

Comparison of model exchange potentials for low-energy e–H_2 collisions with and without polarisation effects

Thomas L Gibson and Michael A Morrison

Department of Physics and Astronomy, University of Oklahoma, Norman, Oklahoma 73019, USA

Received 1 August 1980

Abstract. The utility of several model exchange potentials in e–H_2 scattering calculations from 0·01–1·00 Ryd is investigated. Model potential cross sections and eigenphase sums for the $^2\Sigma_g$, $^2\Pi_g$, $^2\Sigma_u$ and $^2\Pi_u$ e–H_2 symmetries are calculated both with and without polarisation. Their validity is assessed from a comparison with results obtained when exchange is treated via an exact iterative procedure. To ensure meaningful comparisons, the same static and polarisation potentials are used for the model exchange and exact exchange calculations. Results obtained with the tuned free-electron-gas exchange potential are consistently found to have the best overall agreement with exact exchange values. In addition, new exact static exchange polarisation results are reported.

1. Introduction

The behaviour of cross sections for low-energy electron–molecule collisions is governed by static, polarisation and exchange interactions (Lane 1980). The dominant short-range static interaction, which is due to Coulomb forces between the scattering electron and the target, can be accurately and efficiently determined (Morrison 1980, Collins *et al* 1980). The long-range induced polarisation, which is a second-order effect arising from the distortion of the target by the scattering electron, is usually included in the electron–molecule interaction potential via a semi-empirical adiabatic approximation based on the known asymptotic form of the polarisation potential. In the last few years the approximations inherent in this procedure have been examined and more accurate treatments of polarisation proposed (Morrison and Hay 1979, Truhlar *et al* 1979, Klonover and Kaldor 1978, Schneider 1977).

In addition to static and polarisation interactions, any reliable treatment of low-energy electron–molecule scattering must incorporate the quantum-mechanical requirement that the system wavefunction be antisymmetric under pairwise electron interchange. This requirement gives rise to energy-dependent exchange terms in the scattering equations. The non-local character of these terms makes the numerical solution of the resulting equations arduous and tends to obscure the physical nature of exchange. Although recent advances have widened the range of systems for which the exact treatment of exchange is possible (e.g., Collins *et al* 1980, Morrison and Schneider 1977, Levin *et al* 1980, Watson *et al* 1980), it still remains very difficult for all but the simplest systems. This situation has stimulated attempts to model the effects of exchange by including approximate local terms in the interaction potential.

0022-3700/81/040727+13$01.50 © 1981 The Institute of Physics

Two types of model exchange potentials for electron scattering have been investigated in recent years. One such potential is based on a semiclassical exchange (SCE) approximation (Riley and Truhlar 1975, Furness and McCarthy 1973); heretofore use of this model in electron–molecule collisions (Truhlar and Brandt 1976, Rumble and Truhlar 1979, 1980b, Onda and Truhlar 1979a, b, 1980, Siegel *et al* 1980) has been restricted mainly to intermediate-energy scattering ($10{\cdot}0 \leqslant E \leqslant 100{\cdot}0$ eV). The other class of potentials is based on a free-electron-gas (FEG) approximation. Because of the admittedly *ad hoc* nature of these model potentials, extensive systematic studies of their validity are essential for an assessment of their applicability for low-energy electron scattering. Such studies should initially be carried out in the static exchange (SE) approximation, where the absence of polarisation effects enables us to focus on the influence of exchange. Moreover, comparison with results of calculations in which exchange is treated exactly is essential to a meaningful evaluation of the models.

The use of model exchange potentials in low-energy collisions ($E \leqslant 10{\cdot}0$ eV) has been explored for electron–atom scattering (Riley and Truhlar 1975, 1976, Bransden *et al* 1976) and for several electron–molecule systems (Morrison and Collins 1978, 1980, Morrison *et al* 1977, Collins and Norcross 1978, Collins *et al* 1979, Lynch *et al* 1979, Rumble and Truhlar 1980a, Hara 1967, Baille and Darewych 1977). Comparative studies of such model potentials include that of Morrison and Collins (1978), in which FEG potentials were used to calculate cross sections for e–N_2 scattering in the static exchange (SE) and static exchange polarisation (SEP) models and for e–H_2 collisions in the SE approximation. These authors considered only the $^2\Sigma_g$ electron–H_2 symmetry and developed a variant of the usual (Hara 1967) FEG exchange potential in which the introduction of an energy-independent 'tuning' parameter led to a model SE potential capable of reproducing exact $^2\Sigma_g$ SE phaseshifts over three decades of energy (0·01–1·00 Ryd). Since the primary emphasis in their study was the e–N_2 system, Morrison and Collins did not pursue model exchange calculations for other e–H_2 symmetries.

A study of model exchange potentials for e–H_2 scattering by Baille and Darewych (1977) subsequently appeared which contains conclusions markedly different from those of Morrison and Collins. However, Baille and Darewych only reported calculations in which a polarisation term was included in the interaction potential. The presence of this additional interaction could obscure the role of exchange.

To clarify this situation, we have carried out an extensive study of SCE and FEG model potentials for low-energy e–H_2 scattering. We report both SE and SEP calculations for scattering energies from 0·01–1·00 Ryd. The models are assessed by comparison with SE and SEP results in which exchange is treated exactly. For consistency, the same static and polarisation potentials are used in the exact and model exchange calculations.

In § 2 we briefly summarise the collision theory and the model exchange potentials considered in the present work. Section 3 contains a discussion of the calculations we have performed and the results obtained, including new results for SEP e–H_2 scattering in which exchange is treated exactly and the *ab initio* polarisation potential of Lane and Henry (1968) is employed. Our conclusions and final comments about local exchange approximations appear in § 4. Unless otherwise stated, atomic units† are used throughout.

† In atomic units $\hbar = m_e = a_0 = e = 1$. The unit of energy is $\hbar^2/(m_e a_0^2) = 1$ Hartree = 2 Ryd = 27·212 eV. The unit of distance is the first Bohr radius (a_0) = 1 Bohr = $0{\cdot}52918 \times 10^{-10}$ m.

2. Theory

2.1. Static exchange scattering equations

For these calculations we use a body-fixed reference frame in which the $\hat{z}$ axis lies along the internuclear axis $\hat{R}$. We make the Born–Oppenheimer approximation for the wavefunction of the molecule. In addition, we make the fixed-nuclei approximation (Temkin and Vasavada 1967, Temkin *et al* 1969, Hara 1967) in which the molecular orientation $\hat{R}$ and the internuclear separation R are held fixed for the duration of the collision.

In this formulation, we solve the non-relativistic time-independent Schrödinger equation for the scattering electron with coordinate r. For e–H_2 scattering, this equation is (Lane 1980)

$$(-\tfrac{1}{2}\nabla^2 + V_{st}(r) + V_{ex}(r) - \tfrac{1}{2}k^2)y(r) = 0 \tag{2.1}$$

where $V_{st}(r)$ is the Coulomb interaction averaged over the ground electronic wavefunction of the molecule, $y(r)$ is the spatial scattering function, and $\frac{1}{2}k^2$ is the incident scattering energy, E_{inc} (in hartrees). The non-local energy-dependent exchange term is written as

$$V_{ex}(r)y(r) = -\phi(r)\int \phi^*(r')\frac{1}{|r-r'|}y(r')\,dr' \tag{2.2}$$

with $\phi(r')$ being the doubly occupied bound spatial orbital of the molecule.

In order to solve (2.1) we expand the scattering function $y(r)$ in spherical harmonics (all coordinates are referred to the centre of mass of the molecule)

$$y(r) = \frac{1}{r}\sum_{l=0}^{\infty}\sum_{m=-l}^{l} f_l(r)Y_l^m(\hat{r}) \tag{2.3}$$

where $f_l(r)$ is the radial scattering function. Channels are designated by quantum numbers representing the scattering electron's orbital angular momentum (l) and the projection of this angular momentum along the internuclear axis (m). The use of (2.3) leads to a set of body frame coupled radial equations which (due to neglect of the rotational Hamiltonian in this formulation) is uncoupled in m. For a complete discussion of this formulation, see Morrison and Collins (1978).

2.2. Free-electron-gas model exchange potentials

In using a model exchange potential we seek to replace the exact non-local, energy-dependent exchange term (2.2) with a local energy-dependent approximation. First, we consider models based on the FEG approximation, which are similar to a treatment of exchange for bound states proposed by Slater (1951).

We assume that *for the purposes of exchange only*, we can treat the molecular electrons as non-interacting fermions occupying a finite volume (V) within which they experience zero potential. This model leads to the usual Fermi sphere of radius k_F in momentum space, where k_F is the Fermi momentum. For H_2, the FEG bound spatial orbital is written as

$$\phi(r) = V^{-1/2}\exp(ik_F \cdot r). \tag{2.4}$$

Initially, we assume that the distortion of the scattering function in the exchange term can be ignored, leaving

$$y(r) = C \exp(ik \cdot r) \tag{2.5}$$

where C is an arbitrary normalisation constant and k is the wavevector of the scattering electron.

We wish to replace the exact exchange term (2.2) by the product of an approximate local exchange potential $V_{\mathrm{FEG}}(r)$ and the scattering function $y(r)$. To accomplish this we substitute (2.4) and (2.5) into (2.2) and then multiply and divide by $y^*(r)y(r)$, obtaining

$$V_{\mathrm{FEG}}(r) = \frac{-1}{V}\int_V \exp[\mathrm{i}(k-k_{\mathrm{F}})\cdot(r'-r)]\frac{1}{|r-r'|}\,\mathrm{d}r'. \tag{2.6}$$

Performing the integration (Morrison and Collins 1978) leaves

$$V_{\mathrm{FEG}}(r) = -(2/\pi)k_{\mathrm{F}}F(\eta) \tag{2.7}$$

where

$$F(\eta) \equiv \frac{1}{2} + \frac{1-\eta^2}{4\eta}\ln\left|\frac{1+\eta}{1-\eta}\right| \tag{2.8}$$

and $\eta \equiv k/k_{\mathrm{F}}$. The Fermi momentum is related to the FEG density of bound electrons, $\rho = N/V$, by

$$k_{\mathrm{F}} = (3\pi^2\rho)^{1/3}. \tag{2.9}$$

To be consistent with the FEG approximation care must be exercised in defining the energy of the scattering electron. In this model the ionisation continuum begins at an energy of $I_{\mathrm{F}} + \frac{1}{2}k_{\mathrm{F}}^2$ where I_{F} is the FEG ionisation potential (the energy required to promote the Fermi electron into the continuum). Thus, we write the energy of the scattering electron as

$$E_s = E_{\mathrm{inc}} + I_{\mathrm{F}} + \tfrac{1}{2}k_{\mathrm{F}}^2. \tag{2.10}$$

At this point we make some simple, physically reasonable modifications to improve the model. First, we replace the constant FEG density $\rho = N/V$ by the quantum-mechanical charge density $\rho(r)$ of the molecular ground state, thereby introducing an r dependence into the Fermi momentum $k_{\mathrm{F}}(r)$ and hence into $F(\eta)$.

Second, we replace k in η by a local r-dependent momentum $\kappa(r)$. The 'local kinetic energy' of the scattering electron is $\frac{1}{2}\kappa^2(r)$. Substituting these modifications into (2.10), we obtain

$$\kappa^2(r) = 2(E_{\mathrm{inc}} + I) + k_{\mathrm{F}}^2(r) \tag{2.11}$$

where I is the experimentally observed ionisation potential (in hartrees). Using $\eta = \kappa(r)/k_{\mathrm{F}}(r)$ in (2.7) and (2.8) we obtain $V_{\mathrm{FEG}}(r)$. This form is known as the Hara FEG exchange (HFEGE) potential (Hara 1967, Morrison and Collins 1978).

Since $\rho(r)$ and hence $k_{\mathrm{F}}(r)$ go to zero as $r \to \infty$, we see that asymptotically $\frac{1}{2}\kappa^2(r) \to (E_{\mathrm{inc}} + I)$ instead of E_{inc}. Riley and Truhlar (1975) have suggested that one should set the ionisation potential to zero in V_{FEG}, thereby giving $\frac{1}{2}\kappa^2(r)$ the correct asymptotic value. The resulting potential is designated the asymptotically adjusted FEG exchange (AAFEGE) potential.

Morrison and Collins (1978) have found that by adjusting the value of I they can 'tune' the FEG potential for the e–H_2 system at a single energy (0·04 Ryd) and reproduce exact static exchange (ESE) cross sections and eigenphase sums in the $^2\Sigma_g$ symmetry from 0·01–1·00 Ryd. This form is known as the tuned FEG exchange (TFEGE) potential.

2.3. The semiclassical exchange potential

A semiclassical exchange potential has been developed by Riley and Truhlar (1975) which is similar to one proposed by Furness and McCarthy (1973). In this model we replace the integral in the exchange term (2.2) by making the approximation

$$\int \phi^*(r')\frac{1}{|r-r'|}y(r')\,dr' \simeq A(r)y(r) \tag{2.12}$$

where $A(r)$ is assumed to be a slowly varying amplitude function. Since the bound orbital $\phi(r')$ is a slowly varying function, the major contribution to the integral occurs as $|r-r'|\to 0$ if the rapid oscillation of $y(r')$ causes significant cancellation elsewhere. However, one expects the behaviour of $y(r)$ to be slowly varying for low-energy electrons (in the absence of strongly attractive potentials). This is somewhat ameliorated in that the exchange interaction is most important near the target, where the scattering interaction is dominated by the strongly attractive static potential of the nuclei. In the region of the strongly attractive potential the local kinetic energy of the scattering electron will be large, and in so far as a local wavelength is meaningful, it should be short. Near the target $y(r)$ might oscillate rapidly enough to make the SCE approximation reasonable even at moderately low scattering energies.

Riley and Truhlar (1975) expand $A(r)$ in (2.12) in inverse powers of the local kinetic energy $\frac{1}{2}\kappa^2(r)$. This expansion is truncated at the first term by assuming that the local kinetic energy is large. The resulting SCE potential is given by

$$V_{SCE}(r)=\tfrac{1}{2}\{(E_{inc}-V_{st}(r))-[(E_{inc}-V_{st}(r))^2+\beta^2]^{1/2}\} \tag{2.13}$$

where (for closed-shell targets)

$$\beta^2=4\pi\rho(r). \tag{2.14}$$

2.4. The static exchange polarisation interaction potential

For the static exchange polarisation (SEP) interaction potential, $V_{sep}(r)=V_{st}(r)+V_{ex}(r)+V_{pol}(r)$, we use the *ab initio* polarisation potential of Lane and Henry (1968). This potential (which incorporates some non-adiabatic effects) is given by Henry and Lane (1969) as

$$V_{pol}(r)=V_0^{pol}(r)+V_2^{pol}(r)P_2(\cos\theta) \tag{2.15}$$

with

$$V_0^{pol}(r)=\frac{-\alpha_0}{2[r^2+(1\cdot22)^2]^2}\{1-\exp[-(r/1\cdot7)^3]\} \tag{2.16a}$$

$$V_2^{pol}(r)=\begin{cases}\dfrac{-\alpha_2}{2(r^2-0\cdot01)^2}\{1-\exp[-(r/2\cdot0)^4]\} & r\geq 0\cdot5\,a_0 \quad (2.16b)\\ 0 & r<0\cdot5\,a_0 \quad (2.16c)\end{cases}$$

where $\alpha_0 = 5{\cdot}5$ au ($\alpha_2 = 1{\cdot}38$ au) is the spherical (non-spherical) polarisability (Kolos and Wolniewicz 1967). For SEP interactions, $V_{pol}(r)$ is added to $V_{st}(r)$ in (2.1), and if the SCE potential is used, $V_{pol}(r)$ is added to $V_{st}(r)$ in (2.13) as well (Truhlar and Brandt 1976, Bransden *et al* 1976).

3. Calculational procedure and results

3.1. Calculational procedure

The body frame coupled radial scattering equations are solved numerically using an integral equations algorithm (Sams and Kouri 1969, Morrison 1979) for the $^2\Sigma_g$, $^2\Pi_g$, $^2\Sigma_u$ and $^2\Pi_u$ electron–molecule symmetries at incident energies from 0·01–1·00 Ryd. In these calculations we include three channels per symmetry; e.g. in the $^2\Sigma_g$ symmetry the $l = 0$, 2 and 4 terms are retained in the partial-wave expansion (2.3). The solution matrix is propagated on a variable-step-size r-integration mesh extending to a maximum r of 50·0 a_0, where the body frame K matrix is extracted.

To calculate the static and exchange potentials we use the near Hartree–Fock H_2 wavefunction of Fraga and Ransil (1961) corresponding to the equilibrium internuclear separation (1·402 a_0), which yields 0·48 ea_0^2 for the quadrupole moment (Wolniewicz 1966). The molecular charge density $\rho(r)$ is calculated from this wavefunction and expanded in a Legendre polynomial series (Morrison 1980). This expansion of $\rho(r)$ is used to calculate the static (Collins *et al* 1980) and exchange potentials which are also expanded, namely,

$$V_{st(ex)}(r) = \sum_{\lambda=0}^{\lambda_{max}} V_\lambda^{st(ex)}(r) P_\lambda(\cos\theta). \tag{3.1}$$

We find $\lambda_{max} = 4$ is sufficient to give total integrated cross sections converged to approximately 1% or less.

3.2. Static exchange (SE) results

For calculations using the HFEGE potential, the experimentally determined value for the ionisation potential, $I = 0{\cdot}564$ Hartree, is used in equation (2.11). As discussed in § 2.2, Morrison and Collins (1978) determined a value of 0·071 Hartree for this parameter in the TFEGE model, and $I = 0$ is used in the AAFEGE potential.

Total (elastic plus rotational excitation) integrated cross sections including all four e–H_2 symmetries for the model exchange potentials considered in the present study are shown in figure 1 together with the ESE results of Collins *et al* (1980). The latter cross sections were calculated with the same H_2 wavefunction as was used in the present calculations. The behaviour of these cross sections (and the eigenphase sums in table 1) indicates that the HFEGE potential is too weak, while the AAFEGE model is too strong. The TFEGE cross sections give the best overall agreement with the ESE results. The SCE potential yields results of reasonable accuracy, but the incorrect qualitative behaviour of these cross sections at low energy indicates that this potential is also too strong.

Selected cross sections and eigenphase sums for the three dominant e–H_2 symmetries are given in table 1. For incident energies $\leq 0{\cdot}25$ Ryd, the scattering is predominantly s wave in the $^2\Sigma_g$ symmetry. Therefore, although TFEGE and SCE cross sections in this energy range for $^2\Sigma_u$, $^2\Pi_u$ and $^2\Pi_g$ symmetries are not particularly

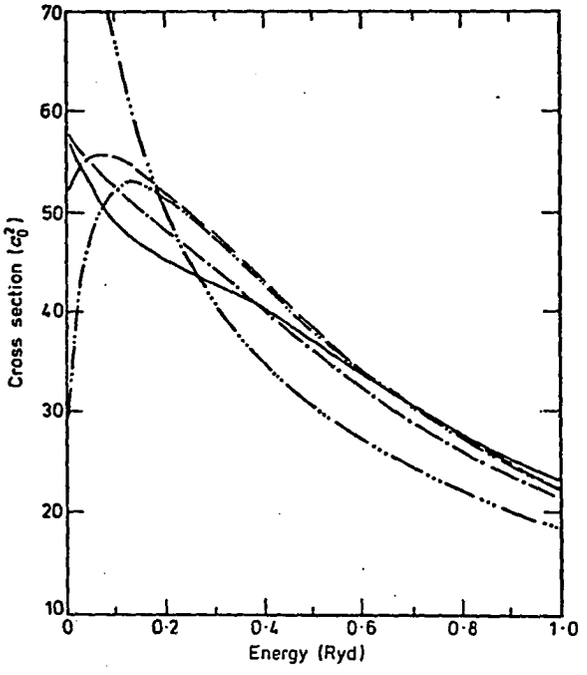


Figure 1. Total, integrated, static exchange cross sections from the following calculations: ———, ESE (Collins *et al* 1980); — —, SCE; – · – ·, TFEGE; – · · – · · –, AAFEGE; – · · · –, HFEGE. These cross sections include the $^2\Sigma_g$, $^2\Pi_g$, $^2\Sigma_u$ and $^2\Pi_u$ symmetries.

accurate, this has little effect on the total cross section. Differential cross sections $d\sigma/d\Omega$ from TFEGE, SCE and ESE calculations at scattering energies of 0·04 and 0·16 Ryd are compared in figure 3.

3.3. Static exchange polarisation (SEP) results

To evaluate the model exchange potentials in the SEP approximation, when polarisation effects are taken into account, we compare SEP cross sections determined using model potentials with their 'exact' SEP (ESEP) counterparts. The latter have been calculated by M A Morrison and L A Collins (1980 private communication) using the Fraga and Ransil static potential described in § 3.1 and the Lane and Henry polarisation potential of equations (2.15)–(2.16). The same static and polarisation potentials were used in the model exchange calculations. Total integrated cross sections from these various calculations are shown in figure 2 and table 2.

Of the model potentials considered, only the TFEGEP and SCEP produce cross sections in reasonable agreement with the ESEP values. These approximate results are essentially identical for scattering energies from 0·01 to 1·00 Ryd and are in fair agreement with their ESEP counterparts except for energies near 0·2 Ryd. The peak in the cross section at this energy is due primarily to a p-wave enhancement of the $^2\Sigma_u$ contribution (Bardsley *et al* 1966a, b). In contrast to the SE case, the dominant contribution to the SEP cross sections for energies above 0·09 Ryd arises from the sum of the $^2\Sigma_u$ and $^2\Pi_u$ symmetries (cf corresponding entries in tables 1 and 3). Because of

Table 1. Selected SE cross sections (in a_0^2) and eigenphase sums (modulo π, in parentheses) for the three dominant symmetries.

Energy (Ryd)		ESE†	TFEGE	SCE	HFEGE	AAFEGE
0·04	$^2\Sigma_g$	53·034	54·29	53·20	81·97	41·40
		(2·7246)	(2·72)	(2·72)	(2·61)	(2·78)
	$^2\Sigma_u$	0·6763	1·01	1·71	0·34	3·44
		(0·0493)	(0·06)	(0·08)	(0·04)	(0·11)
	$^2\Pi_u$	0·0095	0·02	0·26	0·02	0·40
		(0·0045)	(0·01)	(0·02)	(0·00)	(0·03)
0·09	$^2\Sigma_g$	47·896	49·71	49·96	68·38	43·14
		(2·5267)	(2·51)	(2·51)	(2·38)	(2·56)
	$^2\Sigma_u$	1·9397	2·77	4·37	0·76	7·11
		(0·1233)	(0·15)	(0·18)	(0·08)	(0·23)
	$^2\Pi_u$	0·1386	0·25	0·97	0·01	1·02
		(0·0262)	(0·03)	(0·06)	(0·01)	(0·06)
0·25	$^2\Sigma_g$	35·483	37·03	37·23	42·80	35·33
		(2·1679)	(2·13)	(2·13)	(1·99)	(2·17)
	$^2\Sigma_u$	7·5826	8·13	10·45	2·65	12·60
		(0·4084)	(0·42)	(0·48)	(0·24)	(0·53)
	$^2\Pi_u$	1·1592	1·16	2·56	0·21	2·09
		(0·1155)	(0·11)	(0·17)	(0·05)	(0·15)
0·64	$^2\Sigma_g$	19·427	19·62	19·63	19·65	19·56
		(1·7509)	(1·70)	(1·71)	(1·58)	(1·73)
	$^2\Sigma_u$	10·453	9·49	10·10	5·84	10·60
		(0·8361)	(0·78)	(0·82)	(0·59)	(0·84)
	$^2\Pi_u$	2·6449	1·90	2·95	0·83	2·33
		(0·2779)	(0·23)	(0·29)	(0·16)	(0·26)
1·00	$^2\Sigma_g$	12·481	12·30	12·34	11·89	12·37
		(1·5509)	(1·50)	(1·51)	(1·41)	(1·52)
	$^2\Sigma_u$	8·092	7·47	7·59	5·82	7·85
		(0·9591)	(0·91)	(0·92)	(0·77)	(0·94)
	$^2\Pi_u$	2·5535	1·79	2·45	1·07	2·01
		(0·3481)	(0·29)	(0·34)	(0·23)	(0·31)

† From Collins *et al* (1980).

the importance of these symmetries to the SEP cross sections, the errors introduced by the approximate treatment of exchange in these symmetries are more significant than in the SE approximation.

Baille and Darewych (1977) note similar differences between their model exchange cross sections and those of Henry and Lane (1969) and suggest that these differences may be due to the neglect of the 'one-electron exchange terms' in the model studies (cf Riley and Truhlar 1976). However, for e–H_2 scattering, these terms are present only in the $^2\Sigma_g$ symmetry. As table 3 illustrates, the TFEGEP and SCEP results in this symmetry agree with the ESEP cross sections. Therefore, in calculations using these two model exchange potentials, the inclusion of the one-electron exchange terms will be unable to rectify the inaccuracies in the $^2\Sigma_u$ and $^2\Pi_u$ symmetries and hence will effect little improvement in the total cross sections.

This question has been studied by Morrison and Collins (1980) in the SE approximation using the HFEGE and AAFEGE potentials. They explicitly orthogonalised the σ_g continuum orbital to the $1\sigma_g$ bound molecular orbital. Although their orthogonalised

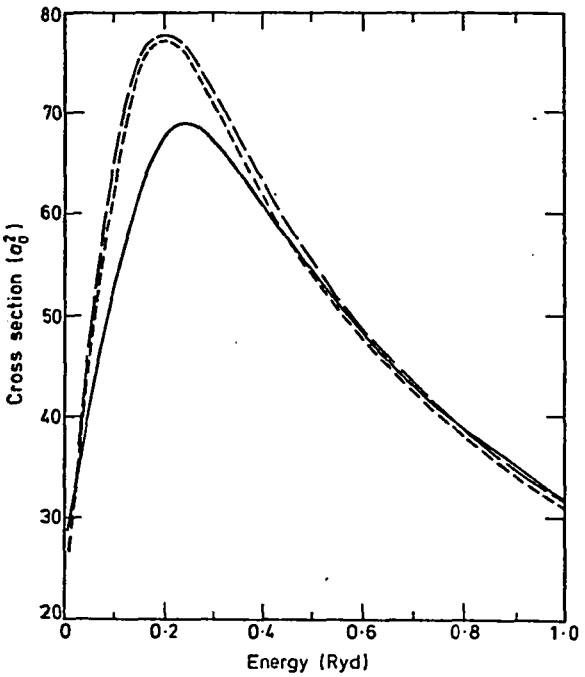


Figure 2. Total, integrated, static exchange polarisation cross sections: ———, ESEP (Morrison and Collins, private communication); – – – –, TFEGEP; — — —, SCEP. The *ab initio* polarisation potential of Lane and Henry (1968) (equations (2.15)-(2.16)) is used throughout. These cross sections include the $^2\Sigma_g$, $^2\Pi_g$, $^2\Sigma_u$ and $^2\Pi_u$ symmetries.

HFEGE e–H_2 cross sections in the $^2\Sigma_g$ symmetry are in better agreement with the ESE results than are the HFEGE cross sections, the orthogonalisation procedure cannot produce results as accurate as those obtained with the TFEGE model.

Total (elastic plus rotational-excitation) differential cross sections $d\sigma/d\Omega$ at 0·04 and 0·16 Ryd from the TFEGEP and SCEP calculations are compared in figure 3 to their ESEP counterparts. A further study at 10·0 eV (not shown) revealed excellent agreement among the three treatments of exchange at this energy.

Finally, we note that Baille and Darewych (1977) also report HFEGEP and AAFEGEP total integrated cross sections using the Lane and Henry polarisation potential of equations (2.15)–(2.16) but a different static potential. However, our results for these cases (cf table 2) are in substantial disagreement with those of Baille and Darewych. Moreover, their SCEP cross sections are consistently larger than those of table 2. The less accurate static potential used by Baille and Darewych (based on the Wang (1928) H_2 wavefunction) may account for some of this disagreement.

4. Summary and conclusions

We have investigated the utility of several model exchange potentials for e–H_2 collisions by comparing model exchange and exact exchange results in the SE and SEP

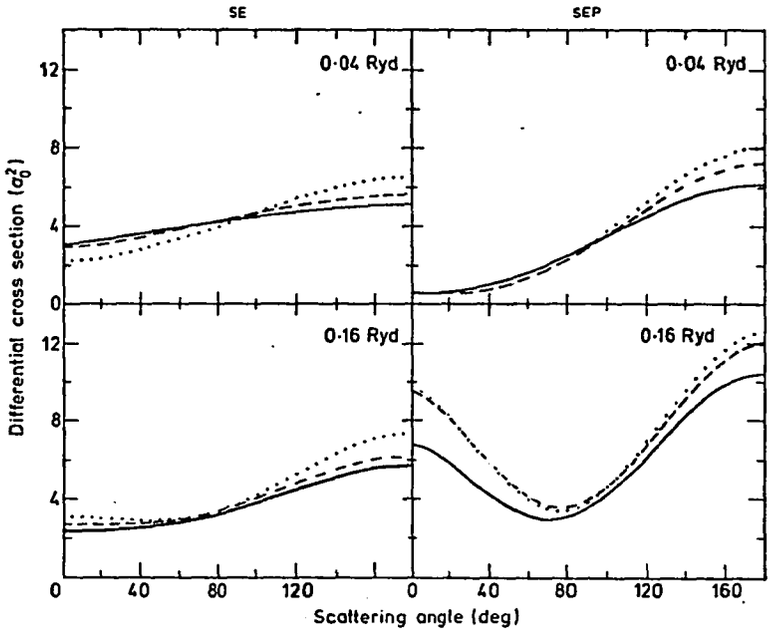


Figure 3. Total, differential, static exchange (left) and static exchange polarisation (right) cross sections for the following treatments of exchange: ———, exact; – – –, tuned FEG; · · · ·, semiclassical exchange. For calculations involving polarisation, the Lane and Henry (1968) polarisation potential (equations (2.15)-(2.16)) is used. The $^2\Sigma_g$, $^2\Pi_g$, $^2\Sigma_u$ and $^2\Pi_u$ symmetries are included in these cross sections.

Table 2. Total (elastic plus rotational-excitation) integrated SEP cross sections (in a_0^2).

Energy (Ryd)	ESEP†	TFEGEP	SCEP	HFEGEP	AAFEGEP
0·01	29·132	26·62	25·70	50·41	11·96
0·04	38·839	40·49	42·81	55·78	61·53
0·09	50·618	60·22	62·23	57·37	100·84
0·16	63·963	75·82	76·20	57·89	100·15
0·25	68·777	74·95	75·72	56·88	85·05
0·36	63·602	65·48	66·73	52·90	70·10
0·64	46·251	45·51	46·42	39·83	47·03
0·735	41·714	40·77	41·54	36·12	41·96
1·00	32·156	31·12	31·63	28·17	31·82

† From Morrison and Collins (private communication).

approximations. All important electron–molecule symmetries are included in this study. To ensure consistency, the same static and polarisation potentials were used throughout and a consistent standard of numerical accuracy was enforced in all calculations. By examining corresponding SE and SEP cross sections, we can determine the extent to which the polarisation interaction alters the effects of various approximate treatments of exchange on these cross sections.

Table 3. Selected SEP cross sections (a_0^2) and eigenphase sums (modulo π, in parentheses) for the three dominant symmetries.

Energy (Ryd)		ESEP†	TFEGEP	SCEP	HFEGEP	AAFEGEP
0·04	$^2\Sigma_g$	33·352	31·53	33·05	52·47	18·91
		(2·825)	(2·83)	(2·83)	(2·73)	(2·91)
	$^2\Sigma_u$	4·404	7·47	7·48	2·60	38·73
		(0·125)	(0·16)	(0·16)	(0·10)	(0·36)
	$^2\Pi_u$	1·026	1·43	2·22	0·65	3·82
		(0·046)	(0·05)	(0·06)	(0·04)	(0·08)
0·09	$^2\Sigma_g$	34·509	33·94	36·06	49·41	27·18
		(2·651)	(2·65)	(2·64)	(2·53)	(2·71)
	$^2\Sigma_u$	13·038	22·26	20·38	6·20	65·62
		(0·322)	(0·42)	(0·40)	(0·22)	(0·77)
	$^2\Pi_u$	2·965	3·92	5·67	1·65	7·91
		(0·114)	(0·13)	(0·15)	(0·09)	(0·18)
0·25	$^2\Sigma_g$	29·978	30·64	31·72	36·67	28·70
		(2·335)	(2·32)	(2·30)	(2·19)	(2·36)
	$^2\Sigma_u$	30·303	35·27	32·47	15·87	43·81
		(0·916)	(1·02)	(0·96)	(0·62)	(1·23)
	$^2\Pi_u$	8·230	8·74	11·20	4·11	12·21
		(0·315)	(0·32)	(0·36)	(0·23)	(0·38)
0·64	$^2\Sigma_g$	18·975	19·29	19·41	19·77	19·13
		(1·982)	(1·95)	(1·94)	(1·84)	(1·98)
	$^2\Sigma_u$	17·437	17·44	16·93	14·18	18·10
		(1·289)	(1·29)	(1·25)	(1·07)	(1·34)
	$^2\Pi_u$	9·185	8·07	9·31	5·31	9·03
		(0·562)	(0·52)	(0·56)	(0·43)	(0·55)
1·00	$^2\Sigma_g$	13·153	13·15	13·18	12·92	13·20
		(1·822)	(1·78)	(1·78)	(1·69)	(1·80)
	$^2\Sigma_u$	11·250	11·15	10·91	9·99	11·37
		(1·327)	(1·31)	(1·28)	(0·18)	(1·34)
	$^2\Pi_u$	6·853	5·89	6·56	4·49	6·27
		(0·633)	(0·58)	(0·62)	(0·51)	(0·60)

† Morrison and Collins (private communication).

The best agreement with the ESE and ESEP e–H_2 cross sections was obtained by using the TFEGE potential of Morrison and Collins (1978). Somewhat surprisingly, the SCE potential is qualitatively successful for this system except at very low energies, where serious deviations from the ESE cross sections occur.

This work should be seen in the context of other very recent research into the applicability of model exchange potentials for electron–molecule scattering. These include a study by Morrison and Collins (1980) of the effects of imposing orthogonality of continuum and bound orbitals (of the same symmetry) in FEG exchange calculations for e–H_2, e–N_2, e–CO and e–LiH collisions and the earlier studies of this question by Collins *et al* (1979, 1980). In addition, Rumble and Truhlar (1980b) have recently reported SE and SEP calculations of e–N_2 cross sections using the HFEGE and SCE potentials. They find that at 1·0 Ryd the SCE potential is much too strong. Indeed, like the AAFEGE potential, which was applied to this system by Morrison and Collins (1978), the SCE is so attractive that it binds the unoccupied $1\pi_g$ orbital of N_2. The SCE potential is not as disastrously inaccurate for the e–H_2 system, as figures 1–3 of the present paper illustrate.

Acknowledgments

We wish to acknowledge support of this research from the US Department of Energy, Office of Basic Energy Sciences and from the Research Corporation. We are most grateful to Dr Neal F Lane for his gentle insistence that this study be performed and to Dr L A Collins for his help with the ESEP calculations reported in § 3.3, for useful discussions regarding exchange, and for reading and commenting on the present manuscript in a preliminary form. We should also like to thank Dr Andy Feldt and Rick Weitzel for reading and commenting on a preliminary form of this manuscript.

References

Baille P and Darewych J W 1977 *J. Phys. B: Atom. Molec. Phys.* **10** L615–21
Bardsley J N, Herzenberg A and Mandl F 1966a *Proc. Phys. Soc.* **89** 305–19
—— 1966b *Proc. Phys. Soc.* **89** 321–40
Bransden B H, McDowell M R C, Noble C J and Scott T 1976 *J. Phys. B: Atom. Molec. Phys.* **9** 1301–17
Collins L A, Henry R J W and Norcross D W 1980 *J. Phys. B: Atom. Molec. Phys.* **13** 2299–307
Collins L A and Norcross D W 1978 *Phys. Rev.* A **18** 467–97
Collins L A, Norcross D W and Schmid G B 1980 *Comput. Phys. Commun.* in press
Collins L A, Robb W D and Morrison M A 1980 *Phys. Rev.* A **21** 488–95
Collins L A, Robb W D and Norcross D W 1979 *Phys. Rev.* A **20** 1838–40
Fraga S and Ransil G J 1961 *J. Chem. Phys.* **35** 1967–77
Furness J B and McCarthy I E 1973 *J. Phys. B: Atom. Molec. Phys.* **6** 2280–91
Hara S 1967 *J. Phys. Soc. Japan* **22** 710–8
Henry R J W and Lane N F 1969 *Phys. Rev.* **183** 221–31
Klonover A and Kaldor J 1978 *J. Phys. B: Atom. Molec. Phys.* **11** 1623–32
Kolos W and Wolniewicz L 1967 *J. Chem. Phys.* **46** 1426–32
Lane N F 1980 *Rev. Mod. Phys.* **52** 29–119
Lane N F and Henry R J W 1968 *Phys. Rev.* **173** 183–90
Levin D A, Fliflet A W and McKoy V 1980 *Phys. Rev.* A **21** 1202–9
Lynch M G, Dill D, Siegel J and Dehmer J L 1979 *J. Chem. Phys.* **71** 4249–54
Morrison M A 1979 *Electron–Molecule and Photon–Molecule Collisions* ed T N Rescigno, V McKoy and B I Schneider (New York: Plenum) pp 15–50
—— 1980 *Comput. Phys. Commun.* in press
Morrison M A and Collins L A 1978 *Phys. Rev.* A **17** 918–38
—— 1980 *Phys. Rev.* A in press
Morrison M A and Hay P J 1979 *Phys. Rev.* A **20** 740–8
Morrison M A, Lane N F and Collins L A 1977 *Phys. Rev.* A **15** 2186–201
Morrison M A and Schneider B I 1977 *Phys. Rev.* A **16** 1003–12
Onda K and Truhlar D G 1979a *J. Chem. Phys.* **71** 5097–106
—— 1979b *J. Chem. Phys.* **71** 5107–23
—— 1980 *J. Chem. Phys.* **72** 1415–7
Riley M E and Truhlar D G 1975 *J. Chem. Phys.* **63** 2182–91
—— 1976 *J. Chem. Phys.* **65** 792–800
Rumble J R and Truhlar D G 1979 *J. Chem. Phys.* **70** 4101–7
—— 1980a *J. Chem. Phys.* **72** 3206–10
—— 1980b *J. Chem. Phys.* **72** 5223–7
Sams W N and Kouri D J 1969 *J. Chem. Phys.* **51** 4809–14
Schneider B I 1977 *Chem. Phys. Lett.* **51** 578–81
Siegel J, Dehmer J L and Dill D 1980 *Phys. Rev.* A **21** 85–94
Slater J C 1951 *Phys. Rev.* **81** 385–90
Temkin A and Vasavada K V 1967 *Phys. Rev.* **160** 109–17
Temkin A, Vasavada K V, Chang E S and Silver A 1969 *Phys. Rev.* **186** 57–66
Truhlar D G and Brandt M A 1976 *J. Chem. Phys.* **65** 3092–101

Truhlar D G, Dixon D A and Eades R A 1979 *J. Phys. B: Atom. Molec. Phys.* **12** 1913–25
Wang S C 1928 *Phys. Rev.* **31** 579–86
Watson D K, Lucchese R R, McKoy V and Rescigno T N 1980 *Phys. Rev.* A **21** 738–44
Wolniewicz L 1966 *J. Chem. Phys.* **45** 515–23

APPENDIX II

EXPANSION OF GAUSSIAN PRIMITIVES

A Gaussian primitive centered on nucleus A is written as

$$\eta(\vec{r}_1) = N_{qrs}(x_A)^q(y_A)^r(z_A)^s e^{-\alpha r_A^2} \tag{1}$$

where N_{qrs} is a normalization constant, α is the exponential coefficient, and the remaining terms are defined in Table 2 of Chapter III. A similar expression can be written for a primitive centered on nucleus B. The types of Gaussian primitives used in this study are given in Eq.(3.29). From Table 2 we write

$$\begin{aligned}\eta(\vec{r}_1) =& N_{qrs}\,(r_1 \sin\theta_1 \cos\phi_1)^q\,(r_1 \sin\theta_1 \sin\phi_1)^r\,(r_1 \cos\theta_1 + |A_z|)^s \\ & \cdot e^{-\alpha(r_1^2+A_z^2)}\, e^{-\alpha 2 r_1 |A_z| \cos\theta_1}.\end{aligned} \tag{2}$$

We seek to expand $\eta(\vec{r}_1)$ as

$$\eta(\vec{r}_1) = \sum_{i=0}^{\infty} \sum_{j=-i}^{i} \frac{1}{r_1}\, a_i^j(r_1)\, Y_i^j(\hat{r}_1). \tag{3}$$

To obtain the expansion coefficients $a_i^j(r_1)$, we utilize the orthonormality of the spherical harmonics, *viz.*,

$$a_i^j(r_1) = r_1 \int d\hat{r}_1\, Y_i^j(\hat{r}_1)^*\, \eta(\vec{r}_1) \tag{4}$$

These integrals can be performed analytically by substituting the appropriate linear combination of spherical harmonics from Table 3 for the angular factors in Eq.(2) and by replacing $e^{-\alpha 2r_1|A_s|\cos\theta_1}$ with the following expansion. We start with the well known Rayleigh expansion for a plane wave

$$e^{ikr_1\cos\theta_1} = \sum_{\ell=0}^{\infty}(i)^{\ell}(2\ell+1)j_{\ell}(kr_1)P_{\ell}(\cos\theta_1) \tag{5}$$

where $j_{\ell}(kr_1)$ is a spherical Bessel function.[64] The modified spherical Bessel functions of the first kind can be written as (for x along the positive real axis)

$$M_{\ell}(x) = e^{-i\ell\pi/2}j_{\ell}(ix). \tag{6}$$

For integral values of ℓ we have

$$M_{\ell}(x) = (-i)^{\ell}\, j_{\ell}(ix) = (i)^{\ell}\, j_{\ell}(-ix). \tag{7}$$

Now, replacing k by $-i\gamma$ in Eq.(5) we are left with

$$e^{\gamma r_1\cos\theta_1} = \sum_{\ell=0}^{\infty}(2\ell+1)(i)^{\ell}\, j_{\ell}(-i\gamma r_1)P_{\ell}(\cos\theta_1) \tag{8}$$

which can be rewritten via Eq.(7) as

$$e^{\gamma r_1\cos\theta_1} = \sum_{\ell=0}^{\infty}(2\ell+1)M_{\ell}(\gamma r_1)P_{\ell}(\cos\theta_1). \tag{9}$$

Also, since $P_{\ell}(-\cos\theta_1) = (-1)^{\ell}P_{\ell}(\cos\theta_1)$, we have

$$e^{-\gamma r_1\cos\theta_1} = \sum_{\ell=0}^{\infty}(-1)^{\ell}(2\ell+1)M_{\ell}(\gamma r_1)P_{\ell}(\cos\theta_1). \tag{10}$$

By letting $\gamma = \alpha 2|A_z|$, we can substitute the expansion in Eq. (10) for $e^{-\alpha 2 r_1 |A_z| \cos\theta_1}$, which leaves us with a series of angular integrals of the form

$$\int d\vec{r}_1 \, Y_i^{j*}(\hat{r}_1) \, Y_\lambda^\mu(\hat{r}_1) \, P_\ell(\cos\theta_1) \tag{11}$$

where the values of λ and μ depend on the particular type of Gaussian (see Table 3). Finally, we can substitute $P_\ell(\cos\theta_1) = \sqrt{\frac{4\pi}{2\ell+1}} \, Y_\ell^0(\hat{r}_1)$ into Eq.(11) leaving

$$\sqrt{\frac{4\pi}{2\ell+1}} \int d\hat{r}_1 \, Y_i^j(\hat{r}_1)^* \, Y_\lambda^\mu(\hat{r}_1) Y_\ell^0(\hat{r}_1) = (-1)^\mu \sqrt{(2i+1)(2\lambda+1)} \cdot \begin{pmatrix} i & \lambda & \ell \\ -\mu & \mu & 0 \end{pmatrix} \begin{pmatrix} i & \lambda & \ell \\ 0 & 0 & 0 \end{pmatrix}. \tag{12}$$